2015

Anterior Cruciate Ligament Biomechanics, Computational Modeling of Mechanical Behavior and Injury Risk

Bharadwaj Cheruvu
Wright State University

ANTERIOR CRUCIATE LIGAMENT BIOMECHANICS, COMPUTATIONAL MODELING OF MECHANICAL BEHAVIOR AND INJURY RISK

A dissertation submitted in partial fulfillment of the
Requirements for the degree of
Doctor of Philosophy

By

BHARADWAJ CHERUVU
B.S., University of Texas at San Antonio, 2001
M.D. Ross University, 2006

2015

Wright State University

WRIGHT STATE UNIVERSITY

GRADUATE SCHOOL

June 2, 2015

I HEREBY RECOMMEND THAT THE DISSERTATION PREPARED UNDER MY SUPERVISION BY Bharadwaj Cheruvu, ENTITLED Anterior Cruciate Ligament Biomechanics, Compuational Modeling of Mechanical Behavior and Injury Risk BE ACCEPTED IN PARTIAL FULFI.LLMENT OF THE REQUIREMENTS FOR THE DEGREE OF Doctor of Philosophy.

_____

Tarun Goswami, D.Sc
Dissertation Director

_____

Ramana Grandhi, Ph.D
Director, Ph.D Engineering

_____

Robert E.W. Fyffe, Ph.D.
Vice President of Research and Dean, Graduate School

Committee on Final Examination

_____
Tarun Goswami, D.Sc

_____
David Reynolds, Ph.D

_____
Nasser Kashou, Ph.D

_____
Aihua Wood, Ph.D

_____
Matthew Lawless M.D

_____
James Tsatalis M.D

Abstract

Cheruvu, Bharadwaj. Department of Biomedical, Industrial, and Human Factors Engineering, Wright State University, 2015. Anterior cruciate ligament Biomechanics, computational modeling of mechanical behavior and injury risk.

Knee joint involves interactions from various structures such as cartilage, bone, muscles, ligaments, tendon, as well as neural control. Anterior cruciate ligament (ACL) tears are one of the most frequent soft tissue injuries of the knee. A torn ACL leaves the joint unstable and at risk for further damage to other soft tissues manifested as pain, dislocation, and osteoarthritis. This injury is quite common in sports such as basketball, soccer and football. Females often tear their ACL 2-8 times more frequently than their male counterparts. An ACL injury can be devastating and significantly increases the athlete's risk for osteoarthritis long term. While many advances have been made in terms of surgical and rehabilitation treatments for ACL injured patients, long term outcome studies show that these patients are at a high risk for developing knee osteoarthritis 10-15 years after ACL injury, regardless of the treatment. Currently, the mechanism of non-contact ACL injury is not well understood.

Therefore, the knowledge of the ACL biomechanics is of importance in various clinical scenarios, since it would be instrumental in its understanding of structure and function which are necessary to diagnose and prevent ACL injury. This dissertation further investigates four areas; demographic studies which relate anatomical features to ACL injury, computer aided diagnostic tools which can be used to diagnose a common complication with ACL injury, computational simulations of ACL biomechanics using representative gait data, and finally risk of injury assessments.

Magnetic resonance images (MRIs) of 32 patients with ACL tears and 40 patients who did not have ACL tears were evaluated from a physician group practice. Digital measurements of femoral condyle length, femoral notch width, ACL width in the frontal and sagittal plane, and the ACL length in the sagittal plane were taken in both groups. Empirical data correlations were performed and trends identified. Similarly, a sample from the Fels gait data was a larger subset which consists of 178 healthy volunteers, out of which 99 were females and the remaining were males.

Finite element (FE) analysis has become an increasingly popular technique in the study of human joint biomechanics, as it allows for detailed analysis of the joint/tissue behavior under complex, clinically relevant loading conditions. A wide variety of modeling techniques have been utilized to model knee joint ligaments. However, the effect of a selected constitutive model to simulate the ligaments on knee kinematics remains unclear. Computational knee joint models were based on patients' medical images. Using a sample from Fels Longitudinal study, loads were determined from the gait profile of healthy volunteers and the stress distributions on the ACL were determined. The anatomical representation of the ligament make it feasible to determine stress distribution across the ligament which in turn provide valuable information about the mechanism of ligament injury. 3D anisotropic hyperelastic model was found to simulate physiological behavior of human knee.

Females have significantly greater abduction angles ($p < 0.005$). Similarly, males have significantly larger adduction angles than the females ($p<0.05$). In this study, the peak ACL force observed during normal walking was less than ½ BW. A combination of tibial and valgus rotations of the tibia had resulted in a Von Mises stress on the ACL as high as 62 MPa which is indicative of ACL injury.

A linear relationship was determined to investigate the relationship between NWI and width of the ACL. This may suggest that NWI plays no significant role in the causes for ACL injury. Sensitivity analysis had shown that there is a linear relationship between the forces applied and risk for ACL injury. The forces which have exceeded the ultimate strength of the ACL result in its injury. The various anatomical features such as NWI, AP width, Sagittal length and width have no bearing on the risk for ACL injury.

The trends identified here will lead to a more practical method of identifying individuals at high risk for an ACL tear. An attempt was made to use demographic data in combination with digital measurements taken from MRI to predict ACL injury. By training the individuals to reduce the valgus and rotational moments can reduce the incidence of ACL injury. A focus on prevention of ACL tears is recommended to prevent lifelong disability in a young and active population.

TABLE OF CONTENTS

List of Figures

List of Tables

ACKNOWLEDGEMENTS

I am privileged to have completed my doctoral dissertation research under guidance of Dr. Tarun Goswami. I am indebted to him for accepting, training, and encouraging me to pursue doctoral degree. I am grateful to Dr. Goswami for his continued guidance, insightful ideas, and help in many ways. In addition, I am extremely grateful to my father, Dr. Narayana Sastry Cheruvu, who have supported me through my ups and downs throughout my educational career. He has always been there to guide, provide insightful ideas, as well as to help in my through understanding of Mathematics and Engineering. My success in obtaining a Ph.D in Engineering cannot have happen without the loving and caring support my wife, Sayuri Cheruvu; my beautiful daughter, Sruthi Cheruvu; my mother, Rajeswari Cheruvu; and my sister, Praveena Cheruvu.

My sincere thanks to all my committee members: Dr. David Reynolds, Dr. Nasser Kashou. Dr. Aihua Wood, Dr. Matthew Lawless, and Dr. James Tsatalis for their valuable time, guidance, and encouragement in efficiently and effectively completing this work. Special thanks Dr. Lawless for letting me observe ACL Reconstruction surgeries and providing with valuable clinical information to better understand the mechanism of its injury.

Thanks to the Ph.D. in Engineering Program for accepting me into the program and helping me stay on track. I would also like to thank the staff of Biomedical, Industrial and Human Factors Engineering department for being accommodating and understanding over the past years. I am also thankful to the following institutes, organizations, and companies for their help: Wright State University's College of Engineering, and School of Medicine; Miami Valley Hospital. I am very thankful to all of the current and past members of the Goswami Labs and Device Development

Center for creating a vibrant and enthusiastic work environment, sporting great attitude, and helping me in many ways. I am eternally obliged to my friends, who over the years have become family. Without their constant encouragement and steadfast.

Chapter 1 Introduction

Injuries of the knee joint are often due to those who participates in sports regardless of age, gender or playing level. It is a major concern among college level or professional athletes from various sports including soccer, basketball, volleyball, football and lacrosse. Among all of the knee injuries, the injury to anterior cruciate ligament (ACL) is most common cause event in these sports. Among the National Collegiate Athletic Association (NCAA) female basketball athletes from 1988 to 2004, 8% of all the injuries related to knee were ACL injuries [Agel, 2007]. In the United States, there were approximately 250,000 ACL injuries which occur each year [Griffin, 2004]. ACL injury can have a compounding impact on both the individual as well as society. Early onset of osteoarthritis and lengthy rehabilitation programs are major areas of concern for the athlete [Lohmander, 2004]. Higher rate of ACL injuries in female athletes and cost for surgery and rehabilitation which has reached as high as 2 billion dollars are a major concern for researchers and health professionals (Hewett, 1999).

Clinically, patients with ACL injury often present with knee pain, swelling and instability of the knee joint. 70% of the ACL injuries are often non-contact injuries which involve early ground contact and its effect on the knee during landing or cutting tasks [Boden 2000]. Several mechanisms of ACL non-contact injuries include planting and cutting, straight knee landing, pivot /shift, and one step stop landing with knee in hyperextension. The pivot shift can be explained as being a rapid slowing down followed by a quick turn

in one direction while the feet are securely fixed on the ground, which is the most common mechanism of injury.

Over the past 30 years, there are approximately 2000 studies which have investigated ACL injuries (Boden, 2000). Majority of these studies (98%) had focused on surgical treatment and diagnosis, post-surgical rehabilitation programs, procedures to facilitate speedy recovery and post injury biomechanics of these injuries. The remaining portion of the studies were dedicated to actual injury mechanisms and prevention strategies, focusing on neuromuscular control and developing strength training to prevent ACL injuries. Prevention programs have been shown to decrease the rate of knee injuries (Gilchrist, 2008; Heidt, 2000; Mandelbaum, 2005). In addition, research was conducted examining the effects of isolated or combined knee loads motion states on ACL loading [Kanamori, 2002, Shelburne, 2004].

Insights in mechanism of ACL injury help us to give specific directions on prevention strategies, rather than using very generalized neuromuscular and proprioceptive training programs. By doing so, it helps us to separate abnormal movement patterns caused by desired neuromuscular adaptation (Van Den Bogert, 2007). Injuries of the ACL occur during the landing and stance phase of the movements, because it is characterized by rapid changes in speed and direction as seen in rotations of tibia (Boden, 2000). There is another scenario in which a combination of valgus and internal rotation on the tibia can be seen in various cutting movements that can increase risk for ACL injury (Besier, 2001). In

addition to movements, other risk factors of ACL injury include body mass index (BMI), joint laxity, femoral intercondylar notch width, and neuromuscular fatigue. It is difficult to ascertain which combinations play a role in increased ACL loading and how it can be affected by anatomical, and soft tissue parameters as a subsequent risk of injury. There is a lot of interest in understanding knee ligament biomechanics among researcher for many years.

Examining previous study helps in isolating the need areas in ACL research. These research areas that were identified for further research include:

- **Demographic studies which relates anatomical features and interdependent relationships:** Using a retrospective clinical database, various anatomical parameters may be measured to determine any relationship to ACL injury. Some of the key risk factors studied are body mass index, notch width index, and any difference which may exist of the size of the female ACL when compared to that of male.

- **Tools that can be integrated with diagnostics of ACL injury:** One of many complications which may arise from ACL injury includes anterior knee pain. Anterior knee pain has many causes; one of which swelling of the infrapatellar fat pad. Using the same clinical database, the volume of the infrapatellar fat pad in patients with acute ACL injury can be compared to matched controls with intact ligament. The volume of the infrapatellar fat pad was measured using a 3D

reconstruction software, ellipsoidal approximation, and MATLAB code. The information can be used to for additional diagnosing tools.

- **Computational simulations of ACL biomechanics using representative gait data:** To develop computational knee joint models which have subject specific geometry and tissue properties by using various loads applied through the gait cycle, and being able to investigate alternations in the stress distributions on the ACL using three different modeling techniques. Gait data used to evaluate differences in kinematic and kinetic patterns of the knee between male and female walkers. The forces of interest are anterior/posterior knee joint load, which can be calculated from sagittal plane joint reaction forces, varus-valgus and internal-external joint moments. By using these forces one is able to calculate the resulting force being applied on the ACL.

- **Risk of injury assessments:** Monte Carlo simulations were used to assess the risk of ACL injury using these parameters as well as force. By using sensitivity analysis, it is possible to determine key parametric relationships on the risk of ACL injury.

This dissertation will describe in detail the methods that are used to build subject specific knee joint models, optimize and validate these models using gait data and subsequently using these models to determine ACL injury mechanisms.

Knee anatomy plays a critical role in the understanding of joint mechanics and subsequently neuromuscular control. It is quite important to be able to understand the anatomy of the knee joint and ligament before understanding the mechanisms to injure the ligament. Chapter 2 provides an introduction into the anatomy of the knee joint and ACL. The second part of Chapter 2 consists of the incidence of ACL injury and various risk factors that are associated with this injury.

Chapter 3 will cover the biomechanics of the ACL as well as a systematic literature review of cadaveric models to measure and compare the material properties between males and females. The second part of Chapter 3 will cover the use of finite element modeling of the ACL as well as the basics of modeling techniques that will be used. Chapter 4 will cover the importance of the gait cycle to better understand the normal every day scenarios. Chapters 5 through 7 will cover the experimental, results, and discussion sections, respectively. The experimental section would cover 4 distinct subsections: Demographic studies which would investigate the relationship between anatomical measures; Tools that can be integrated with diagnostics of ACL injury; Computational simulations to better understand ACL biomechanics with the use of representative gait data, and finally risk of injury using Monte Carlo Simulations.

Chapter 2: BACKGROUND and Literature Review

2.1 BRIEF ANATOMY OF KNEE JOINT

The knee is the largest and one of the most complex joints in the body. It is a hinge-like joint that is subject to constant impact, flexing, twisting from everyday activities as well as the impact of falls and the effects of arthritis. Injury to knee can significantly affect training and sports performance. The treatment ranges from simple physiotherapy exercises to total knee replacement.

Long articulating bones that form the joint are femur and tibia. The articular surfaces are covered with articular cartilage which provides cushioning and smooth relative motion. The joint is protected anteriorly by patella. The proximal end of the patella is connected to quadriceps muscle and the distal portion is connected to anterior tibia through patellar tendon. The hamstring muscles connect to the posterior portion of the tibia. The medial and lateral collateral ligaments connect the femur and the tibia on the medial and lateral sides respectively. The anterior, lateral and medial aspects of the extra-articular structure of the knee joint are shown in Figure 2.1. The knee joint is covered by synovial membrane. The synovial fluid fills the synovial chamber. This fluid acts as a lubricant and a carrier of nutrients. The articular surfaces are covered by articular cartilage. A C-shaped tissue called meniscus fits in the space between tibia and femur. It helps to protect the joint and allows the bones to slide freely on each other.

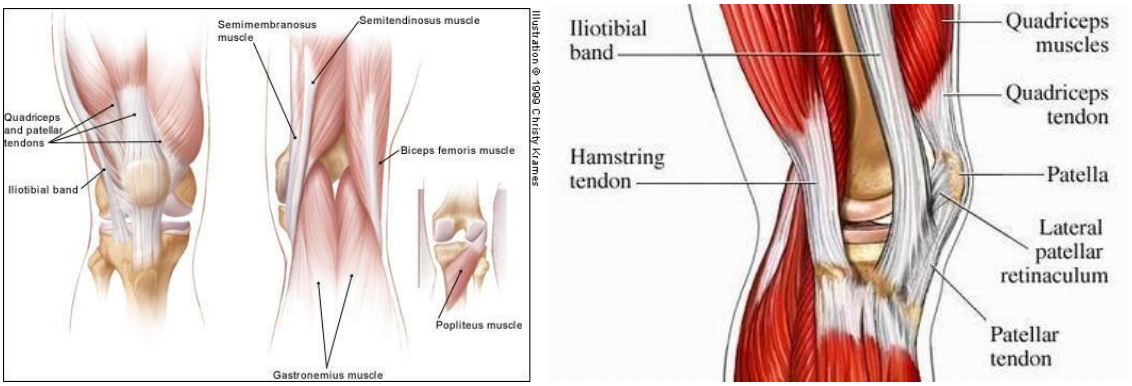

Figure 2.1: Anatomy of knee joint (Netter, 2014)

The end of the femur is shaped as a large notch and it plays an important role in the stability of the knee. This notch is called intercondylar notch. The notch houses two important ligaments of the knee which includes the anterior cruciate ligament (ACL) and the posterior cruciate ligament (PCL). The intra-articular structure of the knee joint is shown in Figure 2.2.

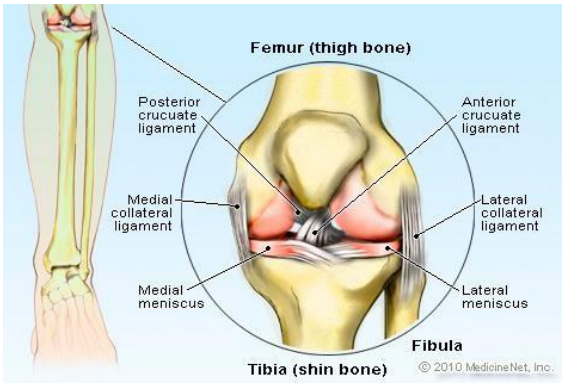

Figure 2.2: Intra-articular structure of knee joint (Medicinenet)

2.2 ACL ANATOMY

The ACL can be divided into distinct functional bundles that represent the varying tension of the fibers through range of motion of the knee. The most widely accepted view is the

classification of fibers into two bundles, anteromedial and posterolateral bundles [Girgis, 1975; Palmer, 2007]. The bundles are named based on their position of insertion into the tibia. The bundles have a clinical application as well as a functional significance. A positive anterior drawer sign is thought to more correspond to a torn anteromedial bundle, whereas a positive Lachman sign is thought to indicate a tear more likely in the posterolateral bundle [Furman, 1976]. During extension of the knee, the posterolateral bundle is stretched and the anteromedial bundle is relaxed. The opposite occurs during flexion when the femoral attachment of the ACL moves into a horizontal position, resulting in stretch of the anteromedial bundle and relaxation of the posterolateral bundle [Amis, 1991].

The overall course of the ACL is to run in an anterior, medial, and distal direction from the femur to the tibia. The femoral ACL attachment lies at the posterior segment of the inner surface of the lateral femoral condyle (Arnoczky, 1983). The fibers fan out as they cross the midline and attach in front of and lateral to the medial intercondylar tubercle (Palmer, 2007). There may be some fibers of the ACL that blend and attach to the anterior and posterior horns of the lateral meniscus as well. The anatomy of the anterior cruciate ligament is closely related to its function as a constraint as knee joint motion. It acts as static stabilizer of the knee for anterior tibial translation and internal tibial rotation. It is also found that the ACL has neuroreceptors that suggests a possible proprioceptive role of the ligament. The ACL is a band of regularly oriented dense connective tissues that

connects the femur and tibia. The ACL is attached to a fossa on the posterior aspect of the medial surface of the lateral femoral condyle. The femoral attachment is in the form of a segment of a circle, with the anterior straight border and the posterior convex border. The long axis of the femoral attachment is tilted slightly forward from the vertical and the posterior convexity is parallel to the posterior articular margin of the lateral femoral condyle.

The ACL is distally attached to the lateral aspect of the anterior tibial plateau. The ACL is covered in a synovial membrane, which makes the ACL an intra-articular structure. The ACL is attached to the femur and tibia as a collection of individual fascicles. The tibial attachment is larger than the femoral attachment. The anteromedial bundle (AMB) consists of fascicles originating from proximal aspect of the femoral attachment and inserting at the anteromedial aspect of the tibial attachment. The posterolateral bundle (PLB) consists of the remaining fascicles that are inserted at posterolateral aspect of the tibial attachment. The average length of the ACL ranges from 22 mm to 41 mm, with a mean of 32 mm. The average width of the ACL ranges from 7 mm to 12 mm [Amis 1991; Odensten, 1985; Kennedy, 1974]. These measurements were all collected during studies using cadavers. More recently, digital measurements using magnetic resonance imaging (MRI) were evaluated for their accuracy [Cohen, 2005]. This study measured the two bundles of the ACL on sagittal and coronal planes of fifty MRIs. These values were then compared to an intraoperative measurement on ten knees that had undergone both MRI and knee

arthroscopy. The agreement between the MRI and intraoperative measurements indicates that MRI measurements of the ACL are clinically reliable (Cohen, 2009). Due to such arrangement of the bundles, the ACL has a characteristic twist and appears hourglass shaped. The ACL courses anteriorly, medially and distally across the joint as it passes from the femur to the tibia (Figure 2.3). Each position of knee flexion is associated with recruitment of different fiber bundles in the ACL. At 0° flexion, both the AMB and the PLB are taut. As the flexion angle increases, the AMB bundles elongates while the PLB becomes lax.

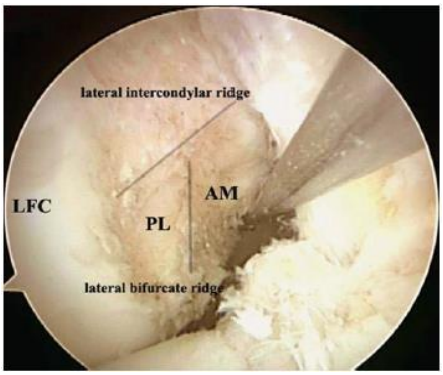

Figure 2.3: Arthroscopic view of the femoral attachments of anteromedial and posterolateral bundles of ACL

2.3 ACL Microanatomy

There are three zones which make up the ACL. Each of these zones have unique materials as seen in table 2.1.

Zone	Composition	Location
Proximal	-Less Solid -Round and Ovoid cells -Contains: fibroblasts, Collagen Type II, glycoproteins	Femoral Attachment
Middle	-High density of collagen fibers - zone of cartilage, elastic fibers and Oxytalan fibers	
Distal	-Mostly solid -Rich in chondroblasts, fibroblasts -low density of collagen fibrils	Tibial attachment

Table 2.1: Composition of the ACL with respect to various zones

In the middle part of the ACL, the oxytalan and elastic fibers play a role in withstanding multidirectional stresses and maximal stresses respectively (Strochhi, 1992). The fusiform cells which are quite prevalent in this region are characterized by longitudinally oriented cells which consists of fusiform shaped nuclei. In addition, the cytoplasm of these cells is intimately attached to extracellular collagen and follow the crimp pattern of the fibers.

The three primary components of the ACL are water, an organic matrix, and fibroblast cells. Water is the most abundant component of the ACL; it constitutes 65 - 70% of the ligament. Type I and type III collagens form 70- 80% of the organic matrix dry weight with a ratio of 9:1 type I to type III collagen [Kirkendall, 2002]. Type III collagen content increases during healing and development, but it is replaced by type I collagen during the tissue remodeling phase [Woo, 2003]. Elastin and proteoglycans are also found in the

organic matrix and represent <5% and <1% of the dry weight, respectively [Kirkendall, 2002].

ACL has been composed of multiple fascicles where the basic unit is the collagen. These fascicles are often range from 250 μm to several millimeters in diameters. These fascicles are surrounded by connective tissue which is known as paratenon. The collagen fibrils (typically consist of Type I collagen) are aligned along the axis of the ACL (figure 2.4). These collagen fibrils gather to form fibril bundles of about 20 micrometers in diameter and a number of such fibril bundles form fascicles that are several hundred micrometers in diameter. These collagen fibrils attach to the bones through a transition zone of fibrocartilage. There are two types of collagen fibrils which make up the ACL and each type plays a unique role. The first type has a variable diameter ranging from 35 to 75 nm. They typically account for 50.3% of the ACL and often produced by fibroblasts. The second type has a more uniform distribution with a peak diameter of 45 nm, and consists about 43.7% of the ACL. These fibrils help in maintaining three dimensional organization of the ligament.

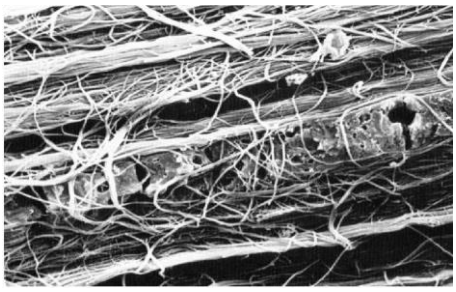

Figure 2.4: Microstructure of the ACL (Jackson, 1993)

Type I collagen is responsible for the tensile strength of the ligament (Amiel, 1989). However the type III collagen is often located in the loose connective tissue which divide the type I collagen fibrils. They are found at maximum concentrations at the attachment zones. The function of type III collagen anchors the vessels to the adjacent matrix and also allows for the ligament to be quite pliable.

At nanoscale, ACL consists of cells called fibroblasts that moderate the synthesis of collagen fibrils in the ACL. The collagen fibrils reinforce the extracellular matrix to form a composite structure (Figure 2.5). The extracellular matrix is made up of ground substance and water. The ground substance, in turn, is made up of substance such as glycosaminoglycan, proteoglycans, and glycoproteins. The water acts as a lubricant for sliding action of collagen fibrils when the ACL is loaded. The water and the ground substance also contribute to the viscoelastic properties of the ACL.

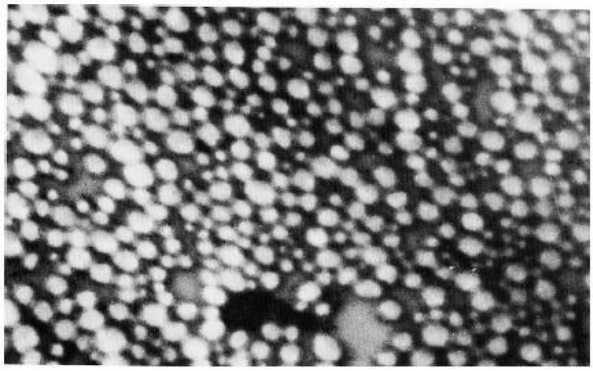

Figure 2.5: Microstructure of the extracellular matrix [Jackson, 1993]

The ligaments in the knee define the motion limits of the articulating surfaces and control and guide the relative motion of the bones. They stretch when the movement of the articulating surfaces is outside the limit. They also participate in transmitting the loads across the joint. The anterior cruciate ligament limits the anterior tibial translation. The AMB is more important in flexion while PLB is more important in extension. The ACL also resists hyperextension of the knee. In full extension, the ACL resists both internal and external tibial rotation. In flexion, it resists internal rotation of tibia only. It also plays role in resisting the medial and valgus displacements of the tibia.

2.4 ACL Injury

There have been many methods of studying the mechanism of injury such as video analysis, interviews with injured subjects, cadaver studies, clinical studies, and mathematical modeling. The typical mechanism of ACL injury occurs with the knee close to full extension and the tibia rotated either internally or externally, leading to a valgus

collapse [Olsen, 2004]. The most devastating force in this sequence is the anterior translation force when the knee is flexed around 20-30º [Boden, 2000].

A material breaks when the force exceeds its mechanical strength. Similarly, the ACL can be injured when it is subjected to a force that exceeds its strength. These forces that are applied on the knee joint include anterior tibial translation, internal and external tibial rotation, hyperextension of the knee, and valgus rotation of the tibia. Majority of ACL injuries are noncontact in nature, which in turn suggests no direct force applied on the ACL. ACL injury commonly can occur in sports such as football, basketball, soccer and skiing.

In the case of skiing, ACL can often get injured in a setting where the anterior tibial translation occurs. As the skier lands, there is a passive drawer force that is applied on the tibia (figure 2.6A). In order to counteract this force, the quadriceps muscle contract which in turn increase the anterior force on the tibia (figure 2.6B). The combination of both of these forces often result in ACL injury.

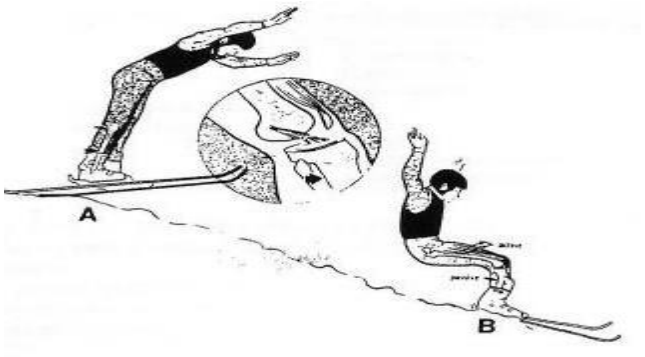

Figure 2.6: ACL injury mechanism during skiing (McConkey, 1986)

Football players often have another mechanism in which the ACL can be injured. These players run and cut on the same side which cause the tibia to be rotated inwards (figure 2.7).

Figure 2.7: ACL Injury as a result of tibial rotation

(http://www.cavalierdaily.com)

Previous scenarios had shown that ACL injury occurs as a result of one component whether it was anterior tibial force or tibial rotation for skiing and football respectively. However, ACL injury can also occur in the case of additive effect as seen in the case with

hyperextension coupled with internal tibial rotation with foot planted. Unfortunately in these cases, there are multiple ligaments which can fail in addition to an ACL injury.

Literature search was performed to determine the incidence of ACL injury among various sports (table 2.2). A number of terms was used for the search parameters such as ‘anterior cruciate ligament’, ‘incidence’ and sports. There were 33 studies which had reported incidence of ACL injury. The most common activity which predispose an athlete to ACL injury was basketball, followed by soccer and football.

		Male and Female			Female			Male			
Sport	**First Author**	**Incidence**	**ACL tear**	**Exposures**	**Incidence**	**ACL tear**	**Exposures**	**Incidence**	**ACL tear**	**Exposures**	**Female : Male**
Basketball	Mihata	0	1,393	8,068,016	0	1,061	3,733,209	0	332	4,334,807	3.50
	Agel	0	682	3,889,954	0	514	1,797,730	0	168	2,092,224	3.63
	Harmon	0	359	1,972,170	0	275	925,501	0	84	1,046,669	
	Arendt	0	238	1,375,974	0	189	639,898	0	49	736,076	4.29
	Gwinn	0	6	21,734	0	5	10,452	0	1	11,282	5.33
	Gwinn	0	5	35,226	0	0	1,360	0	5	33,866	0.00
	Gwinn	0	11	56,960	0	5	11,812	0	6	45,148	3.23
	Gomez				0	11	84,341				
	Messina	0	15	223,566	0	11	92,885	0	4	130,681	4.50
	Bjordal	0	131	1,837,455							
	Mihata	0	1,295	6,283,785	0	871	2,736,615	0	424	3,547,170	2.67
	Agel	0	586	2,840,568	0	394	1,208,994	0	192	1,631,574	2.75
	Harmon	0	317	1,605,004	0	194	604,430	0	123	1,000,574	
	Arendt	0	178	934,971	0	97	308,748	0	81	626,223	2.38
	Gwinn	0	6	18,916	1	5	6,508	0	1	12,408	9.63
	Gwinn	0	12	26,204	3	2	742	0	10	25,462	6.92
	Gwinn	0	18	45,120	1	7	7,250	0	11	37,870	3.34
	Viola	0	31	726,836	0	10	227,766	0	21	499,070	1.00
Lacrosse	Mihata	0	315	1,783,903	0	146	799,611	0	169	984,292	1.06
Football	Scranton							0	61	895,908	
	DeLee							0	37	331,561	
Handball	Mykelbust	0	28	84,690	1	23	40,799	0	5	43,891	5.09
	Seil							0	5	20,462	
Rugby	Levy				0	21	58,296				
	Gwinn	0	7	31,263	0	3	8,475	0	4	22,788	1.94
Wrestling	Gwinn	0	3	11,888	1	1	1,306	0	2	10,582	4.05
Indoor Soccer	Lidenfield	3	10	3,600	5	8	1,536	1	2	2,064	5.37
	Putukian				5	1	190	5	3	600	1.04

Table 2.2: Literature search for the comparison of incidence of ACL injury among various sports

2.5: Risk Factors

Females are found to have 8-9 times higher risk of ACL injury than their male counterparts, which can be due to various causes (table 2.1). The disparity among genders is more evident in certain sports such as basketball, soccer and handball. The injury incidence of females to males is 3.5 times greater in basketball (Arendt, 1995). However among naval servicemen, the ratio reaches as high as 9 among those playing basketball. Non-contact ACL injuries are multifactorial. The causes for non-contact ACL injuries can be subdivided into extrinsic and intrinsic factors. Some of the extrinsic factors include weather, training, and technique. The intrinsic factors which have been studied include ligament laxity and hormone differences. The effect of oral contraceptives have been controversial in their role in protecting ACL injury.

ACL injury has been defined according to a model of risk mechanisms. This model describes ACL injury as the end result of the combination of a predisposed athlete (internal risk factors) in a situation of higher risk (external risk factors) during an event in which the ACL cannot withstand the applied load (Bahr, 2005). The model highlights the role of both qualitative (history of previous injury, skill level, etc.) and quantitative (body weight, intercondylar notch width, etc.). The basic model from Bahr and Krosshaug (2005) was expanded to describe the interplay of risk factors involved in ACL injury during the Hunt Valley II meeting, a gathering of experts in the area of ACL injury research. This updated

model, shown in Figure 2.8, was based on a combination of an epidemiologic model (Meeuwisse, 1994) and a biomechanical model (McIntosh, 2005). Internal risk factors, such as age, gender, health status, anatomy, and skill level establish a baseline risk level leading to a predisposed athlete. This can be considered the first layer of risk in the injury causation model. The predisposed athlete then becomes exposed to external risk factors such as coaching technique, protective equipment used in their sport, and environmental conditions. This defines the second layer of risk, resulting in a susceptible athlete. The final step leading to injury is the occurrence of an inciting event. This could be the particular playing situation, the behavior of those playing the sport, the player biomechanics, or a combination of these events that directly lead to ACL injury.

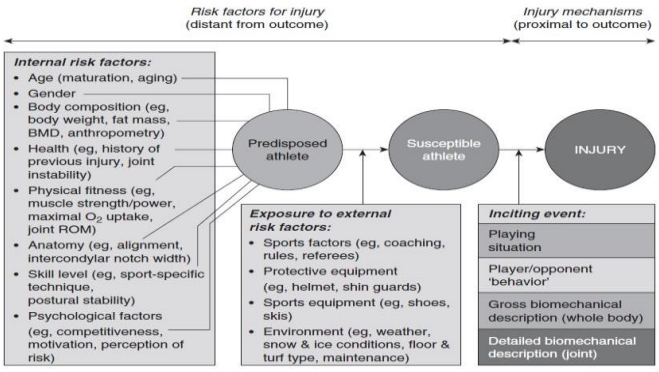

Figure 2.8: Flow chart for the risk factors of ACL injury (Bahr, 2005)

Intrinsic factors are often which cannot be modified. Q-angle can be defined as the angle created by line from anterior-superior iliac spine and patella and like from patella to tibial tubercle (Hutchinson, 1995). Normally, Average Q angle can be 14 and 17 for males and females respectively (Ferber, 2003). Excessive Q-angle result in higher lateral forces on

the quadriceps mechanism. Quadriceps muscles are a major contributor to anterior shear force through the patellar tendon. The increased Q-angle was assumed to be a reason why females have an increased risk for ACL injury. There is no experimental data which support this hypothesis (Ireland, 2002).

Gender variations of the femoral notch morphometry have been studied as one possible explanation for an increased rate of ACL tears in females. Multiple studies have correlated intercondylar notch stenosis with ACL injury [Shelbourne, 1998, Anderson, 1987, LaPrade, 1994, Souryal, 1993], however gender alone has not been consistently correlated with femoral notch stenosis. Several studies have proposed that a smaller, biomechanically weaker ACL may be found in a smaller notch (Souryal, 1988, Davis, 1999, Anderson, 2001). The correlation between notch width and ACL size is controversial. Davis (1999) found a positive correlation, suggesting that a narrow ACL width represents a weaker, more susceptible ACL. However, other studies have found that the size of the notch did not correlate with the size of the ACL (Anderson, 2001; Muneta 1997). Souryal, et al. (1988) used plain radiographs to calculate notch width index (NWI) based on a measured ratio of femoral notch width to femoral bicondylar width. Patients in this study who had sustained bilateral ACL injuries had a statistically smaller NWI than did patients without ACL injuries (Souryal, 1988). Further studies have confirmed this relationship (LaPrade, 1994; Souryal, 1993). Most studies have shown that there is a difference in NWI between

males and females (Shelbourne, 1998; Souryal, 1993; Shelbourne, 1997). Few studies have shown that gender does not correlate with NWI (LaPrade, 1994).

This was quite consistent with a previous work done by LaPrade in 1994. Previous work consisted of 213 athletes in which the Notch Width Index was measured using X-Rays. They were able to conclude the average NWI among injured athletes were 0.193 with a range of 0.17 to 0.21. Comparing among gender, the average NWI was 0.244 and 0.238 for men and women respectively. In the study done by Domzalski, subject's knee were placed in 10 degrees of flexion and T2 weighted image were obtained. The study population in the study done by Domzalski had an average age of 14.7 years with a range of 11 to 16. In this study using MRI, it was found that average notch width size was 0.2438 among those who have ACL injury. Similarly, the notch width size was averaged to be 0.26 among those with an intact ACL. Stein in 2010, studied a large prospective multi-centered study which had involved 160 patients with osteoarthritis. The notch width was determined by the subjects undergoing MRI of the knee. The average age in this study population was 62 years of age, older than what is seen in our study population. The population in this study had a history of osteoarthritis which is not the case in our study population. The results from this study had shown average notch width size of 0.24 and 0.26 for patients with ACL torn and intact ACL, respectively.

ACL can be impinged against the intercondylar notch during tibial external rotation and abduction (Park, 2010). ACL can be impinged at 4 degree abduction and 15 degrees of

external rotation. The force which was measured using FEA methods, to be 36.9 N with a contact area of 19.7mm^2. In addition, contact pressure was observed on the impinged side of the ligament. Maximal principal stresses were observed on the nonimpinged side which can be explained by a combination of ligament bending and stretching. The stresses that were seen had peaked at 8.9 and 3.0 MPa which corresponds with embedded fibers and ground matrix respectively. At the impinged area, the ACL undergoes a process of cell death. The repeated impingement causes a local and cumulative damage of the ligament which can lead to its tear (Fung, 2005). This gives a mechanism in which the ACL can be injured.

Sex hormones such as estrogen and relaxin are shown to have an effect on various organs and ligaments. Estrogen often regulates the structure of the ligament by affecting the synthesis of type I and type III collagen at mRNA level. Doing so, it likely to affect the laxity of the knee and the material properties of ACL. The incidence of ACL injury will likely be higher during the first few days in the menstrual cycle. During this time, the circulating sex-hormones are at its lowest (Slauterbeck, 2002). The incidence of ACL injuries was greater during days 9 to 14 of a typical 28 day cycle, and lower during the post ovulatory phase (defined as after day 15). This finding was supported in a study of recreational alpine skiers. Using serum concentrations of progesterone and estradiol, the phase of the skier's menstrual cycle was determined at the time of ACL injury. Skiers who are in their pre ovulatory phase has a greater risk for ACL injury when compared to post

ovulatory phase (odds ratio 3.22). Among the skiers, 74% of the women had suffered an ACL injury while they are in the preovulatory phase (Beynnon, 2006). There is no direct evidence exists that estrogen alters the properties of human ACL.

Just like how the ligaments are considered to be passive stabilizers of the knee joint, the surrounding muscles of the joint are the active stabilizers of the joint. The active knee stiffness is often dependent upon the strength of these muscles. In general, females have a lower muscle strength than males for a given weight (Anderson, 2001). Among females, the quadriceps be a major player in contributing joint stability. Similarly, males use hamstrings to stabilize the knee.

Slaughterbeck (2006) constructed a model which concluded that all factors will eventually affect the mechanical load placed on the ACL or the magnitude of the ACL load at failure [Slauterbeck, 2006]. Therefore when the load applied on the ACL is greater than the ligament's ultimate failure load is when the ACL injury occur. The applied external load applied on the knee is often resisted by the anterior cruciate ligament. The applied loads on the knee can be attained from ground reaction force, body weight, anatomic structure, and magnitude of muscle contraction. The magnitude of force transmitted to ACL depends on ground reaction force, body mass index and neuromuscular control. The stiffness of the knee can also depend on how the load be transmitted to ACL. In patients with less knee stiffness, a greater proportion of the load be transmitted to ACL.

Females have lesser knee stiffness due to lower muscle co-activation. There are differences in motion patterns, positions and forces generated by the hip among genders. Differences in hip position and motion would directly affect the knee position, loads and stiffness (Putnam, 1993). Coordinated muscle activation plays a key role in production of motion, stabilization of the joint, and development of moments of the joint (Van Ingen Schenau, 1987). In general, females have less hamstring and gluteus medius activation when compared with their male counterparts. Since females have weak hip extensors, they land in more upright hip position due to use of iliopsoas muscles to control the trunk.

Differences in landing techniques and neuromuscular recruitment patterns are modifiable and therefore conducive to intervention via programs that can be implemented to help prevent ACL injuries from occurring. In general, females have a higher tendency to have a risky landing pattern which is associated with ACL injury. Females typically land in a more erect posture than in males and also have greater hip internal rotation and hip adduction when landing [Barber-Westin, 2009]. In addition, their movements involve more external rotation of the tibia which in turn result in increased knee valgus [Huston, 1996]. The muscular strength, timing and recruitment all play a role in the stability of the knee. Hamstrings are key in ACL prevention in that they act as a primary knee flexor which opposes forces to anterior tibial displacement [Renstrom, 2008]. These factors can further explain the role of increased risk for ACL injury among female athletes as well as

used in various prevention programs. Prevention programs have been shown to decrease the rate of knee injuries.

2.6: Complications

Anterior knee pain is a common problem among athletes. Anterior knee pain is often caused by an impingement of the patellofemoral joint caused by edematous changes in the infrapatellar fat pad. Non-invasive methods to determine the size of the infrapatellar fat pad can play role in the preventing this disorder. Using a cohort of patients with acute ACL injury, this study had found that these patients had a greater volume of the infrapatellar fat pad. Due to its location, the changes in morphology of the fat pad is often related to patients with ACL injury.

2.7: ACL Reconstruction

Once the ACL is injured, the patient have to undergo ACL reconstruction. During this surgery, the torn ACL replaced by graft material. Initially, the torn ACL removed and tunnels drilled at the insertion sites of the ACL. The graft placed in the tunnel and secured using various methods. There are two type of graft materials; biological or synthetic. Biological grafts are harvested from one's own body (Autograft) or from cadaver (allografts). The various autografts that are used include the patellar tendon, hamstring tendon, and quadriceps tendon. Patients who have been treated with surgical reconstruction have a success rate of 82 to 95 percent (Wetzler, 1998).

ACL reconstruction can fail due to recurrent instability, arthrofibrosis, and infection. Recurrent instability is the most common cause for ACL reconstruction failure and can be seen in 8% of patients. Reconstruction failure can be subdivided into technical, biological and traumatic scenarios with the primary cause being laxity from ligamentous restraints (Wetzler, 1998).

Technical error is the most common which can account for 77 to 95% of ACL failure (Wetzler, 1998). One of the major causes for technical error is the improper placement of femoral tunnel. By placing the femoral tunnel in a more anterior position, would result in the graft being constrained in flexion and laxity during extension. Similarly, the femoral tunnel in a posterior position result in a loss of fixation. The femoral tunnel in a more central position results in the graft positive pivot shift due to lack of rotational stability. Even though tibial tunnel placement is not a common cause for technical error, the improper position of the tibial tunnel leads to persistent instability. Other causes of technical error include improper graft tensioning, insufficient graft material, and inadequate graft fixation (Petsche, 1999). A lower graft tension causes the knee joint to be unstable with excessive laxity. Whereas a higher graft tension allows for the knee joint to be constrained with a delayed graft incorporation. Graft fixation is also important in that improper fixation result to persistent instability. There are several options for graft fixations. In the case of poor bone stock, the use of post washer or button fixation provides better fixation than interference screws (Wetzler, 1998).

During the healing process of ACL reconstruction, there can be a lack of complete incorporation or ligamentization of the graft material which falls under biological failure (Wetzler, 1998). The primary mechanism of this process be infection and graft rejection. Causes due to infection is seen in approximately 0.3% of ACL reconstruction failures and can be treated with operative irrigation and debridement, intravenous antibiotics, and occasional graft removal (Williams, 1997). Ligamentization is a more delayed process in which the primary cause being bone tunnel osteolysis. Grafts from a cadaver (allograft) can incite a graft rejection. Graft rejection can be lessened with graft being processed by gamma irradiation, freeze drying, and ethylene oxide sterilization. These graft process result in a weakening of the graft which later delay its incorporation (Wetzler, 1998).

Traumatic failure can occur in patients early in postoperative period as well as those returning to full activity. Failure seen in early post-operative period is often due to incomplete graft incorporation often as a result of excessive rehabilitation or non-compliance with activity restrictions. Late failure is often a cause in 5 to 43% of ACL reconstruction failure (Getelman, 1999).

Arthrofibrosis can be defined as the failure to achieve a range of motion in the post-operative period which is equal to that seen in the preoperative stage. It is often due to either an acute scenario or prolonged postoperative immobilization (Wojtys, 1994). Following a traumatic stimulus such as injury or surgery, the knee develops scar tissue. In addition, the joint capsule undergoes shrinkage and tightening of various structures such

as tendons. The tightening process can continue until the femur and tibia are restricted. Afflicted patient presents with inability to straighten or bend the knee. There are some genetic factors which can predispose a patient to develop arthrofibrosis by a way to develop excessive joint scar tissue.

2.8: Prevention programs

Prevention programs have been shown to decrease the rate of knee injuries (Gilchrist, 2008; Heidt, 2000; Mandelbaum, 2005; Myklebust, 2003). The most successful programs involve some combination of stretching, strengthening, aerobic conditioning, agility training, plyometrics, and risk awareness skills. It is not known by which mechanism such prevention programs are effective, however post-program data has shown improvements in balance, strength, and coordination (Griffin, 2006).

A major theory to account for higher knee injury incidence in female athletes is that neuromuscular imbalances. The use of neuromuscular training in a controlled environment can be translated to the court or field and in turn reduce the risk for ACL injury. Neuromuscular training can effectively reduce the relative ACL injury risk among female athletes by an average of 50%. The main reason is that active knee joint be better stabilized in a laboratory setting and which can further explain the reduced injury rate among female athletes.

Four neuromuscular imbalances seen among women. The first imbalance is that females are found to be ligament dominant and have a tendency to allow stresses on the ligament before the muscles in order to absorb ground reaction forces. The ground reaction force controls the direction of motion of lower extremity joint. The lack of muscular control of the joint results increased valgus motion, increased force and high torque at the knee and ACL.

In general, females tend to use their quadriceps which to stabilize the knee joint. However, it accentuates and perpetuates strength and coordination imbalances between knee extensors and flexors. Finally a third imbalance is between muscular strength and coordination on opposite limbs, with 1 limb being greater than the other. Unfortunately, both limbs are at a higher risk for ACL injury. The weaker limb be compromised in its ability to dissipate forces and torques. Whereas, the stronger limb subjected to higher forces and torques as a result of increased dependence and increased loading on that side.

Chapter 3 - ACL BIOMECHANICS

3.1 Biomechanics of ACL

Human knee joint is typically stabilized with the use of four major ligaments; anterior cruciate ligament (ACL), Posterior cruciate ligament (PCL), Medial Collateral ligament (MCL), and lateral collateral ligament (LCL). The use of muscles plays a key role in normal flexion and extension motion of the knee joint. Over a course of daily activity, ground reaction forces and muscles forces are typically transferred to the knee joint and the four ligament stabilize the joint throughout its range of motion. The complex structure of the knee joint allows each of the ligaments to stabilize every degrees of freedom (DOF) of the knee joint motion.

The tibiofemoral knee joint can move in three planes (sagittal, frontal and transverse) with 6 degrees of freedom (3 rotations, and 3 translations) between the femoral condyles and tibial plateau (Woo, 2006). In the sagittal plane, the knee can rotate by flexion and extension. The knee can rotate by abduction and adduction in the frontal plane. Finally, internal and external rotation of the knee joint move in the transverse plane. In addition, the knee can also translate in the sagittal plane anteriorly and posteriorly, in the frontal plane medially and laterally and in the transverse plane by compression.

Each of these motions of the knee joint are often in a relatively limited range. The range of movement is dependent upon age, pubertal status, sex, and race (Quatman, 2008).

Excessive motion of the knee joint beyond the physiological range in these planes can damage the internal knee joint structures.

The transition of the knee takes place in anterior-posterior, proximal-distal and medial lateral aspects. The rotational motion consists of flexion-extension, internal-external rotation and valgus-varus rotation (abduction-adduction), Figure 3.1. The stability of knee is achieved by the three dimensional geometry of the articular surfaces, from the ligaments and musculotendinous units.

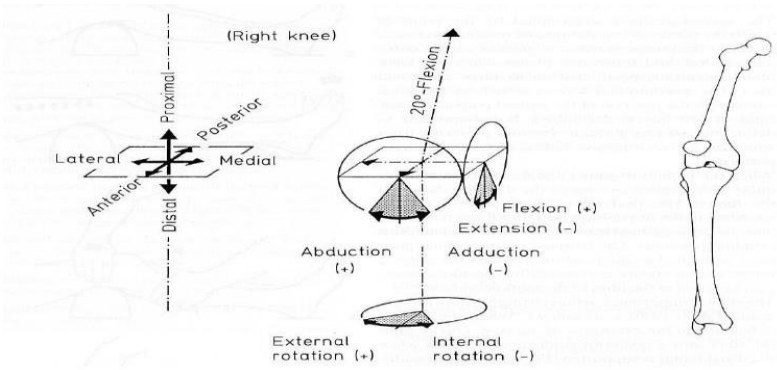

Figure 3.1: Degrees of freedom for Knee joint (Jakob et al., 1992)

The motion of knee joint and the ACL act as a restraint to anterior tibial translation when an anterior force is applied to tibia [Woo, 1999]. However, the ACL becomes unstable when medial and lateral forces are applied on the tibia. Each bundle of the ACL plays a unique role in the flexion extension motion of the knee joint. The AMB is typically tight in flexion and PLB is tight in extension [Amis, 1991].

In case of the passive knee flexion-extension, ACL strain increases with extension while femur is kept horizontal [Woo, et al. 1998]. ACL appears loaded maximally at or near full extension, with minimum loading occurring at approximately 30° of knee flexion [Bach, et al. 1997]. For active flexion-extension, the ACL is again maximally loaded at or near full extension, with the strained or unstrained where transition occurring at a slightly larger (approximately 40°- 50°) knee flexion angle [Beynnon, et al. 1997]. Tension in the ACL is least at 40° to 50°of knee flexion [Beynnon, et al. 1997]. When returning to extension from flexion, the lateral femoral condyle rolls on the tibial surface, whereas the medial femoral condyle, being less convex, translates backward on the tibia continuing its forward roll. This mechanism rotates the tibia laterally and referred as screw home mechanism of the knee in clinical terminology.

ACL plays secondary role in restraining internal-external rotation of the tibia [Markolf, ET al. 1981]. Differences exist while depicting ACL's role in controlling internal external rotation of the tibia. Ahmed and associates [Ahmed, et al. 1987] found that ACL has very little restraining role to play in external rotation, but plays certain restraining role at 40°flexion. But, it is worth noting here that Ahmed's study used strain gauges mounted on certain fiber bundles (typically AMB) of the ACL and may not represent the entire ACL strain. Role of the ACL in varus-valgus knee rotation has been carefully studied by researchers [Hollis, et al. 1991, Markolf, et al.1976, Grood, et al. 1988, Wroble, et al. 1993]. Grood and Markolf studies concluded that ACL plays secondary role to MCL while

restraining the varus-valgus motion at full extension. Wroble and colleagues [Wroble, et al. 1993] reported increase in knee valgus in the ACL deficient knees, whereas, Hollis and colleagues [Hollis, et al. 1991] observed increases in the ACL length during valgus loading.

3.2 Historical review of tensile properties

ACL material response is typically viscoelastic in nature (Woo, 1993), which shows creep with respect to time at constant load. This behavior plays a role in protecting the ligament from rapid deformation cycles (Kwan, 1993). It is because of this property in which cadaveric ligaments should be preconditioned prior to mechanical testing. Due to the function of the ACL, the ligament resists tensile loading while keeping the femoral condyle subluxating from the tibial plateau. The size of the ligament is typically short to be clamped and tested for tension failure. Therefore, mechanical properties of the ACL was determined using tensile testing of a bone-ligament-bone unit. Some of the preliminary studies was performed using animal models such as rabbits (Woo et al, 1987), dogs (Alm et al 1974) and monkeys (Noyes and Grood, 1976).

There are a few studies available in the literature studying the properties of human ACL (Kennedy et al., 1976; Noyes and Grood, 1976; Butler et al., 1986; Woo et al., 1991). Kennedy et al. (1976) had determined the tensile properties of ten isolated anterior cruciate ligaments and reported a mean ultimate load of 620N to failure. Noyes and Grood (1976) had determined the effect of mechanical properties of the human ACL with respect to age.

They divided the donors into two age groups, young (16-26 years) and old (48-86 years), and tested the tensile properties of ACL along the axis of the tibia. It was found that the ultimate load and maximum stress of young human ACL to be 1730 N and 37.8 MPa, respectively. The ultimate load and maximum stress for the older group were determined to be 734 N and 13.3 MPa, respectively. Woo et al (1991) tested the tensile properties of human femur-ACL-tibia complex (FATC) for donors from three age groups; young (22-35 years), middle age (40-50 years) and old (60-97 years). The tensile forces were applied on the ligament in two orientation scenarios; axis of anatomical orientation of the ACL, and along axis of tibia. They reported the ultimate load of 2160N, 1503N and 658 N for young, middle and old age groups, respectively when the FATC was tested in the anatomical orientation (Table 3.1).

Age Group	Specimen orientation	Stiffness (N/mm)	Ultimate Load (N)	Energy Absorbed (N-m)
Young	Anatomical	242	2160	11.6
	Tibial	218	1602	8.3
Middle	Anatomical	220	1503	6.1
	Tibial	192	1160	4.3
Older	Anatomical	180	658	1.8
	Tibial	124	495	1.4

Table 3.1: Comparison of the material properties of the ACL with respect to age (Woo, 1991)

They reported that when the ACL is tested in tibial orientation, the structural properties of the ACL are significantly lower. A schematic of structural and anatomic orientations of FATC is shown in Figure 3.2.

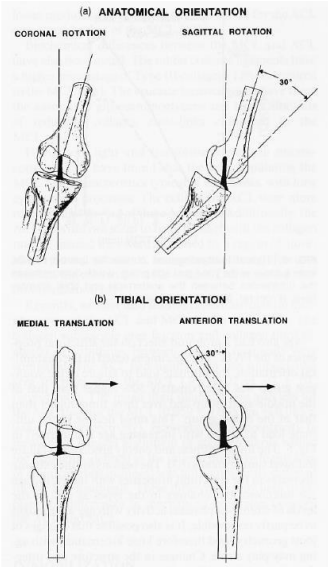

Figure 3.2: Anatomical and tibial orientation of the ACL for tensile testing (Jackson, 1993)

The tensile properties of the ACL decrease with the progression of age [Noyes and Grood (1976); Woo et al. (1991)]. Butler et al. (1986) tested the mechanical properties of individual bundles of ACL and concluded that anterior subunits of the ACL had superior mechanical properties. The anterior bundles were found to have superior mechanical properties when compared to posterior bundles. Further, the tensile properties of some tissues are also known to be affected by the activity level of the subject (Woo et al. 1980).

3.3 Material properties among genders

The exact reason for differences in the incidence of ACL injuries among genders is debatable, however the reasons are quite multifactorial. From an engineering point of view, it is important to investigate the sex based differences in the geometry, tensile properties

and ultrastructure of the ACL (Chandrashekar, 2005). By using cadaveric ligament models, the tensile properties between the males and females were investigated (Chandrashekar, 2005).

The mechanical properties of the ACL in both sexes are seen in Table 3.2. Representative (polynomial fitted) load-deformation and stress-strain curves of the male and female cadavers are seen in figure 3.3. In order to show that sex based differences between materials properties exist, a multivariate regression was performed. It was found that sex was a significant factor in determining elongation ($p=0.03$), ultimate load ($p=0.01$), stiffness ($p=0.05$) and energy absorbed ($p=0.03$) [Chandrashekar, 2005].

There were differences in the stress at failure and modulus of elasticity between sexes which were about 14.29 and 22.49%, respectively. Female ACLs would exhibit less resistance during straining of the ACL (more laxity) and fail at lower stress levels. Females have a lower knee stiffness in torsion in both active and passive states of the muscle, which can explain the higher incidence of knee injury among female athletes. The decreased stiffness and elastic modulus of the ACL seen among females can explain the decreased rotational stiffness in females.

Sex	Elongation at failure (mm)	Load at Failure (N)	Stiffness (N/mm)	Energy absorbed at failure (N-mm)
Male(n=8)	8.95±2.12	1818±699	308±89	7280±3624
Female (n=9)	7.48±2.56	1266±527	199±88	4691±3623
Combined (n=17)	8.17±2.41	1526±658	250±102	5909±3753
% difference between sexes	16.4	30.36	35.3	35.56

Table 3.2: Structural properties of the ACL [Chandrashekar, 2005]

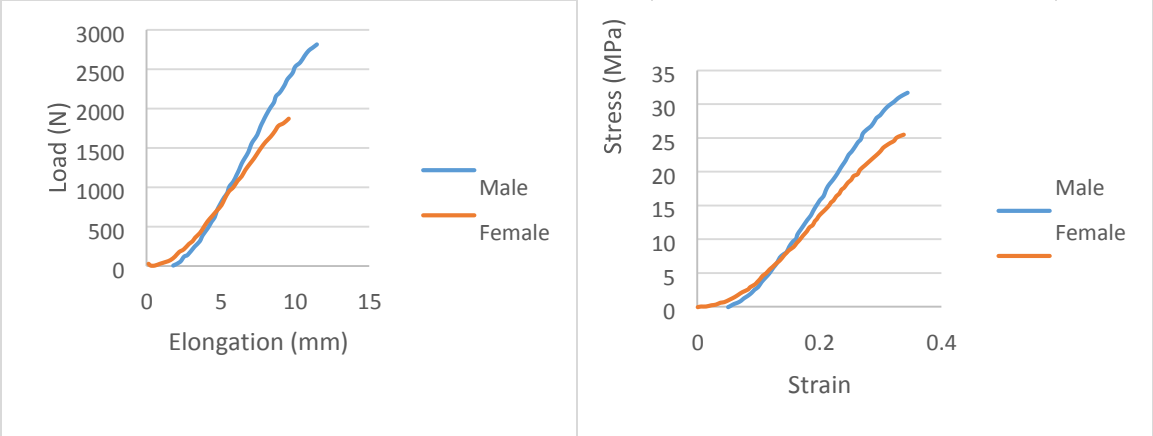

Figure 3.3: Load-Elongation and Stress-Strain curves of a male and female ACL. [Chandrashekar, 2005].

ACL load –elongation curves can be divided into three regions; clinical testing zone, normal physiological loading zone, and injury zone. The curve is predicted to be non-linear in the physiological loading zone. However, the tensile testing performed by Chandrashekar had concluded that this zone is actually linear relationship where the stiffness value to be 308 N/mm and 199 N/mm for males and females, respectively. The strain at failure load was found to be 10% and 3% for young and older adults, respectively. Previous studies have shown that the material properties of the ACL are dependent upon

the age and gender of the person as well as the orientation of the applied load. ACL fails at a lower loads when applied in a line that is not to the longitudinal axis.

3.4 Material properties of Collagen fibrils

Collagen is generally made of fibrous protein which provides structural support for various tissues in the body. The fibrils have little strength in either bending or in torsion, but the presence of the cross-links have allowed for ability to resist high tensile stresses (Parry, 1988). By doing so, the cross links acts as reinforcing fibers in bone and being able to transmit stress in soft tissue such as ligaments.

The mechanical properties of collagen fibrils were studied by using X-ray diffraction with simultaneous tensile testing on tissues. Using changes in the D-period that was detected from X-ray diffraction corresponds to strain on the collagen fibrils. Two methods contribute to the elongation of the fibrils. The first mechanism can be defined by actual stretching of the collagen molecule. The second mechanism is defined by the sliding of the collagen molecules which further increases the D period. Using a constant load, continuous sliding of collagen molecules can occur for 300 seconds which can explain the viscous behavior of these fibrils (Mosler, 1985).

Using an Atomic Force Microscope (AFM) based micro-dissection technique, the properties at the center and the surface of the collagen fibrils isolated from calfskin were probed by Strasser and co-workers (2007). Nano-indentation was performed both at the surface and the center of the fibril.

A Young's modulus of 1.2 GPa without significant difference in the elasticity between core and shell was obtained from the measurements (Table 3.3). However, they found a higher adhesion at the surface of the fibril compared to the central region, which they related to a higher number of cross-links near the fibril surface than in the central region as also suggested by Gutsmann (2004).

	Ultimate strength (MPa)	Modulus of elasticity (GPa)
ACL	37.8	0.128
Collagen	50	1.2

Table 3.3: Comparison in the material properties between ACL and collagen fibrils.

3.5 C_{10} Coefficients of Collagen

The fibril network can be represented as an isotropic biphasic matrix that contributes to the mechanical response of tissues under loading (Korhonen et al. 2003). Thus, the total stress becomes:

$$\sigma t = \sigma nf + \sigma fibril - pI$$

Where σ_{nf} and σ_{fibril} represents nonfibrillar and fibril network stresses, respectively. The isotropic biphasic nonfibrillar matrix has been modeled as Hookean or Neo-Hookean materials with Darcy's law for the fluid flow. The material parameters for the nonfibrillar part are the Young's modulus (E_m), Poisson's ratio (ν_m) and permeability (k). The fibril network properties are controlled by the Young's modulus of the fibril network (E_f). Elastic properties of the fibril network have been characterized with a nonlinear relation.

Neo-hookean coefficients were determined based on curve fitting using mechanical data from mechanical data (figure 3.4).

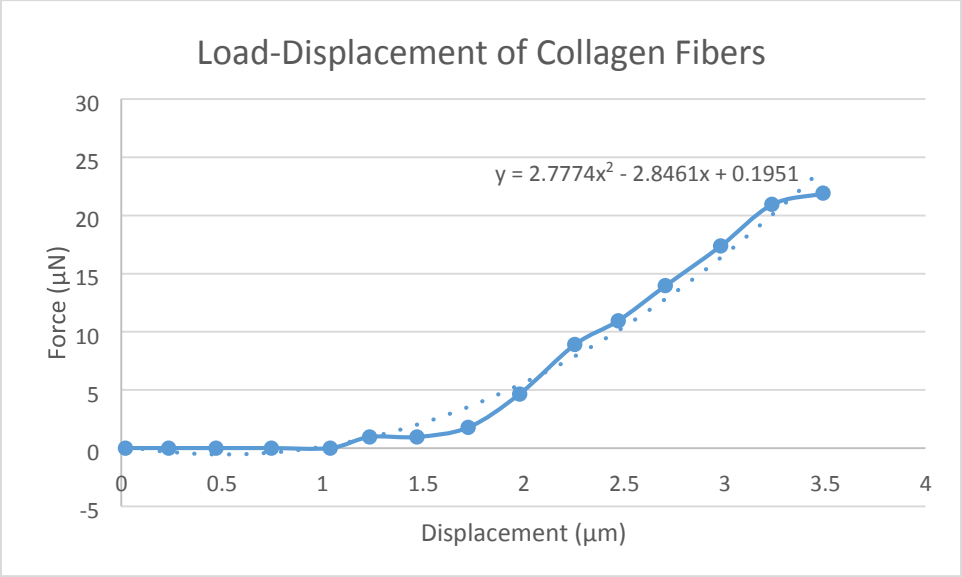

Figure 3.4: Load vs displacement for Collagen fibrils to determine C_{10} values

The increasing rate of physical activity and sports injuries around the world has prompted investigation into the factors that increase an individual's susceptibility to injury. Because of ethical reasons, *in vivo* studies, which mimic possible injury situation, are not feasible. The use of musculo-skeletal modeling and simulation can offer the possibility to study injury situations in a computer environment and estimate ACL forces and strain (McLean, 2004) and thus a potential risk. McLean had used a series of Monte Carlo simulations to study random perturbations in initial trunk and joint kinematics on knee joint loading during a side step cutting task (McLean, 2004).

3.6: Finite Element modeling of the ACL

Quantitative in vivo data on the biomechanics of knee ligaments and their behavior under stress are important tools to understand the pathogenesis of knee ligament injuries. To understand the causes in which ACL can be injured, it is important to accurately measure strains on and in the ligament. Previous studies investigate the material properties of the ACL. These studies do have some pitfalls which include difficulty in measuring strains on and in the ligament. Even in cases with uniaxial tensile loading, it has been found that there are no conditions in which all of the fiber bundles of the ACL are uniformly loaded and stretched. The ligament properties are influenced by its geometry measured by Butler, 1990. It is not clearly understood the nonuniform distribution of strain on the fibers within the ligament. A possible reason for this difficulty may be due to intra-articular ligament which possesses a complex three dimensional shape. Studies on extra-articular ligament such as the MCL has been studied to measure the biaxial strain [Weiss, 1992].

The experiments on the actual ligament have been performed on cadaveric ligaments. The cadaveric ligaments which have previously studied do not provide accurate information about the in vivo ligament. The in vivo methods are typically invasive and cannot be used to study dynamic sport movements. In addition, the study of ACL injury mechanism as each knee specimen can only be injured once not be economically feasible. Cadaveric models be acceptable alternative to study the relationship between external loads applied

on the joint and its distribution among the anatomical structures. These external loads are often affected by agonist and antagonist muscle activation. In addition, it is difficult to get specimens within a specific age group and the activity level of the specimen is not known.

There are a number of techniques which quantify ACL loading. Cadaveric models provide basic insight to the passive biomechanics of the joint. To fully understand the joint behavior in a dynamic setting, computational modeling will be valuable information using different loading conditions. The cadaveric models do not actually represent the true living ligament. They are also limited by high costs, differences in strain rate, and variability between each specimen. However, computational models be dependent upon non subject specific joint geometry, assumed tissue properties, and high computational costs and time. Loading of the ACL during passive knee loading may simplify or neglect the dynamic effects of muscles. Therefore, the loading patterns of the ACL in these scenarios often do not represent the actual loading conditions in a living human. However, determination of the ACL strain in vivo requires a more accurate ACL response to various joint loading conditions. The strain of the ACL can be determined by using implantable differential Variable Reluctance Transducers (DVR). DVR transducers during different activities such as squatting, stair climbing, and weight bearing knee flexion (Beynnon, 1999; Beynnon, 1997; Fleming, 1999). This particular transducer was implanted on the Anteromedial bundle of the ACL, and strain of the ligament was recorded while subjects performed different tasks (figure 3.5).

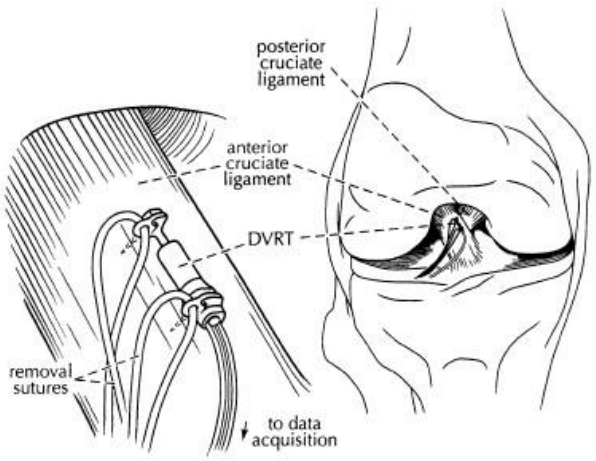

Figure 3.5: DVR transducer to measure the strain of the ACL (Beynnon, 1998).

The primary advantage of these numerical approaches lies in precise control over boundary conditions, material properties, and structural alterations in parametric studies. Moreover, the ligament forces/ strains, contact forces/areas, and stress/strain distribution across all soft and hard tissue structures are invaluable products of such model-based studies, which are challenging, if not impossible, to obtain experimentally.

The computational models can be divided into movement mechanics models and joint mechanics models. Movement mechanics models predict the overall forces produced at the knee joint. However, joint mechanics estimate the loads experienced on an individual structure of the joint. ACL injury can be defined when the peak joint loads exceeding the moment thresholds which reaches as high as 2000 N and 210 Nm respectively (McLean, 2004).

Limitations from the use of cadavers can be overcome by using computational models. These models may be used to simulate injury often in order to study the underlying mechanisms. Use of computational models consider the dynamic muscle activation and offer the potential to study injury events. Therefore, validated computational models can be effective in estimating the forces and stresses in ligaments. Due to these advantages that computational models have over cadaveric models, various studies have developed models to study knee joint biomechanics.

Mesh convergence analysis performed in a finite element study helps in deciding the appropriate element number to be used for the structures. To perform simulations and analyze the results with sufficient accuracy and to follow a good practice of finite element methods, it is necessary to check and ensure that changing the mesh size does not influence the results obtained. An appropriate element size (in turn the element number) is to be decided before performing an analysis.

Over a course of three decades, a variety of modeling techniques have been used to model knee joint ligaments (Abdel-Rahman, 1998). In earlier studies, uniaxial elements such as truss or spring with simplified material properties have been used to model ligaments (Beillas, 2004). This assumption fail to predict non uniform 3D stresses and strains across the tissue. More recently, ligaments were modeled as isotropic hyperelastic material models with use of image processing tools (Bendjaballah, 1997; Gardiner, 2001; Dhaher, 2010; Limbert, 2004).

Two strategies have been used to study loads experienced on the ligaments. In the first approach, a model of the entire joint is constructed which includes all of the supporting soft tissue structures (Bandak, 2001; Penrose, 2002). The influence of arbitrary external loads and/or displacements on joint kinematics and ligament mechanics can then be studied. This approach can predict joint kinematics, ligament stresses, strains, insertion site forces and load transfer to the bones via contact. However, these models are quite complex which in turn make it difficult to implement require detailed experimental studies to validate the model. In the second approach, a single ligament is represented in the FE model. The motion of the ligament insertion sites, or alternatively the bones to which it is attached, is prescribed based on experimental kinematic measurements (Hirokawa, 2000; Gardiner 2003; Song 2004; Debski 2005; Limbert 2004). This approach provides predictions of ligament stresses, strains, insertion site forces and load transfer to the bones via contact, but not joint kinematics, since the motion of the bones must be prescribed. FE models of this kind are considerably easier to implement and validate. Since the overall stiffness characteristics of joints from different donors/animals routinely differ by a factor of two or more, this approach generally requires subject-specific measurements of joint kinematics (Gardiner, 2003).

Ligaments have been commonly modelled as spring elements in the 3D models of the knee joint. Nonlinear material behavior (normally quadratic stress-strain relationship) is often used for the toe region up to ~6% tensile strain, which is twice of the so-called

nonlinear spring parameter (Bendjaballah et al. 1995, Blankevoort and Huiskes 1991, G. Li et al. 1999). The stress-strain relationship for strains greater than 6% is considered linear. The tensile stiffness of the spring elements can be determined accordingly, provided that the ligament geometry is known. The compressive stiffness is taken to be zero, because the ligament does not support load when it is slack. Some level of prestrain exists in ligaments before the joint is subjected to external loads
(ACL, MCL and LCL are in pretension and PCL in pre-compression) (Ahmed et al. 1992, Blankevoort and Huiskes 1991, Butler et al. 1986), which are often incorporated into the material model of the ligaments.

Extensive computational models have been proposed for ligaments and tendons. Since the ligaments' mechanical response is dominated by the collagen fibers, the majority of proposed models focused on the collagen constitutive behavior to predict the response of ligaments. Fung (1967) proposed a one-dimensional constitutive model based on an exponential stress-strain relationship accounting for nonlinear behavior of ligament under finite deformations. The model was later extended to biaxial and three-dimensional cases (Hildebrandt et al. 1969). Some other models were proposed assuming strain rate independence, and negligible hysteresis effect, i.e. the time-dependent response was neglected and elasticity was assumed. In these one-dimensional studies, bundles of linear elastic elements were used to model ligaments. To capture the nonlinear behavior of the

tissue, individual linear elastic fibers in a ligament were assumed slack when the ligament was not externally loaded, and were recruited gradually in resisting increased tension (Decraemer et al. 1980a, Frisén et al. 1969, Kwan and Woo 1989, Lanir 1980, Soong and Huang 1973, Viidik 1968).

Various computational models were found in the literature to evaluate ligament behavior [60, 61]. Finite element method has been shown to be effective approach in characterizing stress distributions in the ACL. In addition, computational modeling of the knee allows for a better understanding of the relationship between hard and soft tissue components of the knee during normal and pathological functions [62]. These validated models play a key role in the design of knee implant systems by understanding the mechanics of the restored knee and optimizing design in order to closely replicate the healthy knee.

Analysis by mathematical model can be effective in that it can simulate a wide variety of conditions, which in turn overcome some of the difficulties in actually measuring the stress/strain measurements. Constitutive equations have been derived from microstructural models of ligaments and tendons (Woo, 1993). However the microstructural approach can result in highly sophisticated formulations which can be difficult to implement using Finite element methods. Another approach, a phenomenological approach has been described by Hirokawa (2000) which can be more practical.

Because of ethical reasons, in vivo studies, which mimic possible injury situations are not feasible. The use of musculo-skeletal modeling and simulation can offer the possibility to study injury situations in a computer environment and estimate ACL forces and strain [67]. These computerized models have an advantage in that a wide variety of condition can be simulated, and thus overcoming the difficulties in making actual stress/strain measurements. There are a number of studies in which constitutive equations were derived from microstructural models of ligaments and tendons [67]. The microstructural approach can result complex formulations which are difficult to implement through finite element methods.

There is a fine balance between mathematical simplicity and structural accuracy. The approach can be made based on assumptions which have been supported by histological and anatomical studies. On modelling ligaments, two important assumptions were made. First, no difference in the material behavior between the ligament body and its insertion were considered. Second, material characteristics depending on time, such as viscoelasticity, creep and relaxation were neglected (Hirokawa and Tsuruno, 2000) due again to the high ratio between the viscoelastic time constant of the material and the loading time of interest in this study.

Strain energy and hyperelasticity have been extensively used in studies of ligaments (Hurschler et al. 1997, Gardiner and Weiss 2001, 2003, Lanir 1983, Quapp and Weiss 1998, Weiss et al. 1996, 2002). A method based on strain energy was proposed to

describe the three-dimensional behavior of the ligament (Lanir 1983). The matrix response was simplified as hydrostatic pressure and the majority of the total strain energy was resulted from the stretch in collagen fibers (Lanir 1983). Weiss and coauthors proposed hyperelastic continuum models of ligaments based on the incompressibility assumption (Weiss et al. 1996, 2002). In their modelling, collagen fibers, ground substance matrix and the fiber-matrix interaction contributed to the tissue response. Incompressibility was enforced in their models based on the assumption that fluid is trapped in the tissue during loading, and therefore no fluid exudation occurs.

3.7 Neo Hookean Hyper-elasticity

Materials which are considered to be hyperelastic have a unique feature to respond elasticity when subjected to very large strains. In the case of a hyperelastic material, the stress-strain relationship is derived from an elastic energy function which is a measure of stored energy in the material under loading. Since the material behavior is elastic, the constitutive behavior is only a function of the current state of deformation (unlike viscoelastic materials where the history of deformation contributes in the current state of stress).

ACL were modeled as a transversely isotropic hyperelastic material model assumed to be nearly incompressible (Pena, 2005). It can be represented with a strain energy function (W) which is defined as follows (Limbert, 2004):

$$W = W_{iso}(I_1, I_4) + W_{vol}(J)$$

$$W = c_1(I_1 - 3) + \frac{1}{D_1}(J-1)^2$$

$$W = c_1(I_1 - 3) + \frac{c_2}{2c_3}(exp^{c_4(I_4-1)^2} + \frac{1}{D_1}(J-1)^2$$

Where W_{iso}, W_{vol} are the isotropic and volumetric parts respectively. In these equations I_1=tr(C), $C=F^TF$ can be defined as the modified right Cauchy-Green Tensor, The incompressibility penalty function $(J-1)^2$ and D_1 was defined to be inverse of the bulk modulus .

The fibers were assumed to be extensible and uniformly distributed in the ground substance and perfectly bonded to the matrix where it is isotropic and hyperelastic. These tension tests (Pioletti, 1997) were performed on a small sample of specimens which can be difficult to develop a distribution of the material coefficients. A simple neo-hookean model was developed to estimate the variations of the soft tissue properties from structural tests. The strain energy function that was used to describe a neo-hookean model can be given with a strain energy function of:

$$W = C_{10}(I - 3) + \frac{1}{D_1}(J_e - 1)^2$$

Where, C_{10} and D_1 are material constants. ACL was described as a homogenized neo-hookean material law (C_{10}=1.95 MPa, and D_1=6.83GPa^{-1}) (Bischoff, 2008). The stiffness of ACL is determined by C10 coefficient, higher C10 values implying stiffer ACL.

3.7.1 Taylor Series

Assuming, $x=I_1 -3$, the taylor series for $\alpha e^{\beta x}$ can be determined as

$$\alpha e^{\beta x} = \alpha(1 + \beta x + \frac{\beta^2 x^2}{2!} + \frac{\beta^3 x^3}{3!} + \frac{\beta^4 x^4}{4!} + \cdots)$$

Given the values for α and β, the coefficients for the first, second and third orders are 2.951, 16.74693, and 63.3592, respectively. The coefficients for the first and second and third orders can correspond with C_{10}, C_{20}, and C_{30} ,respectively.

Numerical Modeling of the ligament:

From the use of the material properties, it is useful to represent the observed response mathematically for predictive modeling. This mathematical interpretation of the material is to develop constitutive relationships that objectively describe the interaction of stress, strain and other state variables such as strain rate and time. Neo-Hookean coefficients can be determined using curve fitting of experimental results (Abramowitch, 2004). Coefficients were curve fitting data using uni-axial mechanical testing performed by Chandrashekar, 2005 (figure 3.6).

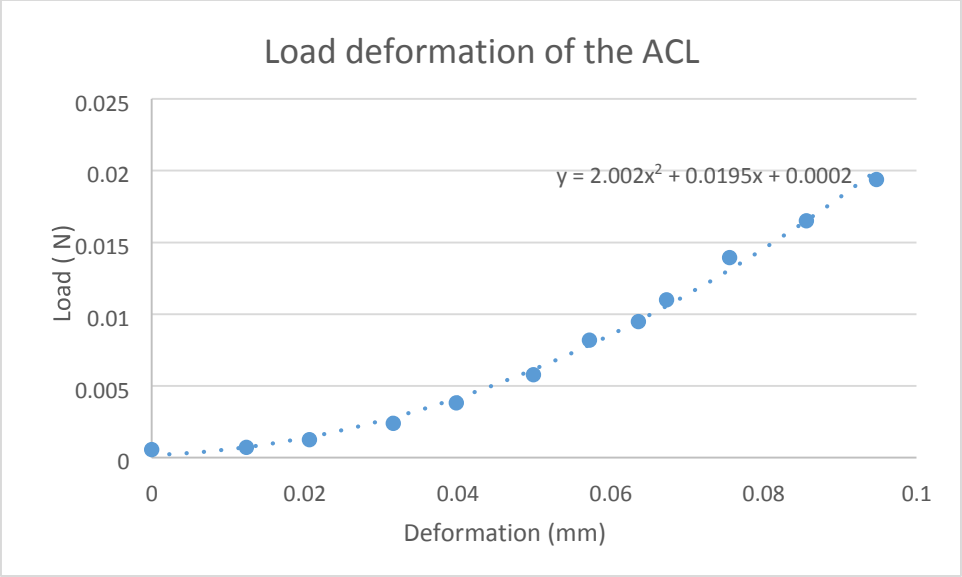

Figure 3.6: Load – Deformation of the ACL to compute C_{10} values

Material properties can be optimized using inverse FE analysis methods (Cox, 2006). An FE model be constructed in which the material properties are considered to be a variable. The simulations were performed and results from the simulation compared to data from experiments.

Another strain energy function for the ACL has been determined (Veronda, 2001).

$$W_e = \alpha e^{(I_1-3)} + C_1(I_2 - 3)$$

Where α=0.26, β=11.35 and C_1 =-1.49.

3.7.2 Anisotropic Modeling

Anatomic representations of the knee ligaments with anisotropic hyperelastic properties will result in more realistic kinematics. Knee cruciate and collateral ligaments were

modeled as incompressible anisotropic hyperelastic structures using the Holzapfel-Gasser-Ogden (HGO) material model (Gasser, 2006). HGO model is a hyperelastic, anisotropic material model that was developed to model the criss-crossed fibrous soft tissues like the illiac adventitia (Shepard, 1999). Briefly, isotropic non-collagenous ground matrix is modeled by the incompressible hyperelastic neo-Hookean component of the strain energy density (SED) function, whereas the transversely isotropic fibrous component is modeled by the following function developed by Gasser *et al*. (2006):

$$\bar{\varphi}(\bar{C}, H_i) = \overline{\varphi_g}(\bar{C}) + \sum_{i=1}^{2} \varphi_{fi}\,(\bar{C}, H_i(a_{oi}, k)$$

Where ψ_g and ψ_{fi} defined to represent the isotropic and anisotropic components, respectively. A_0 can be defined as being the mean orientation of the fibers. A statistical function allows for a spatial distribution of the orientation of the fibers.

Chapter 4: Gait Cycle

4.1 Gait cycle

The knee is a complex synovial joint in the human body and can withstand as high as 7 times body weight. For example, an average jogger can undergo 16,000 impacts per week. Each individual has a unique gait. A person's gait can be affected by injury and disease process. The gait cycle is a time interval or sequence of motion which occurs from heelstrike to heel strike of the same foot. This cycle can be divided into distinct phases: stance phase and swing phase. The stance phase can be described as the time in which the foot is on the ground.

The stance phase generally occupies approximately 60% of stride and consist of periods of double limb support. This support has been defined as the moment when the contralateral foot is in contact with ground. This phase can be divided into 6 subsections. The first section, initial contact, is the time when foot makes contact with ground. Loading response is the time when the sole of the foot is in contact with floor and subsequently the body weight is supported by the supporting limb. The next phase, midstance, is the period of time when the tibia rotates in the direction of motion. During this phase, body weight is supported by a single limb is approximately 10-30% of the stride. The last section of this phase, terminal stance, is the time in which the weight of the body is transferred from the hind foot and midfoot regions onto the forefoot. A

transition phase exists between the stance and swing phase which is known as preswing. During this transition phase, body weight is supported by the contralateral limb as the body prepares for the swing phase.

Swing phase typically covers the last 40% of the gait cycle, and is divided into three periods. The three periods of the swing phase are known as initial swing, mid swing, and terminal swing. The initial swing phase occupies approximately a third of the swing phase which can be described from the toe off until the swinging foot is opposite to stance foot. Mid swing phase can be defined as the time when tibia is vertically oriented.

In addition to the gait phases, there is also some common parameters that exist with gait. Those parameters are stride length, cadence and velocity. The stride length can be defined as the distance covered in one gait cycle. Cadence is defined as the number of steps per unit time. The velocity uses both stride length, and cadence to determine the distance covered per unit of time.

There are structural differences between males and females. Women have a larger hip width to femoral length ratio which result in greater hip adduction. Increased angle in the femur result in higher valgus among women (Benas, 1984). It has also been observed that females exhibit increased hip internal rotation when compared to males. The anatomical differences in females including increased hip adduction, hip internal rotation and valgus of the femur explain the larger Q angle that is observed in females

(Livingston, 1998). The increased Q angle can play a role in the incidence of patellofemoral disorders which have been observed among females (Almeida , 1998). The anatomical differences which females exhibit at the hip and knee can here explain differences in the gait patterns among females. There have been a few studies which have investigated differences in lower extremity mechanics during walking among genders. Even though some studies have concluded there is no difference in the ground reaction forces (GRF) among genders (Keller, 1996). However it is also been shown that females exhibit greater vertical GRF when compared to males (Li, 2001). During walking, it was observed that females have greater hip flexion angle than compared to males (Kerrigan, 1998).

4.2 Anatomical Considerations:

During the gait cycle, the various joints in the body undergo various movements. For example, the hip joint can move in three axis; flexion-extension, adduction-abduction, and internal-external rotation. It has been observed that the flexion-extension movements are of the highest amplitude when compared with other movements. It is of a coordinated effort from all axis develop typical gait pattern in the hip and other joints.

The knee joint typically move with three degrees of freedom of angular rotation during gait. The key player would be flexion and extension movement. Typically, the knee generally be flexed to a maximum of 70 degrees during the course of the gait cycle (figure 4.1).

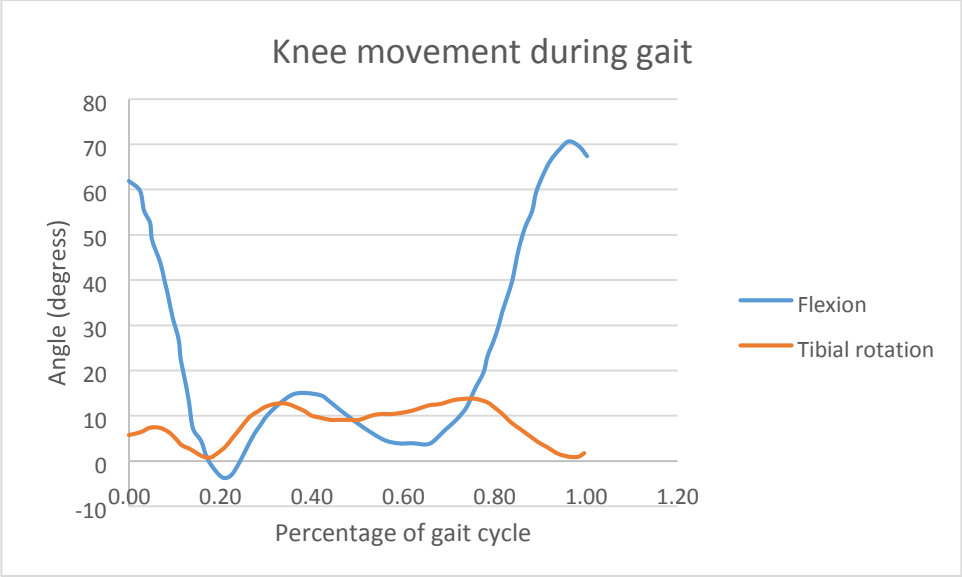

Figure 4.1: Knee Movement during gait

During the gait cycle, there is some amount of internal and external rotation of the tibia which can occur. As seen in figure 4.1, the tibial rotation is of a lesser amplitude which is due to soft tissue and bony constraints that restrict the motion.

4.3 Loading of ACL with respect to gait

In order to have a better understanding of ACL injury mechanisms, it is imperative to determine in-vivo ACL forces. There have been in-vitro studies which have measured the forces on the ACL as a result of various loads applied to the knee (Li, 2006). Each of the in-vitro studies had used different measurement techniques such as buckle transducers (Ahmed, 1992), implantable pressure transducers (Claes, 1985), and robotic techniques (Li, 2004). The loads applied on the ACL were determined by anterior tibial loads (Li, 2004), simulated muscles loads (Claes, 1985) and rotational moments to the

knee joint (Fleming, 2001). However, the loads on the ACL can actually be higher during in vivo activities than the forces measured in vitro studies (Nagura, 2002). The loads that are applied in vivo are higher in order to simulate more physiological conditions. In addition, in vitro studies rarely had used the contribution of the other surrounding structures such as muscles which can determine loading in the knee.

The force on the ACL can be determined by five forces; patellar tendon force (quadriceps), hamstring force, gastrocnemius force, tibio-femoral contact force, and knee ligament force. The largest forces that are applied at the knee were caused by vasti and gastrocnemius. The peak forces were 1188 N and 849 N caused by vasti and gastrocnemius, respectively, during the contralateral toe off. The force that is applied on the ACL can be due to a balance of muscle forces, joint contact forces, and ground reaction forces which all result in a shear force on the knee. The patellar tendon, gastrocnemius and tibiofemoral contact forces develop an anterior shear force on the knee. Similarly, the posterior shear forces are due to hamstring and ground reaction forces. The ACL is often loaded when the resultant shear force is anteriorly directed. Early in the stance phase, the shear force caused by patellar tendon be a major force in resultant shear force on the tibia, thus the maximum force is applied on the ACL. Shear forces caused by the patellar tendon is directly related to quadriceps because of the anatomical location of the patellar tendon. During late stance phase, the posterior component of the ground reaction forces are equal to the sum of anterior shear forces

caused by patellar tendon, gastrocnemius, and tibiofemoral contact results in the ACL loads to be small.

ACL force can be estimated using a linear equation (Kanamori, 2001).

$$F_{ACL} = F_{AP} + 2.5 * |M_{VV}| + 8 * |M_{IE}|$$

Where F_{AP} is defined as the anterior-posterior joint load calculated from sagittal plane joint reaction and muscle forces, M_{VV} and M_{IE} are the varus-valgus and internal-external joint moments respectively.

4.4 Gait analysis differences gender (Knee Joint)

The walking patterns among genders are different due to differences in the skeletal dimensions. Females often walked with shorter step lengths, but with a greater cadence when compared to their male counterparts. Differences in the walking speed can be explained by the differences in skeletal size. However, there is no difference in the pace of walking among the genders.

Gender differences in a healthy population has shown conflicting results in regards to kinetic and kinematic parameters of gait. Some studies indicate that there are no gender differences in the knee joint kinetics, while another study had reported different kinematics between genders during gait.

4.5 Methods for gait analysis

A number of methods to measure various gait characteristics including stride analysis, angular kinematics, force plate and foot pressure analysis, and electromyographic (EMG) analysis are available in literature. To measure stride, simple instruments such as stopwatch used to measure temporal sequence of stance and swing phase. Angular kinematics can be measured by using electrogoniometers which are attached to body segments to directly measure angular displacement. In the case of the lower extremity, two markers are placed on the right and left anterior superior iliac spines (ASIS), as seen in figure 4.2. The position of markers (2 cm in diameter, weighing approximately 4.4g, developed in this study) and was selected to satisfy the rigid body assumption as well as other practical requirements (Cappazzo). Two markers are placed on the right and left anterior superior iliac spines (ASIS). One other marker is placed on a stick 10 cm long extending from the top of the sacrum (L4-L5) and in the spinal plane. It is stabilized by a flexible triangular plate attached to the body with an elastic belt. Four other markers are placed on the following locations of the particular limb under consideration: greater trochanter, directly lateral to the estimated average axis of rotation of the knee joint, lateral malleolus, and space between the second and third metatarsal heads.

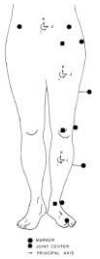

Figure 4.2: Marker configuration and its coordinate systems (Kadaba, 1990)

The art of walking is a complex activity in which it utilizes a joint coordination of various muscles, bones and joints of the lower limbs. The use of various gait analysis be able to reveal defect which are normally difficult to ascertain with ordinary observation and physical examination. It can provide valuable information in patients with complicated neuromuscular disorders such as cerebral palsy, muscular dystrophy, myelomeningocele, arthritis, and traumatic brain injury.

A digital video system is used to retain a permanent visual record of the patient's gait pattern. This equipment allows slow-motion viewing of the patient from front and side. The Vicon three-dimensional movement analysis system uses five cameras to follow the precise position of markers attached to the patient (figure 4.3). With the use of the force plates, the ground reaction forces are determined based on the foot landing on the floor. These data are combined to calculate the various loads acting on the joints and muscles, and their corresponding movements. The computer, using advanced software, constructs a model of the patient's musculo-skeletal system.

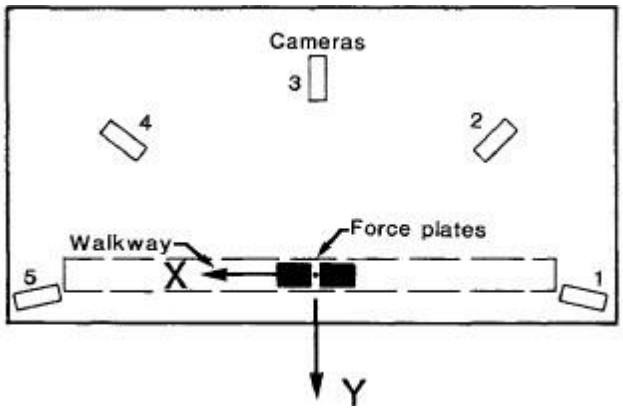

Figure 4.3: Schematic drawing of gait under controlled environment

Chapter 5: Experimental Methods

5.1 Subjects

5.1.1 MRI Retrospective study

After receiving approval from the Miami Valley Hospital institutional review board, the surgery records for knee procedures taking place at Miami Valley Hospital of two full-time orthopedists were reviewed from 2006-2013. Patients having knee procedures were tagged and further investigated to find if they had received an MRI during their diagnostic workup. The study group consisted of patients whose ACL was torn or partially torn based on the radiologists' impression from the MRI. The control group was made of patients whose ACL was described as intact, however patients were still included in the study if pathology other than an ACL tear or partial tear was discovered. Therefore the study group consisted of 32 patients and 40 patients in the control group. All MRI scans were performed on a 1.5 Tesla General Electric (Milwaukee, Wis.) Signa MRI scanner. T1-weighted images in 4mm-thick cuts were evaluated based on the integrity of the image.

The average age of the patients who had ACL injuries was 32 years, and the age range was 12 to 59 years. The control group (group 2) consisted of 40 patients (28 males and 12 females). Of the patients with intact ACLs, the average age was 35 years, and the age range was 12 to 76 years. There were no significant differences in the average ages, genders, sides of injury, injury mechanisms, or average BMIs of the study and control

groups. The average BMIs of the study and control groups were 29 and 28 years, respectively. Clinically, malnutrition has been defined as a BMI less than 14. Therefore, for the patients considered in this study, the fat tissue was not influenced by nutrition. Group matching was performed according to the following factors: gender, age, injury mechanism, and BMI.

5.2 Anatomical measurements

MRI measurements were digitally obtained using IDX Imagecast iPACS Viewer developed by IDX Systems Corporation tools used to position and tracing the length of the object being measured. The femoral condyle width and the notch width measurements were taken in the same T1 coronal cut, which together form the Notch Width Index (NWI) (Figure 5.1). This method was reproduced as described by Domzalski et al. (2010), which defines the NWI as being a ratio of the width of the intercondylar notch at the level of the popliteal groove to the bicondylar width at the same level. The sagittal ACL measurements of width and length were taken in the cut in which the full length of the ACL was in view (Figure 5.2). This value was extrapolated in the MRIs containing an ACL tear or partial tear. The sagittal ACL width was measured at the midpoint. The coronal ACL width was measured in the slice in which the ACL crossed the posterior cruciate ligament (PCL), in which the ACL midsubstance could best be visualized (Figure 5.3).

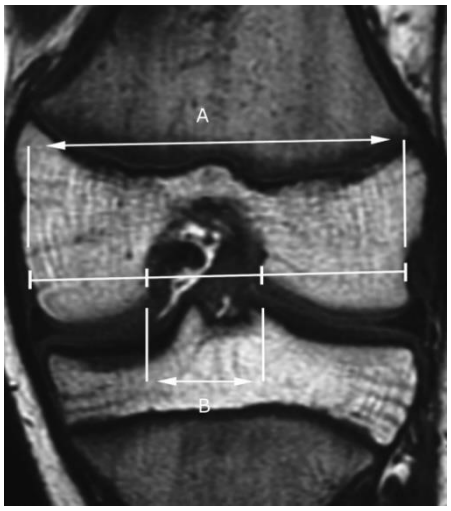

Figure 5.1: Measurement of notch width index using MRI (Domzalski, 2010)

A.  B. 

Figure 5.2: Measurement of sagittal ACL width (solid white line), taken at the midsubstance, and measurement of sagittal ACL length (dashed white line) from femoral to tibial attachment sites. Sample from control group in panel A and sample from study group in panel B.

A.  B. 

Figure 5.3: Measurement of frontal ACL width in control (A) and study (B) groups

Notch Width Index (NWI) = femoral notch width /femoral condyle width (**Eq 5.1**)

Data was statistically analyzed using Chi-square tests and one-way Anovas. A p value less than 0.05 was considered statistically significant.

5.3 Diagnostics/Fat Pad

The infrapatellar fat pad is bounded anteriorly by the patella and posteriorly by the synovial-lined knee joint (figure 5.4) (Dragoo, 2012). It is made up subcutaneous tissue that contains a network of fibrous cords. It consists of columns of fat that are confined in small chambers of fibrous connective tissue (Skiadas, 2013). These columns are often reinforced by a network of transverse and diagonal elastic fibers that connect the outside walls of the sepate (Han, 2014). This fat tissue is not influenced by nutrition, and therefore, the size and volume of the fat pad vary widely among individuals. The fat pad is often metabolized only in cases of severe malnutrition (Ballegaard, 2014).

Anterior knee pain is often caused by an impingement between the patellofemoral or femorotibial joints due to edematous changes in the infrapatellar fat pad (Collins, 2012). Because of the anatomical location of the infrapatellar fat pad, a patient with an anterior cruciate ligament (ACL) injury can suffer a subsequent injury to the infrapatellar fat pad (Alentorn-Geli, 2009). This phenomenon occurs in a torn ACL, which produces instability in the knee that can then cause posterior femoral translation with respect to the tibia (Agel, 2005) Instability of the knee joint due to an ACL injury can generate patterns of lesions in the infrapatellar fat pad. Common injuries to the infrapatellar fat pad include edema, tears, scars, and synovial proliferation (Dragoo, 2012). Edema can be defined as an increased signal intensity within the fat pad detected by magnetic resonance imaging (MRI) (Agel 2005; Dragoo 2012). In a retrospective study of 100 patients with ACL injuries, edema was found in 48% of patients with torn ACLs but just 24% of patients with intact ACLs (Agel, 2005).

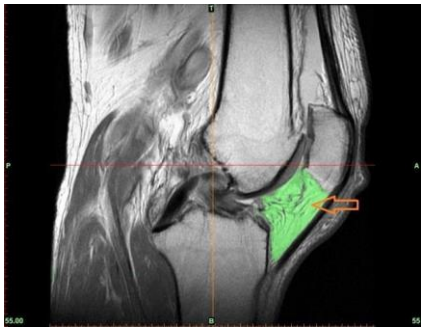

Figure 5.4: Sagittal view from a T2 MRI. The arrow points to the location of the infrapatellar fat pad.

5.3.1 Volumetric analysis of the fat pad

The infrapatellar fat pad volume was measured from axial-plane images using three-dimensional (3D) reconstruction software (Mimics, Materialise Inc., Belgium). The MRI images were imported into the software using the threshold segmentation algorithm to select the region of interest. The "Edit mask in 3D" option in Mimics was used to construct the infrapatellar fat pad based on prior knowledge of human anatomical data. Figure 5.5 shows a 3D reconstruction of an infrapatellar fat pad used in the analysis. The cross-sectional area of each slice was measured by the software using a region-growing strategy based on the pixilation threshold. The volume of the 3D reconstructed image can be determined using the software and also using an ellipsoidal approximation expressed by the following equation (Chuckpaiwong, 2010):

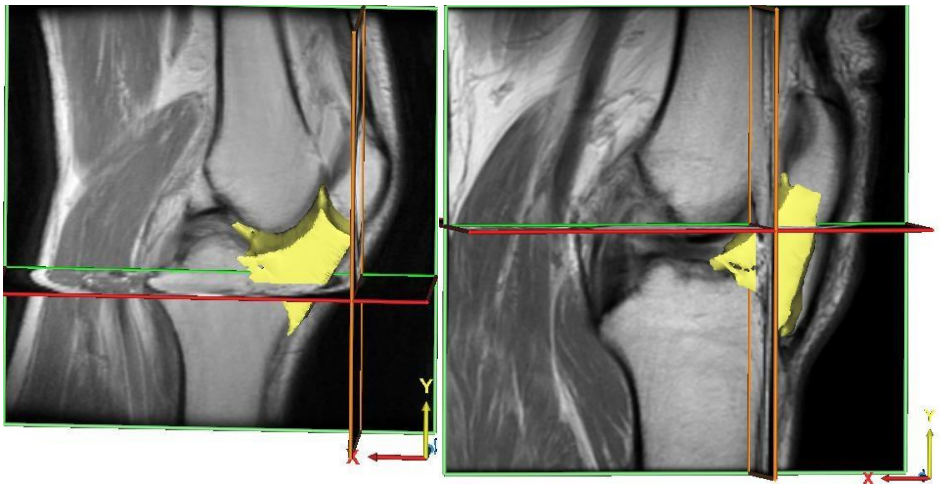

Figure 5.5: 3D reconstruction of the fat pad used for analysis. The left panel is the infrapatellar fat pad in a patient with an intact ACL. The right panel is an infrapatellar fat in a patient with a torn ACL. In both panels, the X axis is the anterior–posterior view, and the Y axis is the superior–inferior view.

$$Ellipsoidal\ volume = \left(\left(\frac{Height}{2}\right) * \left(\frac{width}{2}\right) * \left(\frac{depth}{2}\right) * \left(\frac{4}{3}\right) * \pi\right) \quad (\boldsymbol{Equation\ 5.2})$$

The height, width, and length were determined based on measurements taken from the 3D images (figure 5.6).

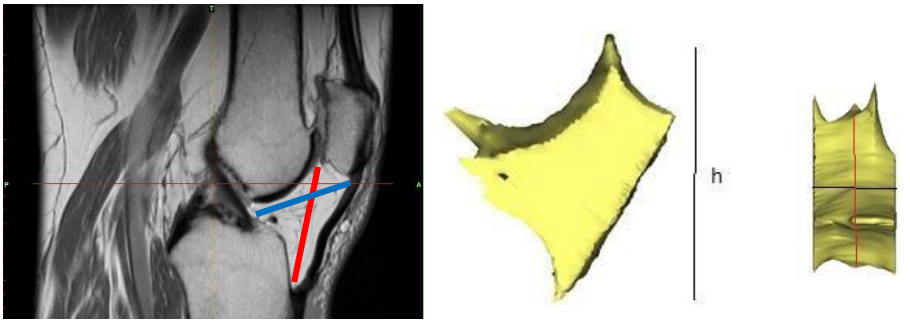

Figure 5.6: The annotations for measuring the fat pad for ellipsoidal calculation. The red line indicates the width, and the black line indicates the depth, as seen in the right panel.

The infrapatellar fat pad volume was also determined using a MATLAB (Mathworks, Inc., Natick, Massachusetts, USA) software code. All of the axial slices from the tibial tuberosity to the slice before the inferior patellar pole were used. A manual trace of each slice was performed to define the region of interest (ROI) (figure 5.7a). The ROI is a portion of the image that allows the image to have a filter. The ROI creates a binary mask in which the pixels that define the ROI are set to 1 and the others are set to zero. This binary mask was modified so that the pixels that define the ROI were set to 1 and placed within the image (figure 5.7b). A semi-automated process was then used to determine the area of the region (figure 5.7c). Once the tracing was input by the user, the area was

determined based on the MATLAB function, which determines the total number of pixels found within the region. The volume was calculated based on a planar summation multiplied by the slice thickness.

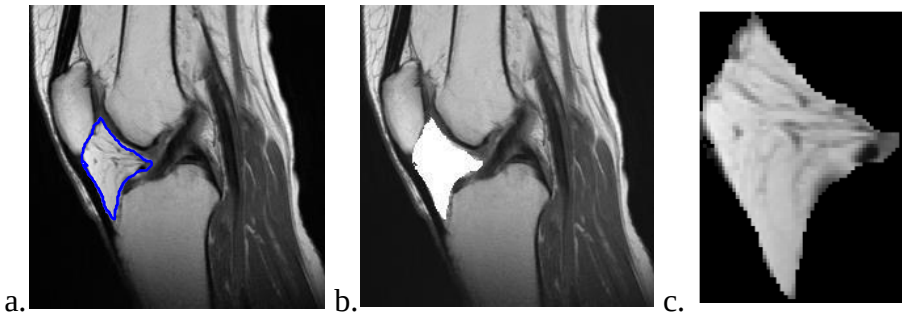

Figure 5.7: Gray-scale image used in the MATLAB program. (a) The blue line represents the user-input trace. (b) The ROI removed from the 2D MRI slice is shown. (c) The infrapatellar fat pad removed from the slice to measure its area is shown.

5.3.2 Statistical analysis

Statistical analyses were performed using JMP 7.0 (SAS institute, 2007). The significance level was set to $P < 0.05$. Differences between the two groups were assessed using independent-sample t-tests. The mean volumes and surface areas of the fat pads of the control patients and the patients with acute ACL injuries were compared using two-tailed t-tests. BMI was treated as a continuous variable.

The methods used to determine infrapatellar fat pad volumes were assumed to be independent in their methodologies. Bland–Altman plots were used to evaluate the methods for measuring fat pad volumes with a high degree of accuracy.

5.4 Biomechanical Evaluation

5.4.1 Finite element modeling

5.4.1.1 Model development

Following IRB approval, computerized tomography (CT) and magnetic resonance imaging (MRI) scans on 24 patients (6 adult males and 6 adult females) were used to capture bony and soft tissue geometry respectively. Scans were obtained while the subjects were supine with leg in an unloaded and neutral position. 3D geometry of the femur and tibia were reconstructed from CT images in all three anatomical planes. 3D geometry of the ACL was constructed from MR images in all three planes. These geometries were then converted into solid 4 node tetrahedral elements and imported into ABAQUS FE package v 6.10 (SIMULIA, Providence, RI USA) to generate FE model (Figure 5.8). The mesh was refined in such a way that the results get converged to less than 5% difference.

Figure 5.8: 3D FEA model of the knee

The mesh was refined in such a way that the results get converged. Von Mises stress of the ACL for each load under different mesh sizes are provided in figure 5.9. For all of the loads the optimized global size was found to be 0.095, which is quite smaller than previous works. In the literature, the size of the global size was approximately two times larger, as well as had used hexahedral elements. The key difference is the elements which are used to construct the ACL. The elements that were used in this study had consisted of tetrahedral elements. In general, tetrahedral elements would allow the results more closely to that of theoretical ones. In addition, the mesh was refined in such a way that the results get converged to less than 5% difference which allowed for more accurate results. Therefore it is important that the ACL to be modeled with tetrahedral elements.

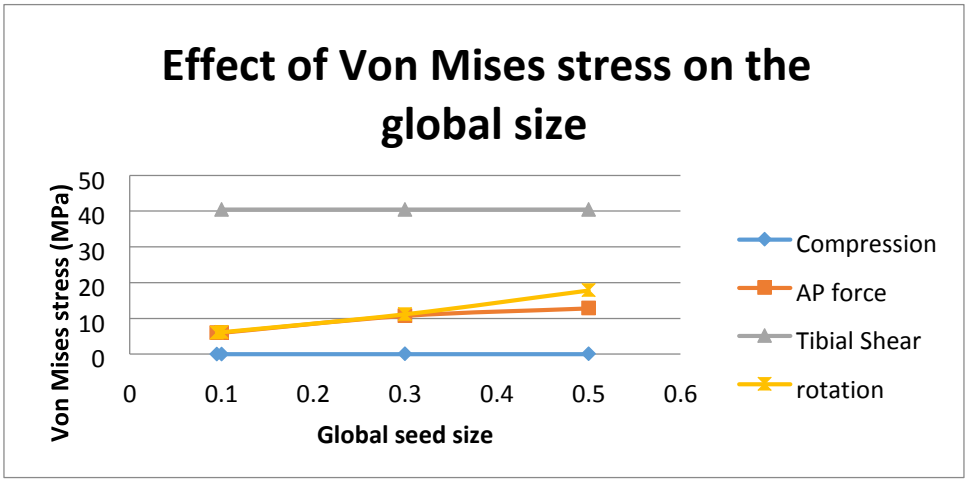

Figure 5.9: Effect of Von Mises stress on the ACL with respect to global seed size.

5.6.1.2 Boundary and Load Conditions:

The tibial origin is located on the tibial axis that can be found between two intercondylar eminences. The femoral origin can be located on the distal bony point midway between the femoral condyles. The proximal –distal translation was along the axis which had passed between through the tibial origin. The medial-lateral translation can be defined as parallel to the femoral transepicondylar line. The varus-valgus, internal-external and flexion-extension rotations were defined along the axis 'x', 'y', and 'z', respectively.

In order to simulate clinical testing, the boundary condition of this joint model was defined as follows: femur fixed in all degrees of freedom and tibia was free to move in all directions.

Visco step with a time period of one gait cycle was selected for analyzing the Von Mises Stresses in the ACL under three loading conditions. Three different loading conditions a) Axial Force, b) internal/external rotation, and c) Anterior/Posterior force observed during a person's gait cycle were selected to determine the stresses developed on the ACL (figure 5.10). Axial force was applied on the proximal surface of the tibia. In case of rotation loading, a reference point was created above the center of the distal surface of the tibia and a coupling constraint was defined in such a way that the torsion in tibia was simulated by applying moment with a rotation angle that was observed during gait. Anterior/posterior force was applied on the frontal surface of the tibia. Anterior shear force of a 100 N was applied onto the tibia.

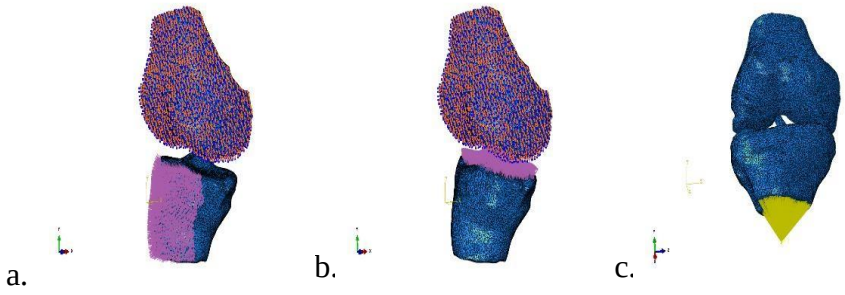

Figure 5.10: The (a) panel is the Anterior/Posterior force which is acting on the knee joint during gait cycle. The (b) panel is the compression force which is acting on the knee joint. The (c) panel is the tibial rotation.

During the gait cycle, the knee joint experiences three forces; compression, anterior tibial load, and tibial rotation (Figure 5.11). Compressive and anterior tibial loads are expressed in terms of multiples of body weight, where it reach as high as 4 and 0.17 times, respectively. During the gait cycle, the tibia rotates to a maximum of 15 degrees. The loading data obtained from both these studies was used to simulate the mechanical environment in the knee joint for measuring the Von Mises and contact stresses developed in the ACL under the applied boundary conditions.

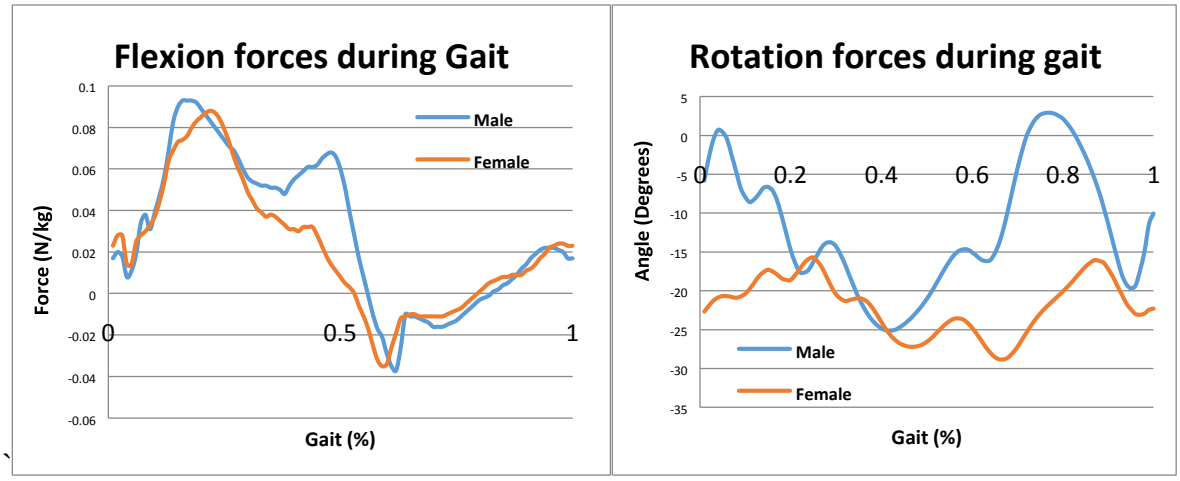

Figure 5.11: Loads and rotation applied on the knee joint during gait

The stress analysis was conducted in this study were the Von Mises stress across the ACL. Changes in the Von Mises and contact stress values w.r.t applied load across the entire gait cycle were determined by measuring the maximum stress values at each 0.01 increment of the gait cycle (normalized). Average Von Mises stress across the ACL was determined by averaging the sum of maximum stress values observed in the corresponding elements of the ligament during the entire gait cycle.

Based on the analysis conducted in this study surface, sub-surface, cross-sectional Von Mises across the ligament were derived. Surface stresses include only the stresses that are observed on the outer surface layer of the liner component and stresses inside the ligament were obtained by cross-sectioning the ligament axially into thin slices. Changes in the Von Mises and contact stress values at each 0.01 increment of the gait cycle (normalized) w.r.t applied load were determined by measuring the stress values in the element that shows

maximum stresses at the point of maximum load. Average Von Mises and contact stress values across the ligament were determined by averaging the sum of maximum stress values observed in all the corresponding elements of the ligament during the entire gait cycle.

5.4.2 Gait Analysis

Participants

A cross-sectional subset of participants from the Fels Longitudinal Study (FLS) was selected for inclusion in the present study. The FLS is the currently the world's largest and longest-running longitudinal study of human growth, development and aging (Sherwood and Duren, 2013). Participants are primarily of European descent and live mainly in or near southwest Ohio. The FLS is a study of normal population variation, since participants are/were not recruited on the basis of any health condition or disease.

To be included in the present study, FLS participants had to have at least one gait analysis test in our database, between the ages of 21 and 50 years at the time of testing to exclude gait variation due to growth or aging. To ensure that the present analysis included only people with normal gait, participants were excluded for obesity (BMI > 30.0); chronic musculoskeletal conditions; acute lower limb, pelvic, or vertebral skeletal or soft tissue injury ≤ 1 year prior to testing; toe-walking; or prescription shoe inserts. If participants had more than one gait test in the database, only the most recent available and eligible test was included. This resulted in a cross-sectional sample of 178 participants, including 79 males and 99 females.

Data collection

All data collection occurred at the Lifespan Health Research Center (LHRC), Wright State University. All study procedures were approved by the Wright State University Institutional Review Board, and each participant gave his or her informed consent prior to any testing.

Anthropometric measurements were taken using standard methods (Lohman et al., 1988) on barefoot participants wearing light clothes, and included stature, body weight, sitting height, and bicristal breadth; BMI was determined from weight and height; subischial leg length was calculated as: height – sitting height.

Gait analysis occurred in the LHRC's Motion Analysis Laboratory, equipped with six highspeed Hawk cameras (Motion Analysis Corp., Santa Rosa, CA) synchronized with three force plates embedded in a 15m walkway (two AMTI OR6-7-1000, Advanced Medical Technology, Inc., Watertown, MA; one Kistler Type 9281B11, Kistler Instruments, Winterthur, Switzerland). External passive reflective markers were placed on joints and body segments (Helen Hayes system: Kadaba, 1990) and motion capture was performed using EvArt software (Motion Analysis Corp., Santa Rosa, CA). Five-second static trials were recorded with the participant standing, feet shoulder-width apart and arms spread laterally. Walking trials at self-selected speed (wearing socks) were then recorded for each participant. The three best trials (clean force plate strikes and high-fidelity marker recognition) were selected, and each participant's average values across those three trials

were derived for analysis. Data were processed in OrthoTrak software (Motion Analysis Corp., Santa Rosa, CA) with hip joint centers calculated as offsets from anterior superior iliac spine (ASIS) and sacral markers. Spatiotemporal variables were normalized for subischial leg length (Hof, 1996), and step width was normalized to base of support as: bicristal breadth / step width (Sutherland et al., 1988). Kinetic variables were calculated form inverse dynamics and normalized for weight. The moments described here are external moments. Data were for the most part analyzed as averages combining both limbs, but inter-limb asymmetries were also assessed.

Statistical analysis

All analyses were performed using SAS version 9.2 (SAS Inc.,Cary, NC, USA), and were twosided with a = 0.05 as the significance level. Sexes were analyzed separately. Gait variables were normalized by expressing temporal measures as percentages of a single gait cycle, adjusting spatial measures for lower limb length, and calculating base of support by dividing bicristal breath by step width [5, 17, 18]. These transformations removed the effects of lower limb length as a confounder of age effects, since, at any age, lower limb length influences raw values of gait parameters.

5.4.3 Collagen distribution

Mechanical properties of various soft tissues are dependent upon the structural components. The ACL are often shown to be non-homogenous structures with respect to

its collagen distribution. The collagen distribution is often dependent upon the age of the individual. In the elderly, the fibril concentration would increase to as high as 50% of the ACL which is approximately twice as high when compared to younger population (Strocchi, 1996). This increase in the concentration may explain a possible mechanism in which the ligament being more pliable.

In this dissertation, the concentration of collagen in the ACL was assumed to be 15%, 20% and 25%, that is commonly seen among younger individuals. The load-displacement curve for this amount of fibrils can be seen in figure 3.4. The C_{10} that is used in this dissertation was determined by coefficients of the curve fitting of its load-displacement curve.

5.4.4 Monte Carlo Simulations

A series of Monte Carlo simulations (n=2000) was generated to investigate the effect of force and anatomical features during gait. The anatomical features used were NWI, AP width, sagittal width and sagittal length. The random numbers were generated on these parameters assuming a Gaussian distribution with means and standard deviations derived from a retrospective database of 40 patients with intact ACL. Random numbers on the forces were generated assuming a Gamma distribution. The distribution of forces is seen in Figure 5.12.

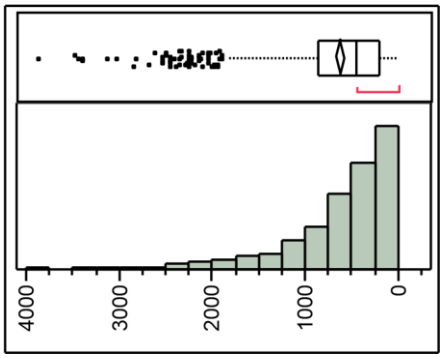

Figure 5.12: Distribution of forces using Monte Carlo Simulations (N=2000)

The purpose of this study was to use the multiplanar imaging and soft tissue visualization strengths of MRI to measure dimensions of the knee joint. The measurements were analyzed to determine whether significant relationships exist between demographic variables, width and length of the ACL, NWI, and ACL injury. Additionally, Monte Carlo simulation technique was used to generate representative random numbers from the population to conduct the risk of ACL injury and comment on the injury risk for a larger population (n=2000).

Chapter 6- Results

6.1 *Subjects*

This dissertation had utilized subjects based on two methods: MRI database and FELs Gait Data. The MRI database had consisted of patients who have undergone MRI between 2006 and 2013. Patients were selected based on surgical records for knee procedures performed by two full-time orthopedists. Fels gait data was based on a subset of patients part of the Fels Longitudinal Study. Fels Longitudinal study was founded in Yellow Springs, Ohio in 1929. The purpose of the Fels study is to focus on physical growth, skeletal maturation, body compositions, risk factors for cardiovascular disease and obesity, skeletal and dental biology, longitudinal biostatistical analyses and aging.

The scope of this dissertation is to better understand the mechanism for ACL injury. Therefore, subjects that are mainly healthy volunteers and their gait behavior studied further. In the retrospective portion of this study, there were 40 patients that were undergone MRI from 2009 to 2013. Similarly, a sample from the Fels gait data was a larger subset which consists of 178 healthy volunteers, out of which 99 were females and the remaining were males. However the average age in both of portions were the same at 35 years of old (Table 6.1).

	# males	Females	Avg. age
Retrospective	28	12	35
FELs Gait data	79	99	35

Table 6.1: Population demographics among healthy individuals

6.2 Anatomical Measurements

6.2.1 MRI retrospective study

The demographic information is presented in Table 6.2. The mean age of the study population was 32±11 years old (range 12-59) and for the control group the mean age was 35±15 (range 12-76). There were no significant differences between the gender, side of injury, mechanism, or BMI between study and control groups. A cutoff of 25 was used to separate the BMI between those of normal weight (BMI <25) and those who are overweight and obese (BMI ≥ 25).

Demographic		Study (#)	Control (#)	Test Variable	P Value
Total number of cases		32	40		
Gender	Male	21	28	Chi = 0.157	0.801
	Female	11	12		
Side	Right	15	22	Chi = 0.640	0.479
	Left	17	17		
Age	Average (years)	32	35	T = -2.082	0.43
	Range (years)	12-59	12-76		
Mechanism	Contact	12	9	Chi = 2.761	0.100
	Noncontact	14	26		
	Unknown	6	5		
BMI	< 25	8	11	Chi = 0.164	0.692
	≥ 25	14	19		
	Unknown	10	10		

Table 6.2: Demographic data for the MRI database

MRI measurements were compared between torn and non-torn individuals, males and females, and those of normal weight (BMI <25) and those who were overweight and obese (BMI >25) (Table 6.3). The length of the ACL in the sagittal plane was significantly different between males and females ($p = 0.000$). The NWI was also significantly different between torn and non-torn individuals ($p = 0.035$). However, the NWI was not significantly different between genders ($p=0.40$).

	Gender		P Value	BMI		P Value
	Female	Male		<25	≥ 25	
APW	6.82	7.07	0.603	7.29	6.92	0.535
SW	6.77	6.81	0.946	6.38	6.98	0.409
SL	34.98	40.17	0.000*	37.53	39.33	0.238
NWI	0.27	0.26	0.69	0.26	0.27	0.418
Standard deviation	0.03	0.03		0.03		

Table 6.3: Comparison of anatomical measurements between various groups

6.3 Diagnostics/Fat Pad

A summary of the results are shown in table 6.4. There is a strong correlation between the volumes determined by ellipsoidal model and MRI. It was determined that the coefficient of determination to be 0.9966. The volume estimated by MATLAB was found to be within a band of ±x2 MRI values (27.29 mm^3; R^2=0.647) and may be considered with high statistical confidence. No significant difference was observed between the two groups (p of 0.87 and 0.83) for ellipsoidal and MATLAB respectively (Figures 6.1a and 6.1b).

Group	Thresholding	Equation	Tracing
Study:	36.16	36.32	37.85
Control	23.79	23.76	24.99
Standard Deviation	13.75	13.37	13.24

Table 6.4: Comparison of volume determinations with respect to various methods.

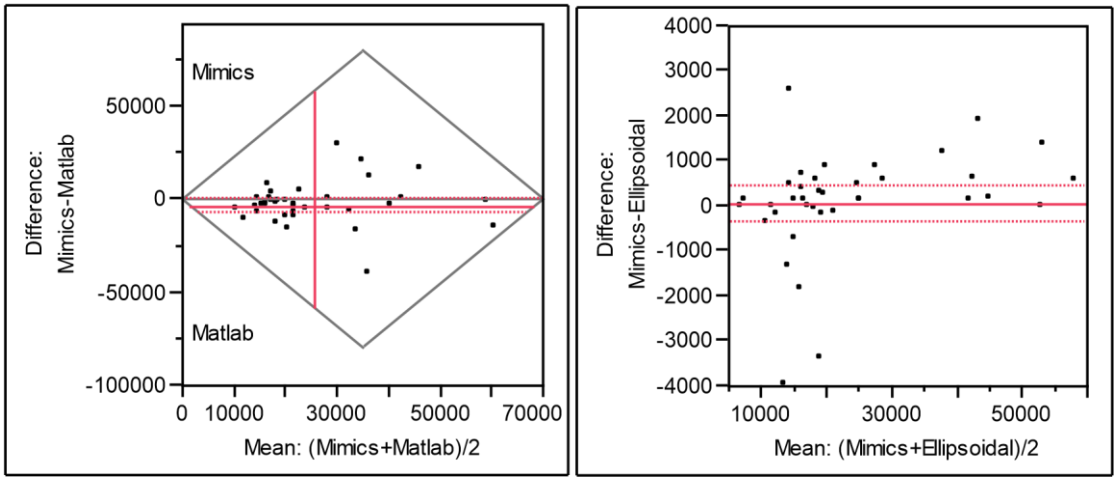

Figure 6.1: Comparison of the volume determined by various methods

Significant differences were observed in the mean volume of the fat pad of the knee between patients with an intact ACL and those with acute ACL injury (table 6.5). Significant differences were also seen in the mean surface area of the fat pad of the knee between the two groups.

Characteristic	Study	Control	P value
Volume (mL)			
Mean	36.160	23.788	0.010
Range	12-85	11.6-52.8	
Standard Deviation	21.7	13.7	
Surface Area (mm^2)	9868.07	7685.88	0.041
Range Surface area (mm^2)	4287-17693	4403 - 19750	
Standard Deviation	4560		

Table 6.5: Volume comparison between two groups

6.4 Biomechanic Evaluation

6.4.1 Finite Element Modeling (FEM)

Four different types of loads were applied to the knee models and the corresponding stresses in the ligament were obtained. Cross-sectional and gross (stresses observed across the entire ligament) stress values of respective knee models and their loads applied are provided in table 6.6.

Model	Elastic		Hyperelastic		Viscoelastic	
	Males	Females	Males	Females	Males	Females
Maximum Cross-sectional Von Mises Stress (MPa)						
Compression	0.258	0.258	0.0689	0.211	0.0807	0.0789
Rotation	154	118	6.68	11.48	12.67	9.89
Anterior tibial	146.22	146.22	6.044	5.79	7.26	6.92
Tibial shear	36.62	36.62	28.5	32.32	25.653	24.4
Maximum Gross Von Mises Stress (MPa)						
Compression	0.258	0.258	0.0689	0.211	0.0807	0.0789
Rotation	154	118	6.68	11.48	12.67	9.89
Anterior tibial	146.22	146.22	6.044	5.79	7.26	6.92
Tibial shear	36.62	36.62	28.5	32.32	25.653	24.4
Average Gross Von Mises Stress (MPa)						
Compression	0.0124	0.0124	0.00404	0.0105	0.00477	0.00469
Rotation	18	13.8	1.68	3.32	3.09	2.62
Anterior tibial	29.26	29.26	1.27	1.21	1.39	1.34
Tibial shear	4.96	4.96	2.59	2.47	4.29	4.16

Table 6.6: Maximum and Average Von Mises stress data under various loads

Based on the obtained results it can be observed that the hyperelastic ACL model from the male knee have shown lower Von Mises stress values (cross sectional and gross stresses)

under compression, rotation, and AP tibial loading conditions. In both males and females, tibial shear loads had resulted in the highest Von Mises stress values (cross sectional and gross stresses). Among all modeling techniques and genders, the ACL as an elastic model had resulted in the highest Von Mises stress values under compression, rotation, AP tibial conditions when compared to hyperelastic and viscoelastic modeling techniques.

During the loads experienced on the knee joint, the tibial rotation had resulted in the highest stresses on the ligament regardless of the modeling technique used. There were statistical significant difference among the stresses found on the female ligament when compared to that of the male ligament ($p\text{-value}<0.05$). The maximal stress found on each load applied can be found on the femoral attachment on the ACL (figure 6.2 and 6.3).

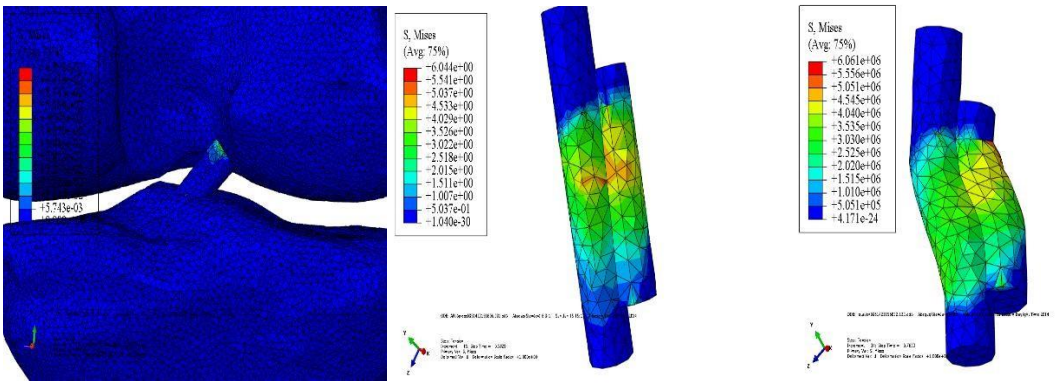

Figure 6.2: Von Mises stresses on the ACL during various loads when modeled as a hyperelastic male ligament

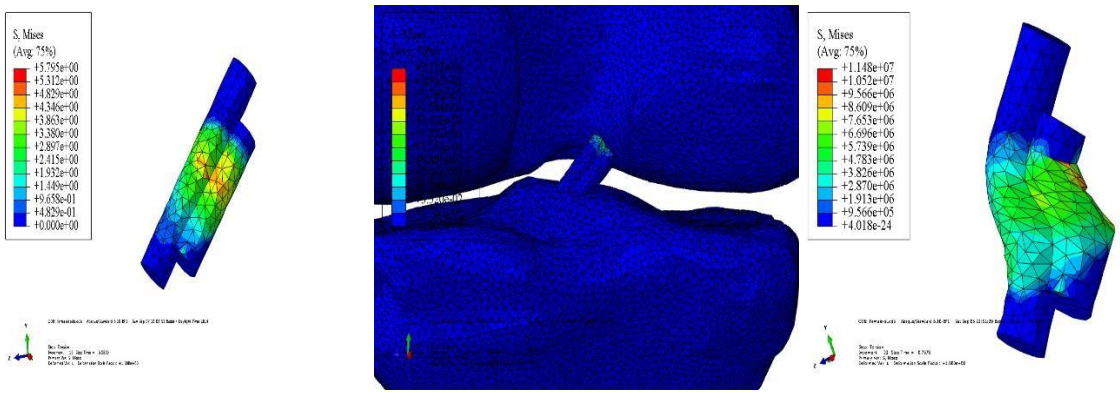

Figure 6.3: Von Mises stresses on the ACL during various loads when modeled as a hyperelastic female ligament

The ACL was modeled as a three dimensional elastic structure. The Von Mises stress experienced by the ACL under the loading conditions are found on figure 6.4 and 6.5. Males and females ACL ligament had shown no difference in the Von Mises stresses under compression, A/P tibial, and tibial shear loading conditions. Tibial rotation of the same degrees, had revealed that females have a significantly different Von Mises stresses when compared to males.

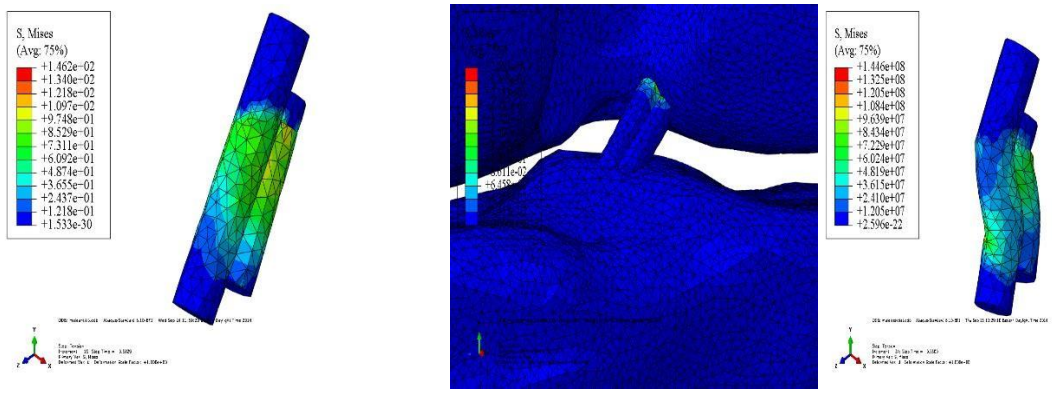

Figure 6.4: Von Mises stress on the male ACL as an elastic structure with respect to load.

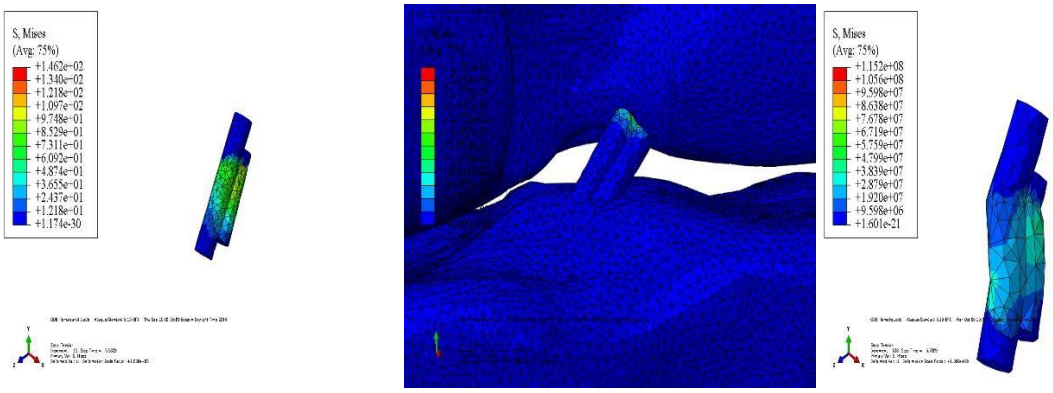

Figure 6.5: Von Mises stress on the female ACL as an elastic structure with respect to load.

The ACL was modeled as a three dimensional viscoelastic structure. The Von Mises stress experienced by the ACL under the loading conditions are found on figure 6.6 and 6.7.

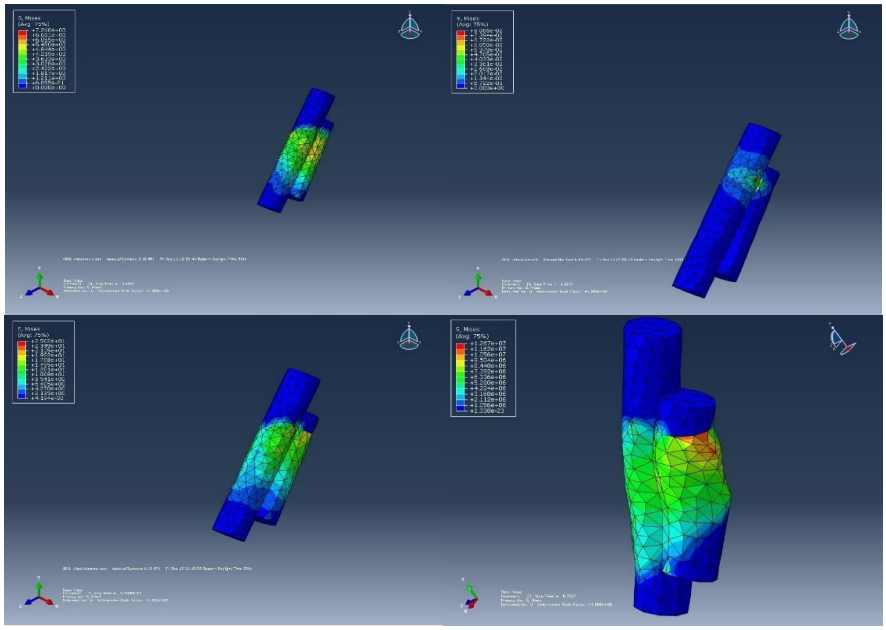

Figure 6.6: Von Mises stress on the male ACL as a viscoelastic structure with respect to load.

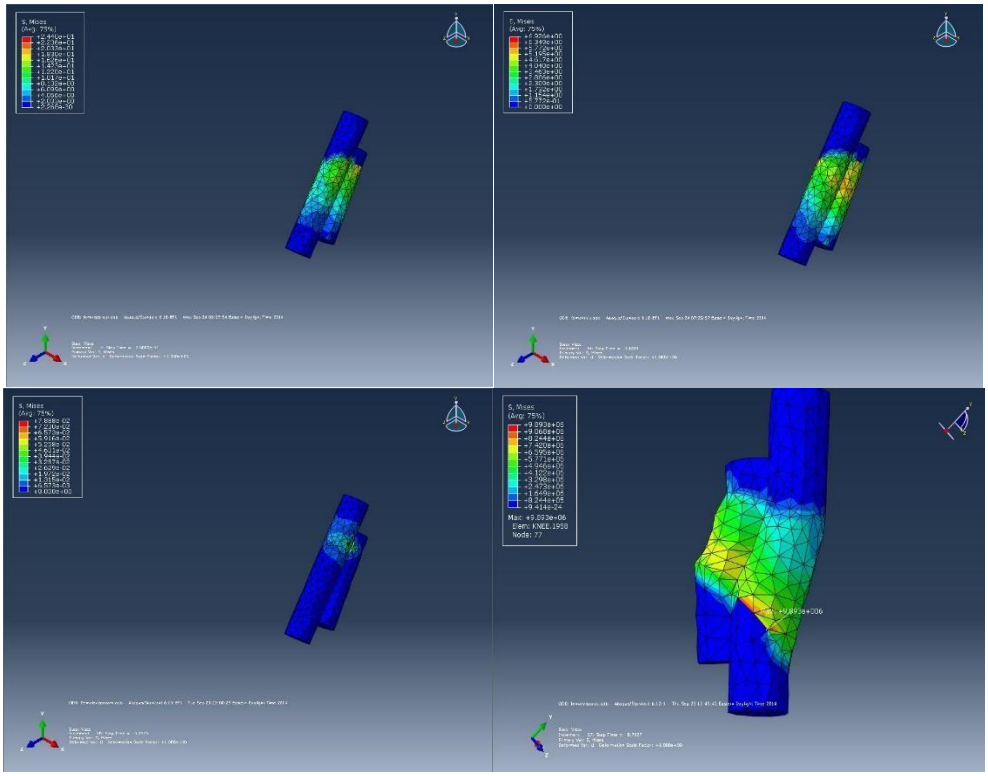

Figure 6.7: Von Mises stress on the female ACL as a viscoelastic structure with respect to load.

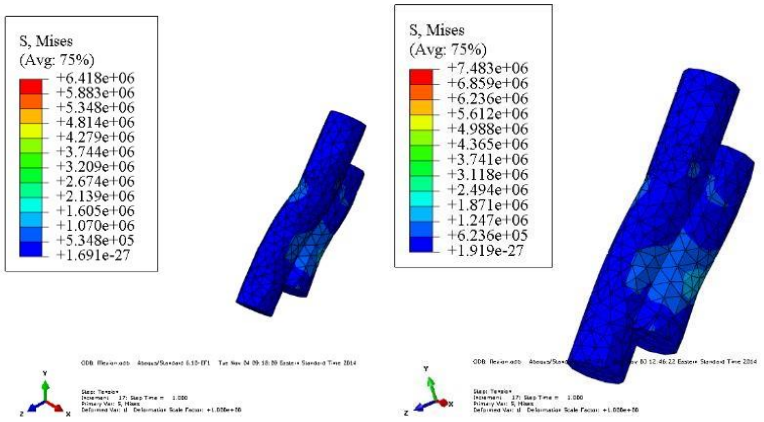

Figure 6.8: Effect of Flexion on the Von Mises stress with respect to gender

Effect of geometric shape on stresses

6.4.1.1 Mesh optimization

The mesh was refined in such a way that the results get converged. Von Mises stress of the ACL for each load under different mesh sizes are provided in figure 6.9. For all of the loads the optimized global size was found to be 0.5.

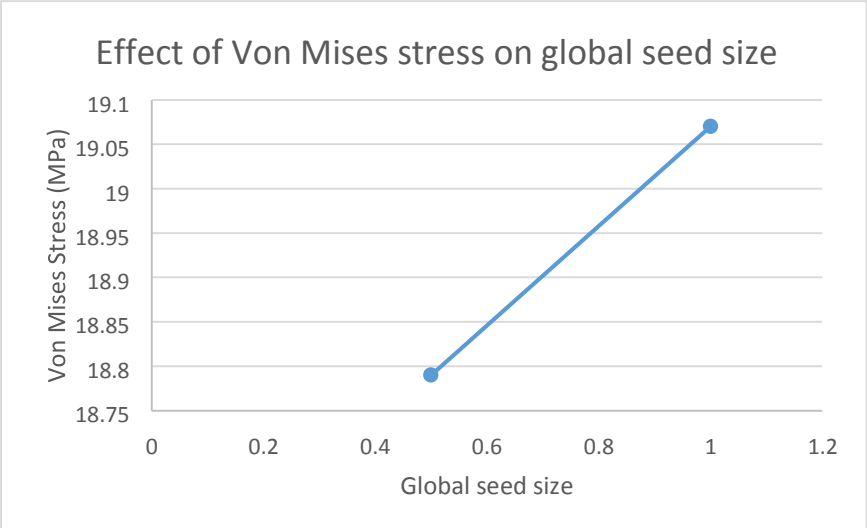

Figure 6.9: Optimized mesh size of the anatomical shaped ligament

The ACL was modeled as two distinct shapes; cylinders and anatomical shape from the MRI. The ACL can be divided into distinct functional bundles that represent the varying tension of the fibers through range of motion of the knee. Cross-sectional and gross (stresses observed across the entire ligament) stress values of respective knee models and their loads applied are provided in table 6.7.

Model	Cylinders		Anatomical	
	Males	Females	Males	Females
Maximum Cross-sectional Von Mises Stress (MPa)				
Compression	0.0689	0.211	0.0313	0.0289
Rotation	6.68	24	3.026	2.64
AP tibial	6.044	5.79	17.74	16.72

Table 6.7: Comparison of geometry shaped ligaments on the Von Mises stresses on the ligament

6.4.2 Anterior tibial force

Under the anterior load, a significant tensile stress had appeared in the posterior part of the ACL, while moderate tensile stress was observed in the anterior part. The highest Von Mises stress had taken place in the posterior region of the tibial insertion of the ACL, with a maximum of 17.79 MPa near the tibial insertion (Figure 6.10). Females had experienced a lower Von Mises stress on the ACL when compared with males.

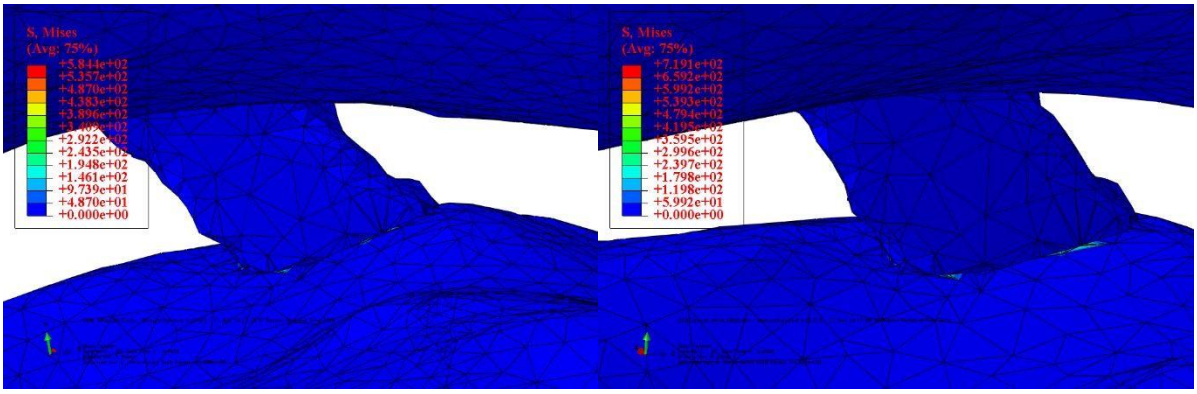

Figure 6.10: Von Mises stress of the ACL under anterior loads

6.4.3 Rotatory load

For every gait cycle, the tibia rotate internally to a maximum of 15 degrees. The ACL can often be injured by direct stretch during internal rotation of the tibia. Failure of the ACL occurs at about 58 degrees of internal tibia rotation (Meyer, 2008). The stresses experienced by the ligament at maximum rotation during gait, seen in figure 6.11.

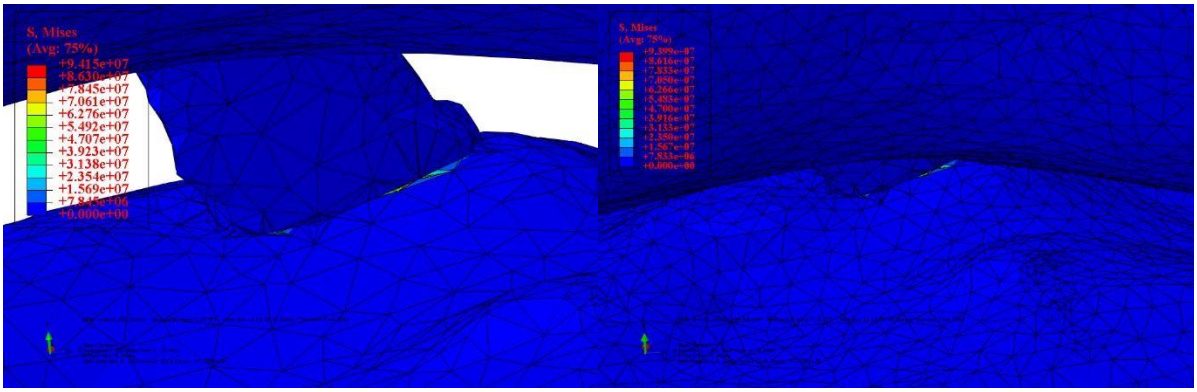

Figure 6.11: Von Mises stress of the ACL under rotation loads

As seen in the above figure, the maximum stress was observed in the posterior region at the femoral insertion site. Von Mises stress experienced on the female ligament be similar to that of the male ligament.

6.4.4 Compression

Compression forces can reach as high as 4 times the body weight through the gait cycle. The maximum Von Mises stress was found on the femoral attachment of the ACL (figure 6.12).

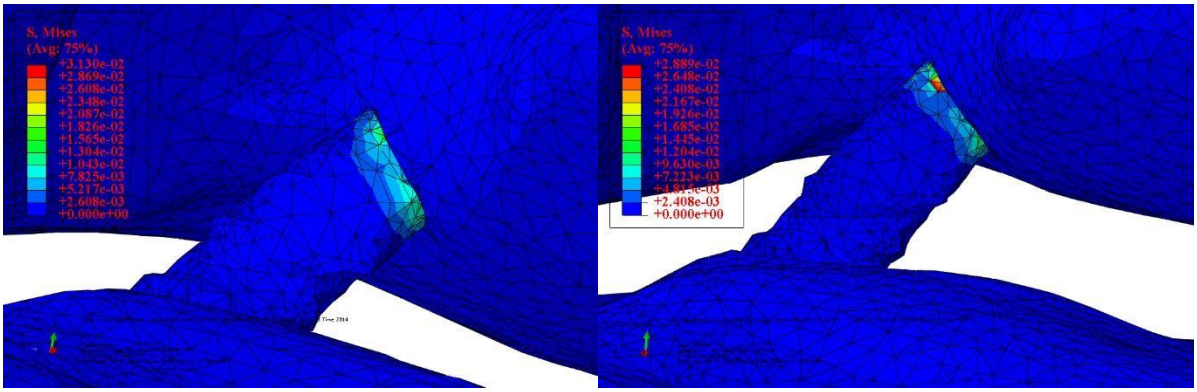

Figure 6.12: Compression forces acting on the knee joint

6.4.5 Effect of C10 parameters

Using the same loads experienced during the gait cycle, the Von Mises stresses on the ACL were determined. As the collagen distribution increases from 15 to 25%, the C10 value also increases. The higher C10 value had shown higher Von Mises stress under the same loading conditions (table 6.8).

Model	**Anatomical** (v=0.5)	**Anatomical** (v=0.4)
	Anisotro	**Anisotro**
Compression	0.08934	0.1391
Rotation	73.63	91.87
AP tibial	37.99	39.11

Table 6.8: Effect of Poisson's ratio with stresses seen with loads.

6.4.6 Anisotropic modeling

Anterior Tibial Force

Under anterior tibial force, the maximum Von Mises stress experienced on the ligament was 0.0788 MPa, which was located on the tibial attachment of the ligament (Figure 6.13). There was an average of 0.0012 MPa.

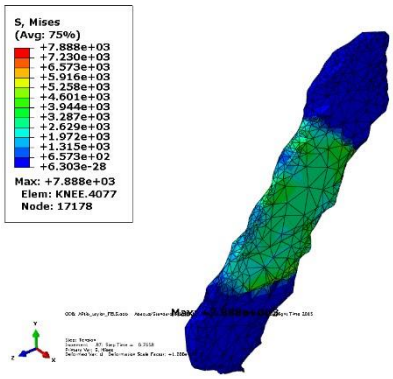

Figure 6.13: Von Mises stress on the ligament as modeled with anisotropic ligament

Rotation

At 15 degrees of tibial rotation, maximum Von Mises stress is observed on the femoral attachment with a value of 7.99 MPa (Figure 6.14). The average Von Mises stress had a value of 1.09 MPa.

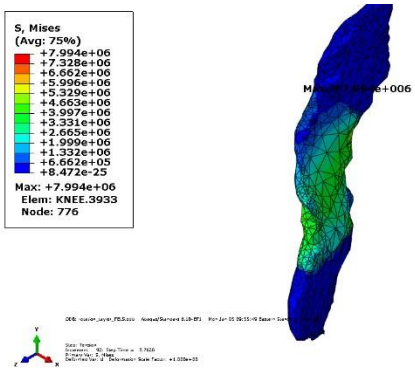

Figure 6.14: Von Mises stress on the ligament as modeled with anisotropic ligament

Compression

At 4 times body weight, the Von Mises stress exhibited on the ACL can be observed (figure 6.15). The maximal Von Mises stress had reached as high 0.07 MPa.

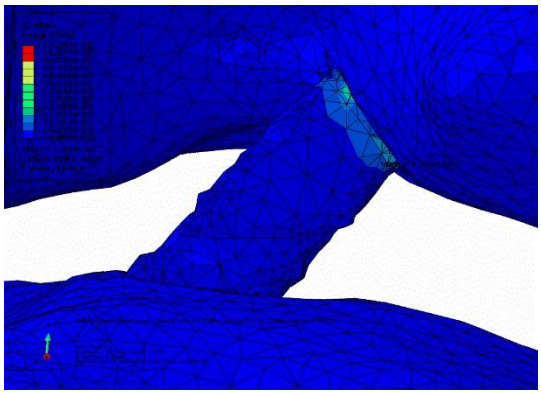

Figure 6.15: Von Mises stress on the ACL under compression loading

6.4.7 Summary of results

Three loading conditions that were seen during gait from healthy volunteers are seen in table 6.9. The Von Mises stress were shown using these loading conditions under different modeling techniques. It is worth to note that the Von Mises stress of the ACL under anisotropic modeling is 100 times less than that seen in anterior tibial loading condition.

Model	Elastic		Hyperelastic		Viscoelastic		Anisotropic	
	Males	Females	Males	Females	Males	Females	Males	Females
Maximum Cross-sectional Von Mises Stress (MPa)								
Compression	0.258	0.258	0.0689	0.211	0.0807	0.0789	0.072	0.072
Rotation	154	118	6.68	11.48	12.67	9.89	7.99	7.99
Anterior tibial	146.22	146.22	6.044	5.79	7.26	6.92	0.0788	0.0788
Maximum Gross Von Mises Stress (MPa)								
Compression	0.258	0.258	0.0689	0.211	0.0807	0.0789	0.072	0.072
Rotation	154	118	6.68	11.48	12.67	9.89	7.99	7.99
Anterior tibial	146.22	146.22	6.044	5.79	7.26	6.92	0.0788	0.0788
Average Gross Von Mises Stress (MPa)								
Compression	0.0124	0.0124	0.00404	0.0105	0.00477	0.00469	0.00485	0.00485
Rotation	18	13.8	1.68	3.32	3.09	2.62	1.05	1.05
Anterior tibial	29.26	29.26	1.27	1.21	1.39	1.34	0.0012	0.0012

Table 6.9: Von Mises of the ACL under various modeling techniques

6.4.8 Validation of the model

FE simulation of experimental uniaxial tensile tests along the longitudinal direction was carried out by Butler, 2006 (figure 6.16). In an effort to validate the FE model, the results displayed in the previous section were compared with in-vivo experimental parameters

measured during the stance phase of gait for both the tibiofemoral and patellofemoral joints.

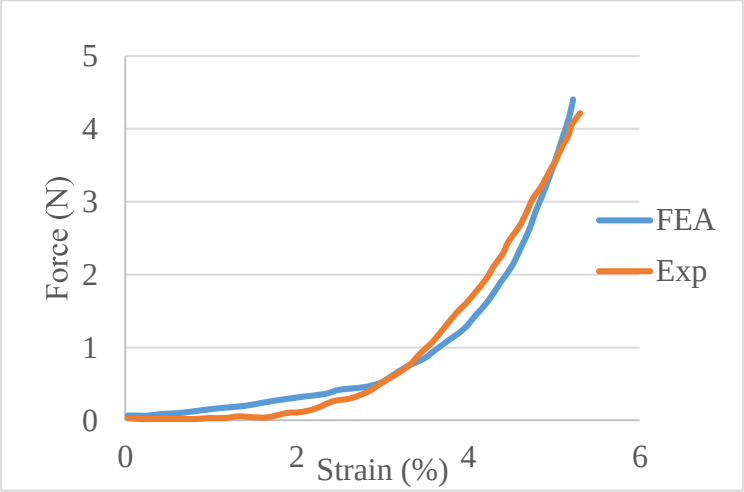

Figure 6.16: FEA model validation using gait data

The load experienced on the tibia reaches as high as 100 N. The translation that is observed on the ligament can reach as high 3mm (figure 6.17). Normally under the same loading conditions the ACL would be displaced about 2 to 5 mm (Wheelers, 2015).

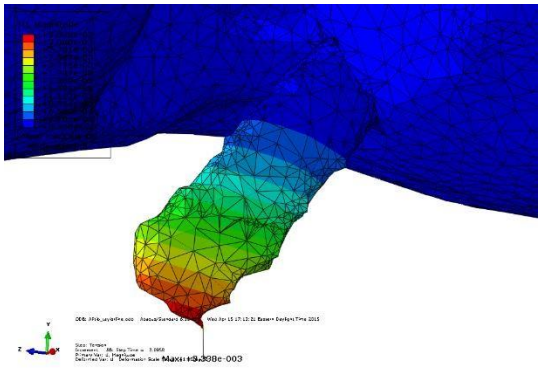

Figure 6.17: Strain of the ACL during the gait cycle

6.4.9 Dynamic Analysis

The stresses on the ACL were determined based on the three loading conditions which occur during gait as previously discussed. On the knee joint, the maximal Von Mises stress were seen on the tibia where the attachment site of the ligament (figure 6.18). The peak Von Mises stress had reached 303.6 MPa at 0.75 of the gait cycle.

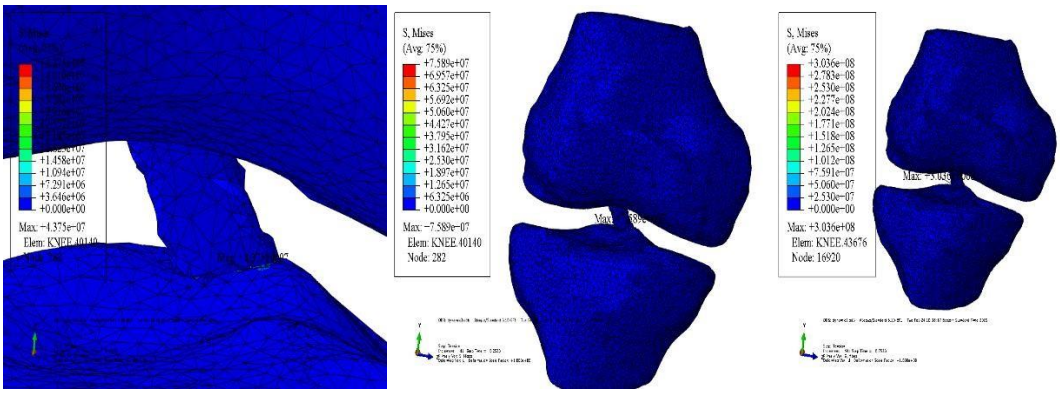

Figure 6.18: Von Mises stress experienced on the knee joint during the gait cycle

Similarly, the ligament would experience a Von Mises stress of 7.99 MPa. The maximum stress was initially found on the femoral attachment of the ligament (figure 6.19). It would then propagate toward the midsubstance of the ligament which is the more common location for injury. The average Von Mises stress that was experienced on the entire ligament had reached 1.05 MPa.

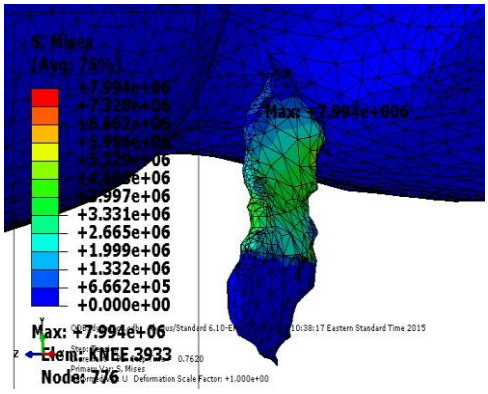

Figure 6.19: Von Mises stress experience on the ligament during the gait cycle.

During a typical gait cycle, the stresses experienced on the ligament can be described as having three peaks; foot strike, support and late swing phase (Figure 6.20). The peak stresses were observed at late swing phase which can be explained by addition of rotation and abduction moments with flexion forces.

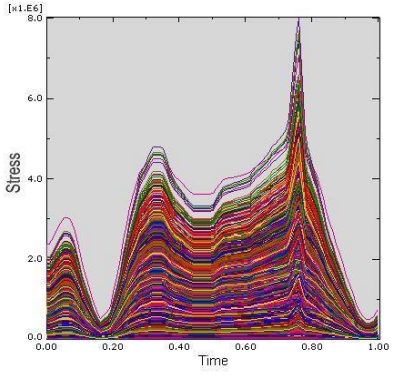

Figure 6.20: Von Mises stress during the entire gait cycle

Maximum Von Mises stresses in the ligament were observed at the point of maximum loads applied.

6.4.10 Valgus Loading/ ACL injury

At 5 degrees of valgus rotation of the tibia, maximum Von Mises stress is observed on the femoral attachment with a value of 1.5 MPa (Figure 6.21). The average Von Mises stress had a value of 0.182 MPa.

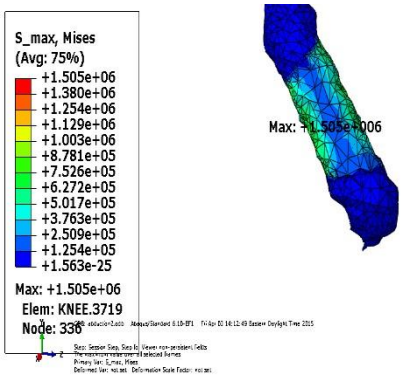

Figure 6.21: Von Mises stress on the ACL under valgus loading conditions

One of the main mechanisms for ACL injury is a combination of valgus and internal rotations of the tibia. This mechanism is often seen among individuals who would land on the leg and quickly pivot in the opposite direction. A combination of these rotatory loads generate Von Mises stress as high as 62 MPa on the ACL ligament (figure 6.22).

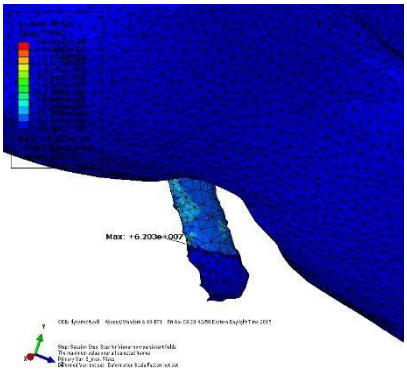

Figure 6.22: Von Mises stress on the ACL under a combination of both Valgus and rotational of the tibia.

6.5 Gait Analysis

The demographics for the participants are listed in table 6.10. The average age among the genders were 35.31 and 35.94 for males and females, respectively. The range found

in both groups was from 21 to 50 years old. No statistical significance difference of age, weight, and forward velocity was found between males and females.

	Males	Females	p-value
N	79	99	
Average Age	35.31	35.94	0.63
Height (cm)	179.84	166.02	
Weight (kg)	78.63	65.09	
BMI	24.23	23.55	0.12
Forward velocity	126.97	128.01	0.6
Cadence	108.86	117.94	<0.05
Step width	11.42	10.08	0.002

Table 6.10: Demographic data for healthy volunteers from Fels Gait data

Females were shorter than their male counterparts ($P < 0.05$). They walked at higher cadence, and a narrower step width ($P < 0.05$). The females walked as fast as the males.

Since it is important to understand the differences in walking mechanics among genders, normalization of joint forces and moments have been performed to eliminate the variation that exists between height and weight. The approach for normalizing joint force and joint moment include dividing moment or force by body mass (Winter, 1991).

The flexion forces were similar in both males and females. Maximal force was observed during support phase of the gait cycle, reaching as high as 0.11 N/kg. During the toe off, females had shown higher flexion force but not significant when compared to males (figure 6.23).

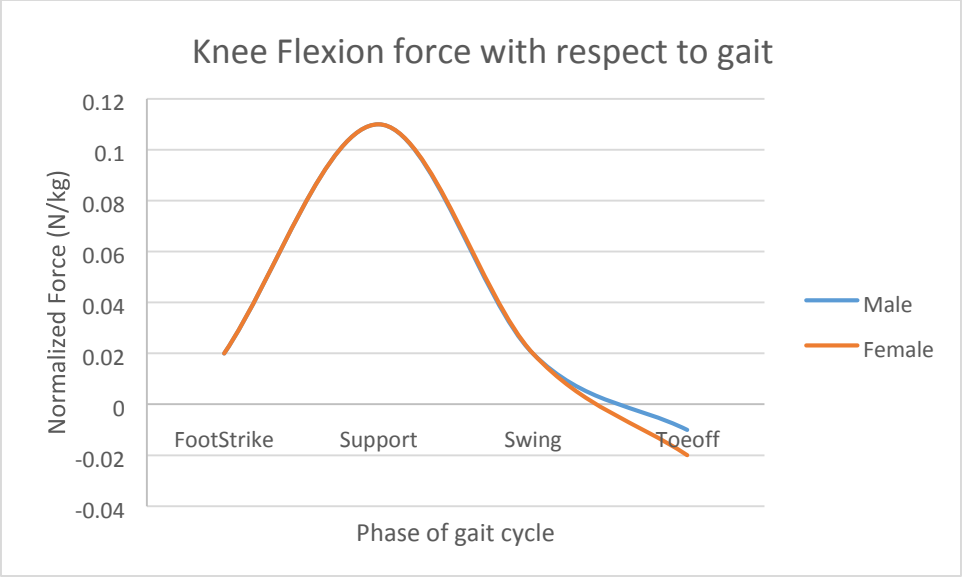

Figure 6.23: Flexion force comparison between genders

The differences in the gait kinetics among gender can be observed in the moment (specifically rotational and abduction moments), as seen in figures 6.24 and 6.25. In the case of rotational moments, the maximal values were observed in the support phase. The rotational moment among the females was significantly lower than that of males (P =0.01). In the remaining phases of the gait cycle, the values were similar among the genders.

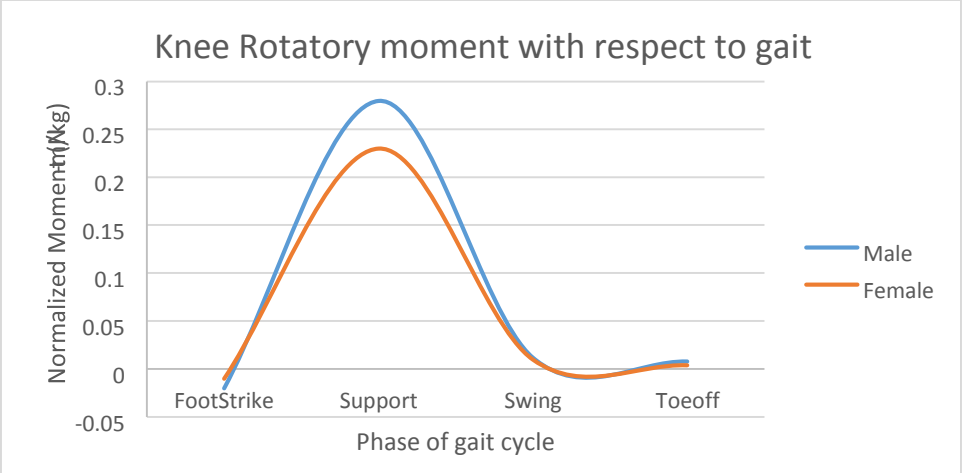

Figure 6.24: Rotatory moment comparison between genders

Similar to rotation moment, maximal values of abduction moment were seen in the support phase. Significant difference was observed during the foot strike phase (P=0.01). However the remaining phases of the gait cycle are not significant (Figure 6.25).

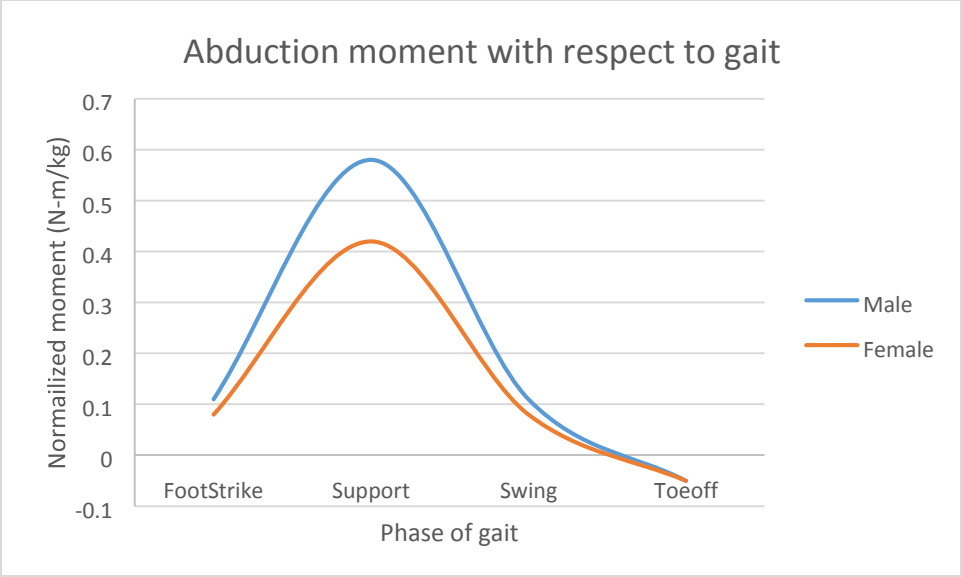

Figure 6.25: Abduction moment between genders

During the gait cycle, there are differences in the kinetics with right leg with respect to left leg. In both genders, there is a significant increase in the rotation angle in the right leg when compared to left leg ($P<0.05$), as seen in table 6.11. Among males, there is also significant differences in other kinetics such as rotation moment, abduction moment, flexion moment, and power.

	Males			Females		
Variable	**Right**	**Left**	**P-value**	**Right**	**Left**	**P-value**
Rotation angle	-20.18	-15.44	0.004	-21.4	-19.58	0.01
Abduction angle	6.91	7.22	0.34	5.38	4.76	0.2
Flexion Angle	62.93	62.26	0.19	62.33	61.65	0.2
Rotation force	1.03	1.03	0.43	1.04	1.03	0.32
Abduction force	0.29	0.28	0.08	0.3	0.29	0.07
Flexion force	0.105	0.11	0.11	0.107	0.104	0.26
Rotation moment	-0.28	-0.24	0.03	-0.23	-0.23	0.49
abduction moment	0.58	0.43	0.02	0.42	0.4	0.29
Flexion moment	0.52	0.43	0.03	0.43	0.38	0.14
Power	0.9	0.77	0.029	0.75	0.75	0.49

Table 6.11: Comparison between right and left legs between genders

During the swing and toe off phase, females are found to have a larger rotation of the tibia when compared to males (P=0.008). Abduction angle is significantly higher among females compared to males in foot strike, support, and swing phases ($P < 0.05$). Flexion force is significantly higher among females compared to males in swing phase (P=0.04). Rotational moment was seen to be significantly higher among males when compared to females in support phase ($P < 0.05$). There is no significant difference seen in the other phases of the gait cycle among genders.

	Gender (Right)				Gender (Left)			
Variable	**Males**	**Females**	**Kinetic**	**P-value**	**Males**	**Females**	**Kinetic**	**P-value**
Rotation angle	-6.07	-2.17	Foot strike	0.04	-15.43	-19.58	Swing	0.008
					-9.32	-13.69	Toe off	0.008
Abduction angle	0.74	-2.04	Foot strike	1.18E-07	0.42	-2.55	Foot strike	5.07E-07
	4.42	2.77	Support (max)	0.00025	4.4	2.5	Support (max)	7.45E-05
	-1.68	-3.66	Support (Min)	0.0003	-1.44	-4.01	Support (Min)	2.21E-05
	6.91	5.38	Swing (Max)	0.02	7.23	4.76	Swing (Max)	0.007
	-3.24	-5.18	Swing (min)	0.001	-4.22	-5.56	Swing (min)	0.04
	2.76	1.36	Toe off	0.02	1.74	0.06	Toe off	0.008
Flexion Angle	7.4	9.5	Foot strike	0.004	8.05	9.61	Foot strike	0.026
	31.82	29.67	Support (max)	0.01	31.26	28.82	Support (max)	0.0068
	5.9	8.97	Swing (min)	0.0003	6.88	9.05	Swing (min)	0.007
	34.07	31.44	Toe off	0.007	33.97	30.86	Toe off	0.001
Rotation force	-0.02	-0.03	Swing (max)	0.004				
Abduction force	-0.09	-0.1	Foot strike	0.03	-0.09	-0.1	Foot strike	0.02
	-0.12	-0.13	Support (Min)	0.03	-0.12	-0.14	Support (min)	0.03
	-0.08	-0.09	Swing (min)	0.01	-0.08	-0.09	Swing (min)	0.0003
	0.008	0.013	Toe off	0.01				
Flexion force	0.025	0.02	Toe off	0.03	0.11	0.1	Support (max)	0.05
	-0.016	-0.018	Swing (min)	0.04				
Rotation moment	0.11	0.13	Support (Max)	0.03				
	-0.28	-0.23	Support (min)	0.01				
Abduction Moment	0.11	0.08	Foot strike	0.03	0.08	0.06	Foot strike	0.04
	0.58	0.42	Support (max)	0.01				
	0.09	0.08	Swing (min)	0.0008				
Flexion moment	0.52	0.42	Support (max)	0.01				
	0.09	0.1	Swing (max)	0.05				
	0.08	0.09	Toe off	0.01				
Power	0.26	0.03	Toe off	0.0002	0.16	0.0001	Toe off	0.0008
	0.9	0.75	Support (max)	0.009	0.13	0.07	Swing (max)	0.0007
	-1.03	-0.9	Support (min)	0.07	-0.62	-0.8	Swing (min)	1.50E-06
	0.19	0.1	Swing (max)	0.0003				
	-0.92	-1.2	Swing (Min(	8.02E-09				

Table 6.12: Comparison between kinetic during gait among genders

6.5.1 ACL force

The ACL is loaded during the entire stance phase of the gait cycle. ACL in the right leg had experienced higher forces when compared to that of the left. Peak ACL force in the right leg was 300 N (Figure 6.26), which had occurred in the first quarter of the gait cycle. The load decreases during the swing phase of the cycle. Peak ACL force in the left leg reaches as high as 150 N, during the swing phase of the cycle.

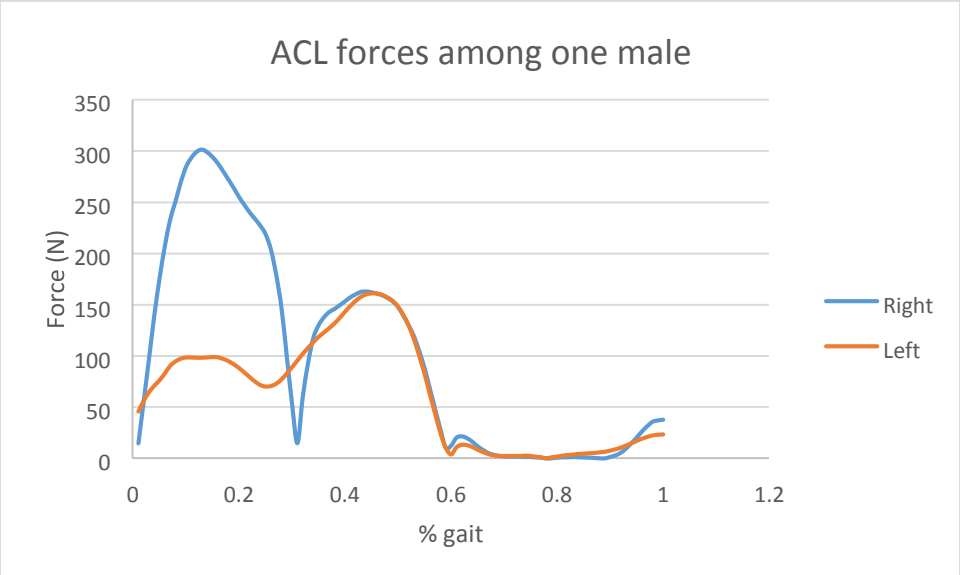

Figure 6.26: ACL forces in one male

ACL forces among females is lower when compared with their male counterparts. The forces experienced in both legs are quite similar (figure 6.27). The peak ACL force was 215 N which had occurred in the swing phase in the gait cycle. The forces in both legs were similar, with one exception. In the stance phase of the gait cycle, the ACL in the right leg had experienced higher forces.

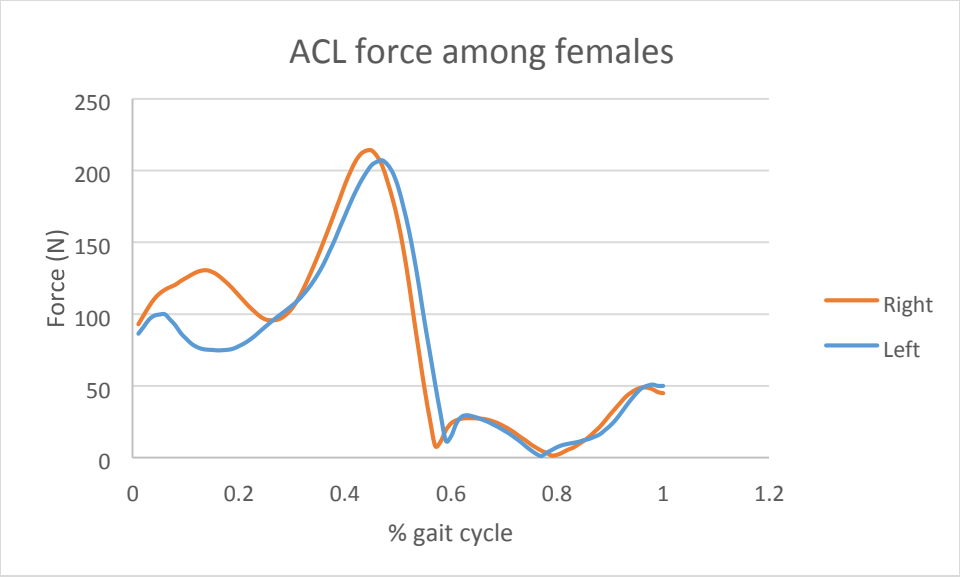

Figure 6.27: ACL forces among females

6.5.2 Comparison between right and left leg

The force of the ACL can be determined with flexion force, rotational moment and abduction moments. In males, rotation moment was significantly higher in the right limb when compared to the left limb (P=0.03). Similarly, abduction moment was also significantly higher in the right limb when compared to left limb (P=0.02). It is due to these differences that the forces experienced on the ACL was higher in the right limb when compared to left limb (Figure 6.28).

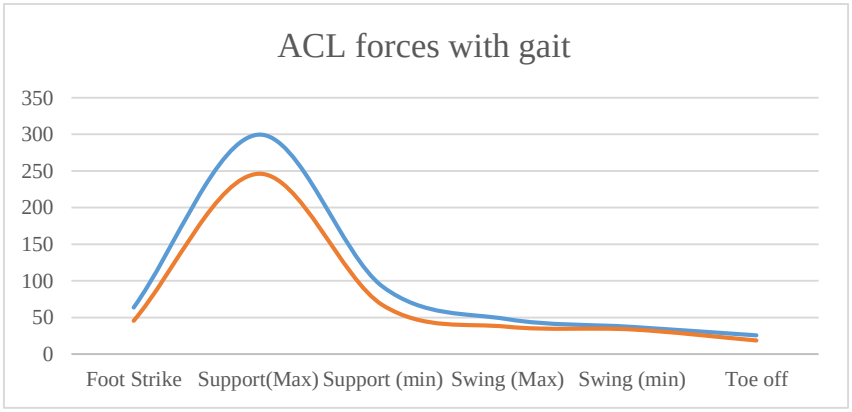

Figure 6.28: Comparison between ACL forces during gait among males

Among females, the forces seen on the ACL were similar when both legs were measured (figure 6.29). In females, flexion force was significantly higher in the right limb when compared to the left limb (P=0.05). Similarly, abduction moment was also significantly higher in the right limb when compare to left limb (P=0.04).

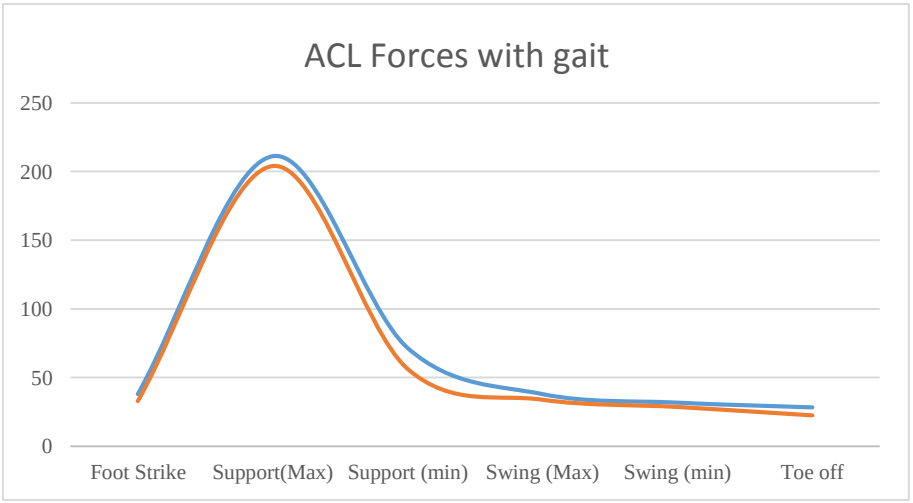

Figure 6.29: ACL forces during gait among females

6.5.3 Base Support

Bivariate analysis was performed to compare the base of support between males and females. Average base of support was found to be 2.69 and 2.92 for males and females, respectively. Females have a significantly narrower base of support when compared to their males counterparts (P =0.02).

Within genders, base of support has no significant effect on the ACL force with p-values of 0.52 and 0.80 for males and females, respectively (Figure 6.30). In addition the effect of abduction moment on the ACL forces are quite significant among genders (P <0.05).

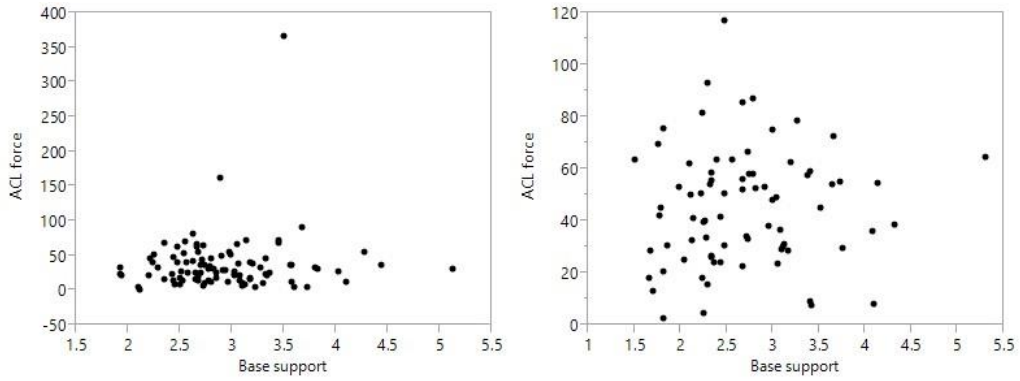

Figure 6.30: Comparison between base of support among genders

6.6 Risk Analysis

A regression plot was compared to investigate the relationship between NWI and sagittal width (Figure 6.31). There appears to be a direct linear relationship between NWI and sagittal width. However, there is no relationship between NWI and sagittal length and

AP width. A prediction equation was developed involving NWI and the ACL measurements in the sagittal plane in control groups (Equation 8.2) to describe individuals who are at greater risk for ACL injury

.

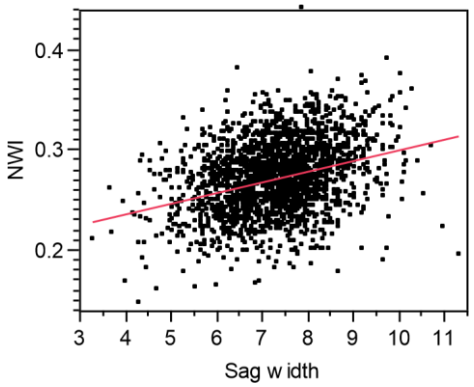

Figure 6.31: Regression plot which describes a linear relationship between NWI and sagittal width of the ACL

$$NWI = 0.19 + 0.01(W) \qquad R^2 = 0.8326 \qquad \text{(Equation 6.2)}$$

Where, W equals the width of the ACL in the sagittal plane. Equation 3 determines the critical dimensions for non-torn ACLs based on NWI data. A strong correlation was found between NWI and sagittal width (r^2=0.32). Similar correlations were performed between other pairs, Table 6.13 An average sagittal width of greater than 7.5 have average NWI of 0.28 (Figure 6.32).

Variable	By Variable	Correlation	Count	Sig Prob
Sag Width	AP Width	-0.0024	2000	0.9146
Sag Length	AP width	-0.0040	2000	0.8596
Sag Length	Sag Width	-0.0289	2000	0.1969
NWI	AP width	0.1117	2000	<0.0001*
NWI	Sag Width	0.3192	2000	<0.0001*
NWI	Sag Length	0.0397	2000	0.0757

Table 6.13: Using Monte Carlo, to investigate relationship of anatomical features

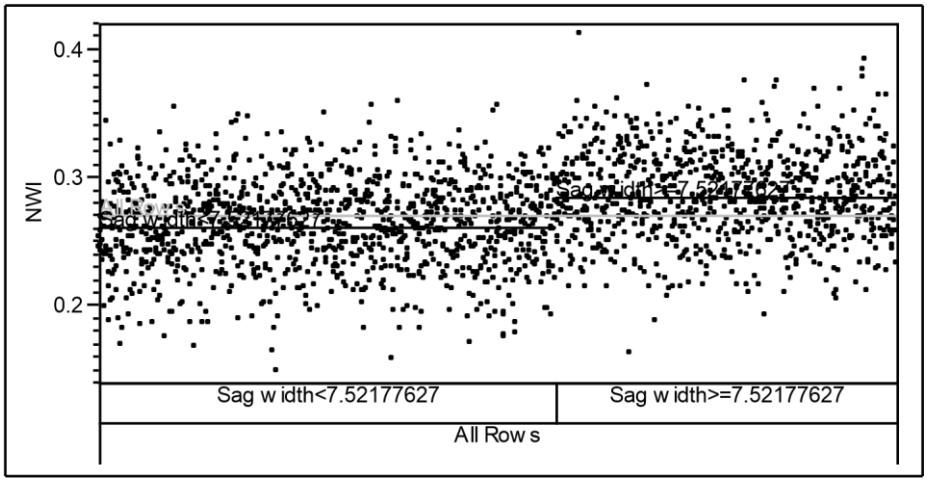

Figure 6.32: Scatter plot of the NWI and sagittal width for larger population. (n=2000)

Sensitivity analysis performed shows that ACL injury is a function of forces as shown in Figure 6.33 assuming the linear relationship between the forces applied and pull-out failure of the ACL. The risk of ACL injury for our assumed population (n=2000) from anatomical data of 40 subjects shows forces from 0 to 100% torn risks at a given NWI. Forces acting on the ligament can be represented as Anterior-Posterior Forces on Tibia or rotation of tibia. The tensile force extend the ACL result in the injury. Other parameters such as NWI, AP width, sagittal width and length are not sensitive to injury risk, Figure 6.34.

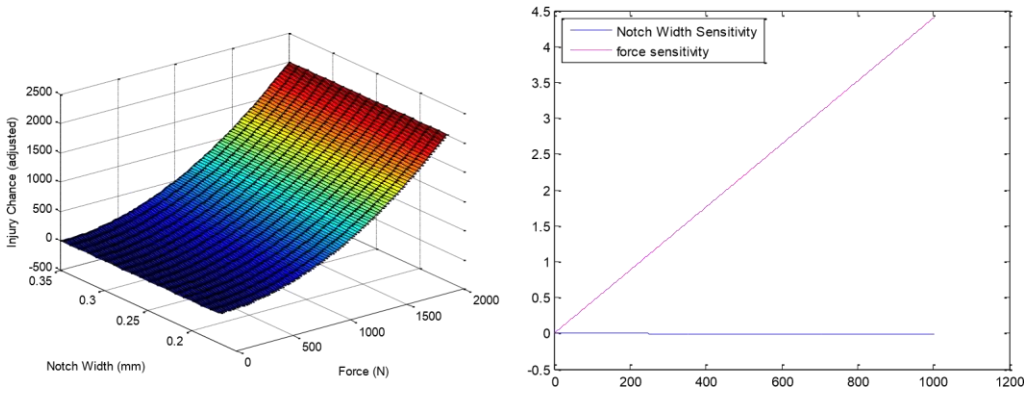

Figure 6.33: Sensitivity analysis of the anatomical features against the ACL injury risk

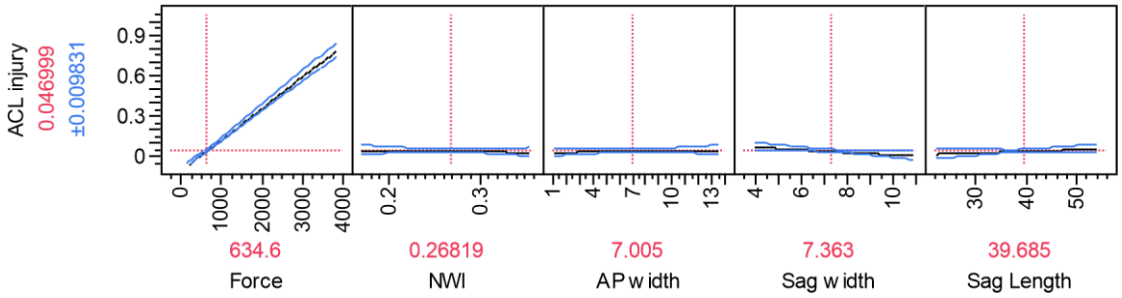

Figure 6.34: Risk assessment of ACL injury when compared with Force and anatomical features of the knee joint.

Monte Carlo simulations (n = 2000) were performed with each model to determine the effects of variability in ACL force using the flexion force, valgus moment and internal rotation moment. These numbers were generated using Gaussian distribution with zero mean and standard deviation in each movement variable calculated from 80 gait trials. Simulations had shown average rotation moment and varus moments of 0.1 Nm/kg and

0.56 Nm/kg respectively. The distribution of the ACL forces can be seen in figure 6.35, which have a Weibull Distribution. The maximum force was determined to be 1533 N.

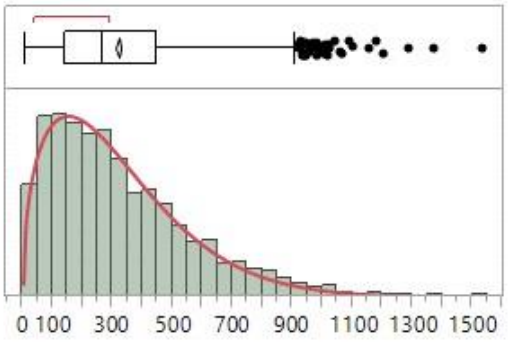

Figure 6.35: Distribution of ACL forces

The force on the ACL is related to the flexion force, abduction moment, and rotation moment. Using sensitivity analysis, it can be determined that both the weight as well as abduction moment are key players in the risk for developing ACL injury (Figure 6.36), with p-value < 0.0001. By doubling the abduction moment and keeping all other factors constant, the force experienced on the ACL also double.

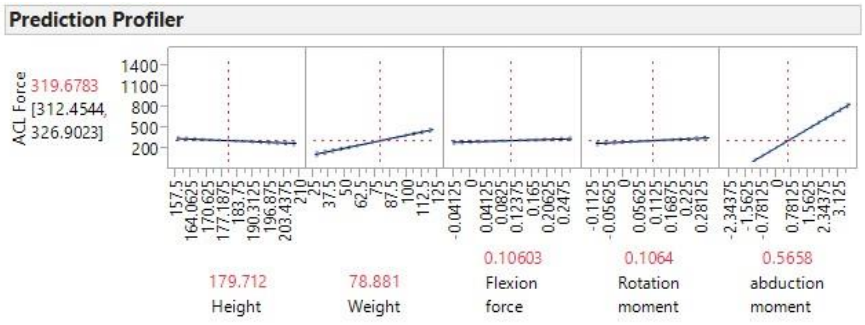

Figure 6.36: Risk assessment of ACL force with different loading conditions

The other factors such as height, flexion force and rotational moment are also quite significant on the force on the ACL as seen in table 6.14.

Source	Nparm	DF	Sum of Squares	F Ratio	Prob > F
Height	1	1	198962	7.3318	0.0068*
Weight	1	1	4562811	168.1412	<.0001*
Flexion force	1	1	105329	3.8814	0.0490*
Rotation moment	1	1	228709	8.4280	0.0037*
abduction moment	1	1	45275772	1668.428	<.0001*

Table 6.14: ANOVA analysis to look at the risk analysis of ACL injury with loading conditions . Significant differences is indicated by *.

There is a linear relationship between tibial shear force and Von Mises stress which can be seen in figure 6.37. Females require a lower shear force to injure the ligament.

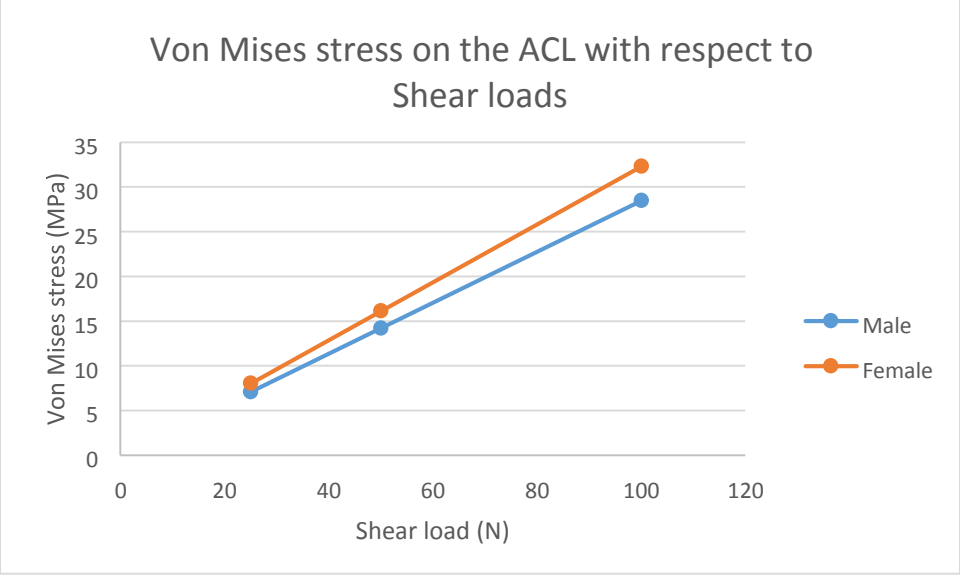

Figure 6.37: Linear regression which describes a relationship between tibial shear and Von Mises stress.

However, there is a non-linear regression which was performed between tibial rotation in degrees and Von Mises stress experienced on the ligament, which can be seen in figure 6.38. There is a greater increase in the Von Mises stresses after it exceeds 20 degrees. At 30 degrees, the Von Mises stress on the ligament was 30 MPa.

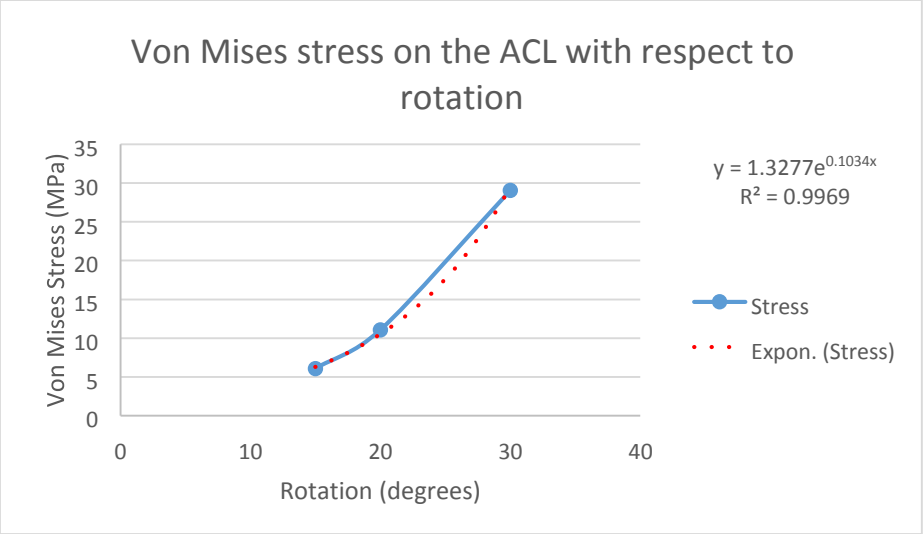

Figure 6.38:Non-linear regression between rotation (degrees) and Von Mises stress

Linear regression was performed using JMP 7.0 to determine a relationship between shear force and Von Mises stress for males and females. However, Von Mises stress increases exponentially with rotation in degrees. The equations for stress with respect to rotation is seen in equation 1 for males, with R^2=0.9969.

$$Stress = 1.3277 * e^{0.1034 * degrees} \quad \text{Equation 6.1}$$

6.7 ACL forces

The force on the ACL can be determined by simultaneously solving equations of dynamic equilibrium. These equations include force vector equilibrium on the tibia in both the y and x directions and an equation for the equilibrium of moments about the joint center.

$$F_{ACL} = 1.68 * weight\ (Kg) + 94.83 * F_{Flexion} + 351.14 * |M_{IE}| + 53.05 * |M_{VV}|$$ Eq. 6.2

Where, M_{IE} and M_{VV} would be defined as the internal-external rotation moment and varus-valgus moments, respectively. $F_{Flexion}$ can be defined as the flexion force which is often seen by anterior-posterior force acting on the tibia.

Chapter 7 Discussion

7.1 Predicting ACL injuries on the basis of anatomical measurements

There was no statistical difference in NWI between males and females overall, however, the NWI was found to be statistically smaller between the study and control groups.

In our population we had found that females had a shorter ACL ligament when compared to males. Although previous work measured smaller ACL length, volume, and cross-sectional area in female cadavers, the length of the ACL has not previously been investigated as a risk factor for ACL tears. These findings suggest a shorter ACL may play a role in ACL injury and may predispose female athletes to a higher rate of ACL injury. The underlying mechanism may be related to a lower collagen fibril concentration and lower percent area of collagen fibrils in women compared to men giving rise to pulling forces longitudinally. Further research is needed to describe this theory as an explanation for the gender difference in ACL tear rates.

7.2 Volume of infrapatellar fat pad

Measurement of fat pad volume from the MR images had appeared to be a useful indicator of fat pad morphology. Recently, a study had validated the fat pad volume from MR against direct measurement of fat pad volumes in porcine knees [Chuckpaiwong, 2010]. In a study of four cadavers aged from 80 to 95 with no medical history of knee surgery,

the infrapatellar fat pad was removed from its surrounding structures, and measurements were made with calipers [Abreu, 2008]. Volume of the fat pad was determined by Archimedes principle. The average volume of the fat pad was 24 ml with a range of 12-36 ml. Here volume was determined with 3D reconstruction of the fat pad, which had average 23.78 ml. Therefore, imaging data reconstruction is able to predict accurately the fat pad generation during ACL injury. We had a larger range of 11 to 44 ml may due mainly to prevalence of bodily fluids in the joint and live subjects. The volume of infrapatellar fat pad in another study of 15 osteoarthritic patients and another 15 aged matched with no history of arthritis or knee pain, population was 20.70 with a standard deviation of 3.3 cm^3 [Chuckpaiwong, 2010]. In a recent study of using MR images, the mean volume of infrapatellar fat pad obtained from asymptomatic knees had determined to be 19.53 with a standard deviation of 3.64 cm^3 [Culvenor, 2011].

Our findings show that there is no relationship between the size of the infrapatellar fat pad of the knee and the BMI ($p=0.7060$). It suggests that the infrapatellar fat pad is not regulated by overall fat adiposity. Present study compared the volume of fat pad among patients with acute ACL injury. The patients with ACL injury have significantly larger infrapatellar fat pad in terms of volume and surface area when compared to age matched control group, p of 0.01 and 0.04, respectively. A possible reason for this finding is that the trauma from the injury may cause hemorrhage in the neighboring structures, which thus increases its volume.

This study was limited by the quality of the MR images, especially to measure the volume of the fat pad. The fat pad is bounded by inferior pole of the patella. The images had shown poor differentiation of fat pad margins proximal to this point. A slice thickness of less than 3.5 mm have resulted in more accurate volume. The average volume of the infrapatellar fat pad has been shown to be varied based on knee flexion. It is unclear about the time frame between the onsets of ACL injury and MRI imaging of the knee. The MRI scans were performed based on physical examination findings and pain level experienced by patients. There were also other factors such as personal preferences for imaging time which pose a problem to standardizing the time between ACL injury and MRI imaging. The other limitation can be that the various risk factors between the two populations not considered in treatment.

7.3 Stress Distribution of the ACL

7.3 Modeling techniques

Based on the obtained results it can be observed that the hyperelastic ACL model from the male knee have shown lower Von Mises stress values (cross sectional and gross stresses) under compression, rotation, and AP tibial loading conditions. In both males and females, tibial shear loads had resulted in the highest Von Mises stress values (cross sectional and gross stresses). Among all modeling techniques and genders, the ACL as an elastic model had resulted in the highest Von Mises stress values under compression, rotation, AP tibial conditions when compared to hyperelastic and viscoelastic modeling techniques.

During the loads experienced on the knee joint, the tibial rotation had resulted in the highest stresses on the ligament regardless of the modeling technique used. There were statistical significant difference among the stresses found on the female ligament when compared to that of the male ligament (p-value<0.05). The maximal stress found on each load applied can be found on the femoral attachment on the ACL.

Males and females ACL ligament had shown no difference in the Von Mises stresses under compression, A/P tibial, and tibial shear loading conditions. Tibial rotation of the same degrees, had revealed that females have a significantly different Von Mises stresses when compared to males.

Recently, 3D representations of knee ligaments with differing degrees of model complexity was attempted (Butler, 1990). An ACL with distinct Anteromedial (AM) and posterolateral (PL) bundles was modeled as hyperelastic model (Song, 2004). Similar model was constructed to evaluate ACL biomechanics under passive tibial translation and flexion of an isolated ACL. There are a limited number of studies which have studied the effects of modeling techniques on joint function.

We have investigated the effect of three most common techniques which can be utilized to model ligament on joint kinematics during gait. Models were constructed from CT and MRI images of both healthy, young males and females. Von Mises stresses on both male and female ACL were compared. During the gait cycle, the knee joint experience 0.17 to

4 times body weight which correspond to maximum anterior tibial load and compression, respectively. Using the same loading conditions with each of the modeling techniques, the maximum Von Mises stresses experienced on the ACL under anterior tibial load conditions were 146.22, 6.044 and 7.26 MPa which corresponds to elastic, hyperelastic and viscoelastic, respectively.

Previous models of the Knee had consisted of bones, ligaments, and menisci. The female model was meshed using hexahedral elements. The ACL was modeled as hyperelastic structure. The elements used in this study were tetrahedral elements. In general, tetrahedral elements allow the results more closely to that of theoretical ones. In addition, the mesh was refined in such a way that the results get converged to less than 5% difference which allowed for more accurate results. Therefore it is important that the ACL to be modeled with tetrahedral elements.

The female ACL are shorter and have lower mechanical properties than that of a male ACL (Chandrashekar, 2005). Microstructurally, the females have a lower collagen fibrils than that of males. The results from this study had revealed that for a given load, the females had experienced significant higher Von Mises stress for all loading conditions except for anterior tibial when the ligament was modeled as hyperelastic. At low tibial shear forces, the Von Mises stress experiences by both males and females are approximately the same. As tibial shear forces increase, the females experience higher Von Mises stress than males. Tibial shear force of greater than 100 N is needed to injure the ligament regardless of the

gender. The higher Von Mises stress experienced by females can be explained by the difference in material properties among genders, and can be a possible reason for increased risk for ACL injury among females.

7.3.1 Effect of geometric shape on stresses

The acquisition of accurate geometry for the ligament and possibly the bones is a fundamental requirement for the construction of three-dimensional FE models of ligaments. Laser scanning and medical imaging are the primary techniques that have been used for this purpose. Laser scanning can be very accurate, but cannot differentiate between the ligament of interest and surrounding bone and soft tissue structures. Further, it can only digitize geometry that is visible directly from the laser source. Both magnetic resonance imaging (MRI) and computed tomography (CT) have been used to acquire ligament geometry (Gardiner 2003; Li 1999). MRI can provide detailed images of soft tissue structure in diarthrodial joints.

Cylinder shaped ligament had exhibited higher Von Mises stresses in both compression and rotational forces when compared to the anatomically shaped ligaments. The cylindrical shaped ligaments overestimate the stresses suggestive of injury. Anatomically accurate 3D representation of such structures coupled with structurally motivated constitutive models (Gasser, 2006) facilitate implementation of realistic ligament mechanical properties such as finite deformation, anisotropy and non-linear incompressible fiber-reinforced structures. Therefore, the anatomical representation of the

ligament make it feasible to determine stress distribution across the ligament which in turn provide valuable information about the mechanism of ligament injury.

Anatomical shaped ligaments had shown that females had a lower Von Mises stress for all the loading conditions when compared to their males counterparts. In both genders, the maximal stress was observed in the posterior region of tibial insertion of the ACL. The highest stress among the cylindrical shaped ligaments was found to be near the femoral intersection area as the ACL wraps around the bone when load is applied.

The results from the anatomical representation had revealed a maximal principal stress of 17.74 MPa which was higher than that observed in a similar study by Peña in 2006. It was reported a maximum principal stress of 15 MPa (Peña, 2006). The results from cylindrical shaped ligaments had revealed a maximum principal stress of 11 MPa. However there are some differences from our study to that of previous study (Peña, 2006). Peña et al.'s model incorporates all four knee ligaments as well as the meniscus. This may cause loads on the ACL to be shared by other ligaments. Our knee model had only consisted of the ACL which allows for the load applied to ligament. Similar to both studies, the model of the ACL was generated using data collected from Magnetic Resonance Imaging (MRI) of each individual patient.

7.3.2 Anisotropic modeling

Study had revealed that the ACL modeled as a hyperelastic structure had exhibited less Von Mises stress when compared with that of both elastic and viscoelastic. This supports

a previous study where it was found that 3D anisotropic hyperelastic model had resulted in more physiological prediction of the human knee motion under a range of physiological loading conditions during gait cycle. Soft tissue modeling is an important criterion to accurately predict joint kinematics using FE analysis. In addition, it is also important to represent such structures as 3D anatomical representations. The appropriate use of soft tissue modeling and anatomical representation facilitates implementation of mechanical properties of ligament. It also permits interactions among the other structures in the joint. In addition, proper anatomical representation of the ligament can be instrumental in determining the local stress-strain distribution across the tissue, which in turn is critical to better understand its injury mechanism.

7.4 Gait

The main purpose of this section is to compare the pattern of forces transmitted to the ACL in normal gait seen by healthy volunteers. The aspects of the analysis had focused on body motions, and leg muscle forces which were obtained from gait analysis among healthy individuals. The forces seen on the Anterior Cruciate ligament were determined based on a linear regression model that was developed based on equations.

$$\text{ACL Force} = 1.66 * \text{weight} + 103.56 * \text{flexion force} + 356.76 * \text{rotation moment} + 52.86 * \text{varus moment} \quad \text{(Eqn. 7.1)}$$

$$\text{ACL Force} = 3.75 * \text{weight} + 158.73 * \text{flexion force} + 196.05 * \text{rotation moment} + 168.85 * \text{varus moment} \quad \text{Eqn 7.2}$$

The major limitation for these analysis was the static equilibrium was assumed in the calculation of ligament forces, similarly the effects of centrifugal and inertial forces were neglected. During the stance phase of the gait, the muscle and gravitational forces play a key role in the forces transmitted to the lower limb joints (Anderson, 2003).

In our study we have noticed differences in the anthropometrics, stride characteristics and walking biomechanics between males and females, that were quite consistent with literature (McKean, 2007; Cho, 2004; Kerrigan, 2000). Significantly higher stride length observed among males can be due to differences in height. This difference in stride length disappears when stride length would be normalized with height.

In our study, female physique was significantly smaller ($P<0.05$), but ANCOVA showed that their shorter leg length could not be one of the gender features of female gait. The unnormalized female pelvic width, which was as wide as of males, could be regarded as greater than that of males with the same height. Thus, wide pelvis can influence the large joints below pelvis, especially in coronal plane.

The female cadence, which was as great as males' inspite of their shorter leg length, did not seem to be influenced by the size of physical size. Also, ANCOVA showed that slower walking speed in female was due to their differences with male BMI ($p=.12$), NWI ($p=.26$), BW ($p<0.05$), height ($p<0.05$), and forward velocity ($p=0.6$). Consequently, the spatiotemporal data did not show any additional effort for females to walk as fast as males. The female stride length, both the female step width, and its ratio to pelvic width were

smaller than the males', ANCOVA. This could imply the females protrude their legs less vigorously with greater hip joint adduction. Since the female's pelvis is wider than the males, it can be assumed that the anatomical or habitual differences can explain their step width to be narrower than the males counterparts.

From an anatomical perspective, the females' greater knee joint valgus seen in our study might contribute to the narrower step width. Because most of our data were derived from gait analysis, we are able to show that females would have significantly greater abduction angles ($p < 0.005$).

Similarly, males would have significantly larger adduction angles than the females ($p<0.05$). Another reason for the narrower step width can be explained by the differences in the narrower base of support. It was observed that females would have narrower base of support which can explain for increased valgus in the joint.

In this study, there were two peaks of ACL loading in stance with the maximum occurring in early stance right around the time of contralateral toe-off, consistent with findings from literature (Collins 1995). Even though the pattern of ACL loading were quite consistent with previous literature, there are significant differences in the predicted values of peak ACL force. In this study, the peak ACL force observed during normal walking was less than ½ BW and is quite similar to loads of ACL seen in various other activities such as isokinetic knee extension exercise. The loads experienced on the ACL can be explained by the shear forces that are acting at the knee joint. The shear force acting on the knee

depends on a balance of muscle forces, ground reaction forces, and joint contact forces applied to the leg. Forces are experienced on the ACL when the shear forces are applied in an anterior direction. In the early stance phase, the shear forces are often caused by the patellar tendon, which is then later transmitted to the ACL. The shear forces caused by the patellar tendon are often large in the stance phase due to forces generated by quadriceps since patellar tendon is located more anteriorly to the long axis of the tibia.

During the heel strike, a component of the ground reaction forces is equal to the sum of anterior shear forces that are generated by the patellar tendon, gastrocnemius, and tibiofemoral contact force. Gastrocnemius would cause anterior shear force since the knee is fully extended just prior to contralateral heel strike, and at small flexion angles the muscle would wrap around the tibia. Similarly, the tibiofemoral contact force cause anterior shear force since the forces would act on the posterior slope of the tibial plateau. The ground reaction forces cause a posterior shear force because of the fact that the resultant force acts behind the knee. This posterior shear forces increased prior to the contralateral heel strike due to increased angle between the shank and ground. During the late stance, the forces acting on the ACL was relatively small because of the fact that sum of the shear forces approaches to zero.

7.5 Risk Analysis

It is important to determine a relationship between notch width and width of the ACL. A linear relationship was determined to investigate the relationship between NWI and width

of the ACL. This prediction equation helps to determine the individuals who are at a greater risk for ACL injury.

Even though there are methods to determine external knee joint loading, there are no studies which analyze the distribution of these forces among internal structures of the knee joint and whether any combination of these load result in ACL injury. Forces which were acting on the ligament represented from loads applied on the external knee joint. Sensitivity analysis had shown that there is a linear relationship between the forces applied and risk for ACL injury. The forces which have exceeded the ultimate strength of the ACL result in its injury. Various anatomical features such as NWI, AP width, Sagittal length and width have no bearing on the risk for ACL injury.

Using the mean joint torques generated during the Monte Carlo simulations in conjunction with the equation used to estimate ACL force had shown that varus-valgus moments have a greater contribution to the loading of ACL than internal-external joint moments. The flexion force alone did not exceed 1000N, therefore the two moments are extremely important in causing injury, based on known strength of the ACL (Woo, 1991). This method would provide valuable information on being able to understand ACL injury mechanisms, as well as being able to assist with preventative methods. In cases where ACL forces greater than 2000 N were simulated, abduction moments and rotational moments were larger than the unperturbed movement. By training the individuals to reduce these moments can reduce the incidence of ACL injury.

Risk equations that corresponds to different amount of forces on the ACL can be seen in equations 7.1 and 7.2. The force on the ACL computed using equation 7.1 can result in a maximum force of 500 N, which is suggestive of 25 % risk for injury. Similarly, the force on the ACL computed using equation 7.2 can result in a maximum force of 1500 N, which is suggestive for 75% risk for an injury. Any additional valgus or varus moments can greatly increase the risk for ACL injury. Prevention programs which would help in the reduction of valgus moments can possibly reduce the incidence of ACL injury.

Chapter 8 - Conclusions

The findings of this study had shown that the risk for ACL injury is greater when resulting force reaches its threshold. Anatomical features such as NWI, Length and width of ACL have no effect on the risk for ACL injury. Probabilistic modeling of ACL injury risk shows the forces needed for a specific percent risk assuming a linear relationship between the force and ACL pull-out failure. Another confounding variable which is present in our study is the different mechanisms in which the ACL is injured and imaging data post injury. Continuation of this study with a larger, age specific, population and injury mechanism should further establish the suggested relationships.

Patients with a torn ACL ligament had a larger infrapatellar fat pad measured from MR compared with their asymptomatic counterparts. The size of the fat pad is not related to BMI. The ellipsoidal model and MATLAB approximation of volume had shown to have no difference when compared to that determined by Mimics, with p-values of 0.87 and 0.83 respectively. There is no statistical significance between BMI and volume of infrapatellar fat pad. Volume determinations using ellipsoidal approximation model had been shown to be comparable to that determined by MRI and MATLAB code within a statistical band of ±x2.

Hyperelastic ACL model from the male knee have shown lower Von Mises stress values (cross sectional and gross stresses) under compression, rotation, and AP tibial loading conditions. In both males and females, tibial shear loads had resulted in the highest Von Mises stress values (cross sectional and gross stresses). Among all modeling techniques and genders, the ACL as an elastic model had resulted in the highest Von Mises stress values under compression, rotation, AP tibial conditions when compared to hyperelastic and viscoelastic modeling techniques.

Cylinder shaped ligament had exhibited higher Von Mises in both compression and rotational forces when compared to the anatomically shaped ligaments. The cylindrical shaped ligaments overestimate the stresses suggestive of injury. Anatomically accurate 3D representation of such structures coupled with structurally motivated constitutive models facilitate implementation of realistic ligament mechanical properties such as finite deformation, anisotropy and non-linear incompressible fiber-reinforced structures. Therefore, the anatomical representation of the ligament make it feasible to determine stress distribution across the ligament which in turn provide valuable information about the mechanism of ligament injury.

3D anisotropic hyperelastic model had resulted in more physiological prediction of the human knee motion under a range of physiological loading conditions during gait cycle. Soft tissue modeling is an important criterion to accurately predict joint kinematics using FE analysis. In addition, it is also important to represent such structures as 3D

anatomical representations. The appropriate use of soft tissue modeling and anatomical representation facilitates implementation of mechanical properties of ligament.

In our study, female physique was significantly smaller ($P<0.05$), but ANCOVA showed that their shorter leg length could not be one of the gender features of female gait. The unnormalized female pelvic width, which was as wide as of males, could be regarded as greater than that of males with the same height. Thus, wide pelvis can influence the large joints below pelvis, especially in coronal plane.

The female cadence, which was similar to males' inspite of their shorter leg length, did not seem to be influenced by physical size. Also, ANCOVA showed that slower walking speed in female was due to their smaller physique, which could not be a gender feature of female gait. Consequently, the spatiotemporal data did not show any additional effort for females to walk as fast as males. The female stride length, both the female step width, and its ratio to pelvic width were smaller than the males' , ANCOVA. This could imply the females protrude their legs less vigorously with greater hip joint adduction. Since the female's pelvis is wider than the males, it can be assumed that the anatomical or habitual differences can explain their step width to be narrower than the males counterparts.

From an anatomical perspective, the females' greater knee joint valgus seen in our study might contribute to the narrower step width. Because most of our data were derived from gait analysis, we are able to show that females would have significantly greater abduction

angles ($p < 0.005$). Similarly, males would have significantly larger adduction angles than the females ($p<0.05$). In this study, the peak ACL force observed during normal walking was less than ½ BW.

A linear relationship was determined to investigate the relationship between NWI and width of the ACL. This may suggest that NWI plays no significant role in the causes for ACL injury. Sensitivity analysis had shown that there is a linear relationship between the forces applied and risk for ACL injury. The forces which have exceeded the ultimate strength of the ACL result in its injury. The various anatomical features such as NWI, AP width, Sagittal length and width have no bearing on the risk for ACL injury.

The trends identified here will lead to a more practical method of identifying individuals at high risk for an ACL tear. An attempt was made to use demographic data in combination with digital measurements taken from MRI to predict ACL injury. A focus on prevention of ACL tears is truly the best method to prevent lifelong disability in a young and active population.

Further work needs to be done with a larger population to strengthen the validity of this data. Injuries of the ACL have been quite prevalent, especially among young athletes who participate in various sports.

References

Agel, J., Evans, T. A., Dick, R., Putukian, M., & Marshall, S. W. (2007). Descriptive epidemiology of collegiate men's soccer injuries: National Collegiate Athletic Association Injury Surveillance System, 1988–1989 through 2002–2003. *Journal of athletic training*, *42*(2), 270.

Griffin LY, Albohm MJ, Arendt EA et al., Understanding and preventing noncontact anterior cruciate ligament injuries: a review of the Hunt Valley II meeting, January 2005. Am.J.Sports Med. 2006; 34 1512-32

Lohmander LS, Ostenberg A, Englund M, Roos H, High prevalence of knee osteoarthritis, pain, and functional limitations in female soccer players twelve years after anterior cruciate ligament injury. Arthritis Rheum. 2004; 50 3145-52

Hewett TE, Lindenfeld TN, Riccobene JV and Noyes FR (1999). The effect of neuromuscular training on the incidence of knee injury in female athletes. A Prospective study. Am J Sports Med 27: 699-706

Boden BP, Dean GS, Feagin JA, and Garrett WE (2000). Mechanism of Anterior Cruciate Ligament Injury. Orthopedics 23: 573-578

Gilchrist J, Mandelbaum BR, Melancon H et al., A randomized controlled trial to prevent noncontact anterior cruciate ligament injury in female collegiate soccer players. Am.J.Sports Med. 2008; 36 1476-83

Heidt, R. S., Sweeterman, L. M., Carlonas, R. L., Traub, J. A., & Tekulve, F. X. (2000). Avoidance of soccer injuries with preseason conditioning. *The American journal of sports medicine*, *28*(5), 659-662

Mandelbaum, B. R., Silvers, H. J., Watanabe, D. S., Knarr, J. F., Thomas, S. D., Griffin, L. Y.,& Garrett, W. (2005). Effectiveness of a Neuromuscular and Proprioceptive Training Program in Preventing Anterior Cruciate Ligament Injuries in Female Athletes 2-Year Follow-up. *The American journal of sports medicine*, *33*(7), 1003-1010.

Kanamori, A., Zeminski, J., Rudy, T. W., Li, G., Fu, F. H., & Woo, S. L. Y. (2002). The effect of axial tibial torque on the function of the anterior cruciate ligament: a

biomechanical study of a simulated pivot shift test. *Arthroscopy: The Journal of Arthroscopic & Related Surgery*, *18*(4), 394-398.

Shelburne, K. B., Pandy, M. G., & Torry, M. R. (2004). Comparison of shear forces and ligament loading in the healthy and ACL-deficient knee during gait. *Journal of biomechanics*, *37*(3), 313-319.

Van den Bogert, A. J., & McLean, S. G. (2007). ACL injuries: do we know the mechanisms?. *Journal of Orthopaedic and Sports Physical Therapy*, *37*(2), A8.

Besier, T. F., Lloyd, D. G., Cochrane, J. L., & Ackland, T. R. (2001). External loading of the knee joint during running and cutting maneuvers. *Medicine and Science in Sports and Exercise*, *33*(7), 1168-1175.

Netter, F. H. (2014). *Atlas of human anatomy*. Elsevier Health Sciences.

Girgis FG, Marshall JL, Monajem A, The cruciate ligaments of the knee joint. Anatomical, functional and experimental analysis. Clin.Orthop.Relat.Res. 1975; (106) 216-31

Palmer I, On the injuries to the ligaments of the knee joint: a clinical study. 1938. Clin.Orthop.Relat.Res. 2007; 454 17,22; discussion 14

Amis AA, Dawkins GP, Functional anatomy of the anterior cruciate ligament. Fibre bundle actions related to ligament replacements and injuries. J.Bone Joint Surg.Br. 1991; 73 260-7

Furman W, Marshall JL, Girgis FG, The anterior cruciate ligament. A functional analysis based on postmortem studies. J.Bone Joint Surg.Am. 1976; 58 179-85

Arnoczky SP, Anatomy of the anterior cruciate ligament. Clin.Orthop.Relat.Res. 1983; (172) 1925

Odensten M, Gillquist J, Functional anatomy of the anterior cruciate ligament and a rationale for reconstruction. J.Bone Joint Surg.Am. 1985; 67 257-62

Kennedy JC, Weinberg HW, Wilson AS, The anatomy and function of the anterior cruciate ligament. As determined by clinical and morphological studies. J.Bone Joint Surg.Am. 1974; 56 223-35

Cohen SB, VanBeek C, Starman JS et al., MRI measurement of the 2 bundles of the normal anterior cruciate ligament. Orthopedics 2009; 32 10.3928/01477447,20090728-35

Jackson DW (Ed). The anterior cruciate ligament : current and future concepts. Raven Press LTD (1993)

McConkey, J. P. (1986). Anterior cruciate ligament rupture in skiing A new mechanism of injury. *The American journal of sports medicine*, *14*(2), 160-164.

Arendt, E., & Dick, R. (1995). Knee injury patterns among men and women in collegiate basketball and soccer NCAA data and review of literature. *The American journal of sports medicine*, *23*(6), 694-701.

Bahr R, Krosshaug T, Understanding injury mechanisms: a key component of preventing injuries in sport. Br.J.Sports Med. 2005; 39 324-9

Meeuwisse W, Assessing causation in sport injury: a multifactorial model. Clin.J.Sport Med.
1994; 4 166-170

McIntosh AS, Risk compensation, motivation, injuries, and biomechanics in competitive sport. Br.J.Sports Med. 2005; 39 2-3

Hutchinson, M. R., & Ireland, M. L. (1995). Knee injuries in female athletes. *Sports Medicine*, *19*(4), 288-302.
Ferber, R., Davis, I. M., & Williams Iii, D. S. (2003). Gender differences in lower extremity mechanics during running. *Clinical biomechanics*, *18*(4), 350-357.

Ireland, M. L. (2002). The female ACL: why is it more prone to injury?. *Orthopedic Clinics of North America*, *33*(4), 637-651.

Shelbourne KD, Davis TJ, Klootwyk TE, The relationship between intercondylar notch width of the femur and the incidence of anterior cruciate ligament tears. A prospective study. Am.J.Sports Med. 1998; 26 402-8

Anderson AF, Lipscomb AB, Liudahl KJ, Addlestone RB, Analysis of the intercondylar notch by computed tomography. Am.J.Sports Med. 1987; 15 547-52

LaPrade, R. F., & Burnett, Q. M. (1994). Femoral Intercondylar Notch Stenosis and Correlation to Anterior Cruciate Ligament Injuries A Prospective Study. *The American Journal of Sports Medicine*, *22*(2), 198-203.

Souryal, T. O., & Freeman, T. R. (1993). Intercondylar notch size and anterior cruciate ligament injuries in athletes A prospective study. *The American Journal of Sports Medicine*, *21*(4), 535539.

Souryal TO, Moore HA, Evans JP, Bilaterality in anterior cruciate ligament injuries: associated intercondylar notch stenosis. Am.J.Sports Med. 1988; 16 449-54

Davis TJ, Shelbourne KD, Klootwyk TE, Correlation of the intercondylar notch width of the femur to the width of the anterior and posterior cruciate ligaments. Knee Surg.Sports Traumatol.Arthrosc. 1999; 7 209-14

Anderson AF, Dome DC, Gautam S et al., Correlation of anthropometric measurements, strength, anterior cruciate ligament size, and intercondylar notch characteristics to sex differences in anterior cruciate ligament tear rates. Am.J.Sports Med. 2001; 29 58-66

Muneta T, Takakuda K, Yamamoto H, Intercondylar notch width and its relation to the configuration and cross-sectional area of the anterior cruciate ligament. A cadaveric knee study. Am.J.Sports Med. 1997; 25 69-72

Shelbourne KD, Facibene WA, Hunt JJ, Radiographic and intraoperative intercondylar notch width measurements in men and women with unilateral and bilateral anterior cruciate ligament tears. Knee Surg.Sports Traumatol.Arthrosc. 1997; 5 229-33

Slauterbeck, J. R., Fuzie, S. F., Smith, M. P., Clark, R. J., Xu, K. T., Starch, D. W., & Hardy, D. M. (2002). The menstrual cycle, sex hormones, and anterior cruciate ligament injury. *Journal of athletic training*, *37*(3), 275.

Beynnon, B. D., Johnson, R. J., Braun, S., Sargent, M., Bernstein, I. M., Skelly, J. M., & Vacek,
P. M. (2006). The Relationship Between Menstrual Cycle Phase and Anterior Cruciate Ligament Injury A Case-Control Study of Recreational Alpine Skiers. *The American journal of sports medicine*, *34*(5), 757-764.

Slauterbeck JR, Hickox JR, Beynnon B, Hardy DM, Anterior cruciate ligament biology and its relationship to injury forces. Orthop.Clin.North Am. 2006; 37 585-91

Putnam, C.A. 1993. Sequential motions of body segments in striking and throwing skills: Descriptions and explanations. *Journal of Biomechanics*, 26: 125–135. suppl. 1

Barber-Westin, S. D., Noyes, F. R., Smith, S. T., & Campbell, T. M. (2009). Reducing the risk of noncontact anterior cruciate ligament injuries in the female athlete. *The Physician and sportsmedicine*, *37*(3), 49-61.

Huston, L. J., & Wojtys, E. M. (1996). Neuromuscular performance characteristics in elite female athletes. *The American Journal of Sports Medicine*, *24*(4), 427-436.

Renstrom, P., Ljungqvist, A., Arendt, E., Beynnon, B., Fukubayashi, T., Garrett, W., ... & Engebretsen, L. (2008). Non-contact ACL injuries in female athletes: an International Olympic Committee current concepts statement. *British journal of sports medicine*, *42*(6), 394-412.

Myklebust G, Engebretsen L, Braekken IH et al., Prevention of anterior cruciate ligament injuries in female team handball players: a prospective intervention study over three seasons. Clin.J.Sport Med. 2003; 13 71-8

Griffin LY, Albohm MJ, Arendt EA et al., Understanding and preventing noncontact anterior cruciate ligament injuries: a review of the Hunt Valley II meeting, January 2005. Am.J.Sports Med. 2006; 34 1512-32

Wetzler, M. J., Getelman, M. H., Friedman, M. J., & Bartolozzi, A. R. (1998). Revision anterior cruciate ligamentsurgery: etiology of failures. *Operative Techniques in Sports Medicine*, *6*(2), 64-70.

Petsche, T. S., & Hutchinson, M. R. (1999). Loss of extension after reconstruction of the anterior cruciate ligament. *Journal of the American Academy of Orthopaedic Surgeons*, *7*(2), 119-127.

Wojtys, E. M., & Huston, L. J. (1994). Neuromuscular performance in normal and anterior cruciate ligament-deficient lower extremities. *The American journal of sports medicine*, *22*(1), 89-104.

Quatman, C. E., Ford, K. R., Myer, G. D., Paterno, M. V., & Hewett, T. E. (2008). The effects of gender and pubertal status on generalized joint laxity in young athletes. *Journal of Science and Medicine in Sport*, *11*(3), 257-263.

Woo, S. L., Debski, R. E., Withrow, J. D., & Janaushek, M. A. (1999). Biomechanics of knee ligaments. *The American journal of sports medicine*, *27*(4), 533-543.

Woo, S. L., Fox, R. J., Sakane, M., Livesay, G. A., Rudy, T. W., & Fu, F. H. (1998).

Biomechanics of the ACL: measurements of in situ force in the ACL and knee kinematics. *The Knee*, *5*(4), 267-288.

Beynnon, B. D., Johnson, R. J., Fleming, B. C., Stankewich, C. J., Renström, P. A., & Nichols, C. E. (1997). The strain behavior of the anterior cruciate ligament during squatting and active flexion-extension a comparison of an open and a closed kinetic chain exercise. *The American Journal of Sports Medicine*, *25*(6), 823-829.

Markolf, K. L., Bargar, W. L., Shoemaker, S. C., & Amstutz, H. C. (1981). The role of joint load in knee stability. *The Journal of Bone & Joint Surgery*, *63*(4), 570-585.

Hollis, J. M., Takai, S., Adams, D. J., Horibe, S., & Woo, S. Y. (1991). The effects of knee motion and external loading on the length of the anterior cruciate ligament (ACL): a kinematic study. *Journal of biomechanical engineering*, *113*(2), 208-214.

Markolf, K. L., Mensch, J. S., & Amstutz, H. C. (1976). Stiffness and laxity of the knee--the contributions of the supporting structures. A quantitative in vitro study. *The Journal of Bone & Joint Surgery*, *58*(5), 583-594.

Grood, E. S., Stowers, S. F., & Noyes, F. R. (1988). Limits of movement in the human knee. Effect of sectioning the posterior cruciate ligament and posterolateral structures. *The Journal of Bone & Joint Surgery*, *70*(1), 88-97.

Wroble, R. R., Grood, E. S., Cummings, J. S., Henderson, J. M., & Noyes, F. R. (1993). The role of the lateral extraarticular restraints in the anterior cruciate ligament-deficient knee. *The American journal of sports medicine*, *21*(2), 257-263.

Woo, S. Y., Johnson, G. A., & Smith, B. A. (1993). Mathematical modeling of ligaments and tendons. *Journal of biomechanical engineering*, *115*(4B), 468-473.

Kwan, M. K., Lin, T. H., & Woo, S. L. (1993). On the viscoelastic properties of the anteromedial bundle of the anterior cruciate ligament. *Journal of biomechanics*, *26*(4), 447-452.

Woo, S. L., Newton, P. O., MacKenna, D. A., & Lyon, R. M. (1992). A comparative evaluation of the mechanical properties of the rabbit medial collateral and anterior cruciate ligaments. *Journal of biomechanics*, *25*(4), 377-386.

Alm, A. N. D. E. R. S., & Strömberg, B. (1974). Vascular anatomy of the patellar and cruciate ligaments. A microangiographic and histologic investigation in the dog. *Acta chirurgica Scandinavica. Supplementum*, *445*, 25.

Noyes, F. R., & Grood, E. S. (1976). The strength of the anterior cruciate ligament in humans and Rhesus monkeys. *The Journal of Bone & Joint Surgery*, *58*(8), 1074-1082.

Butler, D. L., Guan, Y., Kay, M. D., Cummings, J. F., Feder, S. M., & Levy, M. S. (1992). Location-dependent variations in the material properties of the anterior cruciate ligament. *Journal of biomechanics*, *25*(5), 511-518.

Woo, S. L. Y., Hollis, J. M., Adams, D. J., Lyon, R. M., & Takai, S. (1991). Tensile properties of the human femur-anterior cruciate ligament-tibia complex The effects of specimen age and orientation. *The American journal of sports medicine*, *19*(3), 217-225.

Butler, D. L., Kay, M. D., & Stouffer, D. C. (1986). Comparison of material properties in fascicle-bone units from human patellar tendon and knee ligaments. *Journal of biomechanics*, *19*(6), 425-432.

Chandrashekar, N., Slauterbeck, J., & Hashemi, J. (2005). Sex-Based Differences in the Anthropometric Characteristics of the Anterior Cruciate Ligament and Its Relation to Intercondylar Notch Geometry A Cadaveric Study. *The American journal of sports medicine*, *33*(10), 1492-1498.

Parry, D. A. (1988). The molecular fibrillar structure of collagen and its relationship to the mechanical properties of connective tissue. *Biophysical chemistry*, *29*(1), 195-209.

Mosler, E., Folkhard, W., Knörzer, E., Nemetschek-Gansler, H., Nemetschek, T., & Koch, M. H. J. (1985). Stress-induced molecular rearrangement in tendon collagen. *Journal of molecular biology*, *182*(4), 589-596.

Strasser, S., Zink, A., Janko, M., Heckl, W. M., & Thalhammer, S. (2007). Structural investigations on native collagen type I fibrils using AFM. *Biochemical and biophysical research communications*, *354*(1), 27-32.

Gutsmann, T., Fantner, G. E., Kindt, J. H., Venturoni, M., Danielsen, S., & Hansma, P. K. (2004). Force spectroscopy of collagen fibers to investigate their mechanical properties and structural organization. *Biophysical journal*, *86*(5), 3186-3193.

Korhonen, R. K., Laasanen, M. S., Töyräs, J., Lappalainen, R., Helminen, H. J., & Jurvelin, J. S. (2003). Fibril reinforced poroelastic model predicts specifically mechanical behavior of normal, proteoglycan depleted and collagen degraded articular cartilage. *Journal of biomechanics*, *36*(9), 1373-1379.

Butler, D. L., Sheh, M. Y., Stouffer, D. C., Samaranayake, V. A., & Levy, M. S. (1990). Surface strain variation in human patellar tendon and knee cruciate ligaments. *Journal of biomechanical engineering*, *112*(1), 38-45.

Weiss, R. (1992). Viscoelastic Behavior of Lightly Sulfonated Polystyrene Ionomers. *Department of Polymer Engineering*, *67*, 127.

Fleming, B. C., Beynnon, B. D., Renstrom, P. A., Johnson, R. J., Nichols, C. E., Peura, G. D., & Uh, B. S. (1999). The strain behavior of the anterior cruciate ligament during stair climbing: an in vivo study. *Arthroscopy: The Journal of Arthroscopic & Related Surgery*, *15*(2), 185-191.

Beynnon, B. D., & Fleming, B. C. (1998). Anterior cruciate ligament strain in-vivo: a review of previous work. *Journal of biomechanics*, *31*(6), 519-525.

McLean, S. G., Huang, X., Su, A., & Van Den Bogert, A. J. (2004). Sagittal plane biomechanics cannot injure the ACL during sidestep cutting. *Clinical biomechanics*, *19*(8), 828-838.

Abdel-Rahman, E. M., & Hefzy, M. S. (1998). Three-dimensional dynamic behaviour of the human knee joint under impact loading. *Medical engineering & physics*, *20*(4), 276-290.

Bendjaballah, M. Z., Shirazi-Adl, A., & Zukor, D. J. (1997). Finite element analysis of human knee joint in varus-valgus. *Clinical Biomechanics*, *12*(3), 139-148.

Gardiner, J. C., Weiss, J. A., & Rosenberg, T. D. (2001). Strain in the human medial collateral ligament during valgus loading of the knee. *Clinical orthopaedics and related research*, *391*, 266-274.

Dhaher, Y. Y., Kwon, T. H., & Barry, M. (2010). The effect of connective tissue material uncertainties on knee joint mechanics under isolated loading conditions. *Journal of biomechanics*, *43*(16), 3118-3125.

Limbert, G., Taylor, M., & Middleton, J. (2004). Three-dimensional finite element modelling of the human ACL: simulation of passive knee flexion with a stressed and stress-free ACL. *Journal of biomechanics*, *37*(11), 1723-1731.

Hirokawa, S., & Tsuruno, R. (2000). Three-dimensional deformation and stress distribution in an analytical/computational model of the anterior cruciate ligament. *Journal of biomechanics*, *33*(9), 1069-1077.

Gardiner, J. C., & Weiss, J. A. (2003). Subject‐specific finite element analysis of the human medial collateral ligament during valgus knee loading. *Journal of orthopaedic research*, *21*(6), 1098-1106.

Song, Y., Debski, R. E., Musahl, V., Thomas, M., & Woo, S. L. Y. (2004). A three-dimensional finite element model of the human anterior cruciate ligament: a computational analysis with experimental validation. *Journal of biomechanics*, *37*(3), 383-390.

Debski, R. E., Weiss, J. A., Newman, W. J., Moore, S. M., & McMahon, P. J. (2005). Stress and strain in the anterior band of the inferior glenohumeral ligament during a simulated clinical examination. *Journal of shoulder and elbow surgery*, *14*(1), S24-S31.

Limbert, G., Taylor, M., & Middleton, J. (2004). Three-dimensional finite element modelling of the human ACL: simulation of passive knee flexion with a stressed and stress-free ACL. *Journal of biomechanics*, *37*(11), 1723-1731.

Bendjaballah, M. Z., Shirazi-Adl, A., & Zukor, D. J. (1995). Biomechanics of the human knee joint in compression: reconstruction, mesh generation and finite element analysis. *The knee*, *2*(2), 69-79.

Blankevoort, L., & Huiskes, R. (1991). Ligament-bone interaction in a three-dimensional model of the knee. *Journal of Biomechanical Engineering*, *113*(3), 263-269.

Li, G., Rudy, T. W., Sakane, M., Kanamori, A., Ma, C. B., & Woo, S. Y. (1999). The importance of quadriceps and hamstring muscle loading on knee kinematics and in-situ forces in the ACL. *Journal of biomechanics*, *32*(4), 395-400.

Ahmed, A. M., Burke, D. L., Duncan, N. A., & Chan, K. H. (1992). Ligament tension pattern in the flexed knee in combined passive anterior translation and axial rotation. *Journal of Orthopaedic Research*, *10*(6), 854-867.

Butler, D. L., Kay, M. D., & Stouffer, D. C. (1986). Comparison of material properties in fascicle-bone units from human patellar tendon and knee ligaments. *Journal of biomechanics*, *19*(6), 425-432.

Fung, Y.C., 1967. Biorheology of soft tissues. Biorheology 10, 139–155.

Hildebrandt

Decraemer, W. F., Maes, M. A., Vanhuyse, V. J., & Vanpeperstraete, P. (1980). A non-linear viscoelastic constitutive equation for soft biological tissues, based upon a structural model. *Journal of biomechanics*, *13*(7), 559-564.

Frisen, M., Mägi, M., Sonnerup, L., & Viidik, A. (1969). Rheological analysis of soft collagenous tissue: Part I: Theoretical considerations. *Journal of biomechanics*, *2*(1), 13-20.

Kwan, M. K., Lin, T. H., & Woo, S. L. (1993). On the viscoelastic properties of the anteromedial bundle of the anterior cruciate ligament. *Journal of biomechanics*, *26*(4), 447-452.

Lanir 1980

Soong 1973

Viidik, A. (1968). Elasticity and tensile strength of the anterior cruciate ligament in rabbits as influenced by training. *Acta Physiologica Scandinavica*, *74*(3), 372-380.

Woo, S. Y., Johnson, G. A., & Smith, B. A. (1993). Mathematical modeling of ligaments and tendons. *Journal of biomechanical engineering*, *115*(4B), 468-473.

Hurschler, C., Loitz-Ramage, B., Vanderby, R., 1997. A structurally based stress–stretch relationship for tendon and ligament. ASMEJ Biomech. Eng. 119, 392–399.

Gardiner, J., Weiss, J., Rosenberg, T., 2001. Strain in the human medial collateral ligament during valgus lading of the knee. Clinical Orthopaedics and Related Research 391, 266–274.

Lanir, Y. (1983). Constitutive equations for fibrous connective tissues. *Journal of biomechanics*, *16*(1), 1-12.

Quapp, K. M., & Weiss, J. A. (1998). Material characterization of human medial collateral ligament. *Journal of biomechanical engineering*, *120*(6), 757-763.

Weiss, J. A., Maker, B. N., & Govindjee, S. (1996). Finite element implementation of incompressible, transversely isotropic hyperelasticity. *Computer methods in applied mechanics and engineering*, *135*(1), 107-128.

Weiss, J. A., Gardiner, J. C., & Bonifasi-Lista, C. (2002). Ligament material behavior is nonlinear, viscoelastic and rate-independent under shear loading. *Journal of biomechanics*, *35*(7), 943-950.

Sanjeevi, R., Somanathan, N., & Ramaswamy, D. (1982). A viscoelastic model for collagen fibres. *Journal of biomechanics*, *15*(3), 181-183.

Dehoff, P. H. (1978). On the nonlinear viscoelastic behavior of soft biological tissues. *Journal of Biomechanics*, *11*(1), 35-40.

Fung, Y.C., 1993. Biomechanics: Mechanical Properties of Living Tissues. 2nd ed. Springer, New York.

Atkinson, T. S., Haut, R. C., & Altiero, N. J. (1997). A poroelastic model that predicts some phenomenological responses of ligaments and tendons. *Journal of biomechanical engineering*, *119*(4), 400-405.

Yin, L., & Elliott, D. M. (2004). A biphasic and transversely isotropic mechanical model for tendon:: application to mouse tail fascicles in uniaxial tension. *Journal of biomechanics*, *37*(6), 907-916.

Holzapfel, G. A., & Gasser, T. C. (2001). A viscoelastic model for fiber-reinforced composites at finite strains: Continuum basis, computational aspects and applications. *Computer methods in applied mechanics and engineering*, *190*(34), 4379-4403.

Pioletti, D. P., Rakotomanana, L. R., Benvenuti, J. F., & Leyvraz, P. F. (1998). Viscoelastic constitutive law in large deformations: application to human knee ligaments and tendons. *Journal of biomechanics*, *31*(8), 753-757.

Limbert, G., & Middleton, J. (2004). A transversely isotropic viscohyperelastic material: Application to the modeling of biological soft connective tissues. *International Journal of Solids and Structures*, *41*(15), 4237-4260.

Pioletti, D. P., & Rakotomanana, L. R. (2000). Non-linear viscoelastic laws for soft biological tissues. *European Journal of Mechanics A-Solids*, *19*(LBO-ARTICLE-2000-002), 749-759.

Sarver, J. J., Robinson, P. S., & Elliott, D. M. (2003). Methods for quasi-linear viscoelastic modeling of soft tissue: application to incremental stress-relaxation experiments. *Journal of biomechanical engineering*, *125*(5), 754-758.

Toms, S. R., Dakin, G. J., Lemons, J. E., & Eberhardt, A. W. (2002). Quasi-linear viscoelastic behavior of the human periodontal ligament. *Journal of biomechanics*, *35*(10), 1411-1415.

Woo, S. L. (1982). Mechanical properties of tendons and ligaments. I. Quasi-static and nonlinear viscoelastic properties. *Biorheology*, *19*(3), 385.

Woo, S. Y., Gomez, M. A., & Akeson, W. H. (1981). The time and history-dependent viscoelastic properties of the canine medial collateral ligament. *Journal of Biomechanical Engineering*, *103*(4), 293-298.

Pena, E., Martinez, M. A., Calvo, B., Palanca, D., & Doblare, M. (2005). A finite element simulation of the effect of graft stiffness and graft tensioning in ACL reconstruction. *Clinical Biomechanics*, *20*(6), 636-644.

Pioletti, D. P. (1997). Viscoelastic properties of soft tissues.

Bischoff, J. E., Siggelkow, E., Sieber, D., Kersh, M., Ploeg, H., & Münchinger, M. (2008). Advanced material modeling in a virtual biomechanical knee. In *Abaqus Users' Conference*.

Abramowitch, S. D., Woo, S. L., Clineff, T. D., & Debski, R. E. (2004). An evaluation of the quasi-linear viscoelastic properties of the healing medial collateral ligament in a goat model. *Annals of biomedical engineering*, *32*(3), 329-335.

Veronda, D.R., Westmann, R.A., 1970. Mechanical characterization of skin—finite deformations. Journal of Biomechanics 3, 111–124

Gasser, T. C., Ogden, R. W., & Holzapfel, G. A. (2006). Hyperelastic modelling of arterial layers with distributed collagen fibre orientations. *Journal of the royal society interface*, *3*(6), 1535.

Shepherd, D. E., & Seedhom, B. B. (1999). The'instantaneous' compressive modulus of human articular cartilage in joints of the lower limb. *Rheumatology*, *38*(2), 124-132.

Livingston, L. A. (1998). The quadriceps angle: a review of the literature. *Journal of Orthopaedic & Sports Physical Therapy*, *28*(2), 105-109.

Almeida, S.A., Trone, D.W., Leone, D.M., Shaffer, R.A., Patheal, S.L., Long, K., 1999. Gender differences in musculoskeletal injury rates: a function of symptom reporting? Med.Sci.Sports Exerc.31, 1807–1812.
Keller, T. S., Weisberger, A. M., Ray, J. L., Hasan, S. S., Shiavi, R. G., & Spengler, D. M. (1996). Relationship between vertical ground reaction force and speed during walking, slow jogging, and running. *Clinical Biomechanics*, *11*(5), 253-259.

Kerrigan, D. C., Roth, R. S., & Riley, P. O. (1998). The modelling of adult spastic paretic stifflegged gait swing period based on actual kinematic data. *Gait & Posture*, *7*(2), 117-124.

Li, Z., Huang, Q., Li, K., & Duan, X. (2004, April). Stability criterion and pattern planning for humanoid running. In *Robotics and Automation, 2004. Proceedings. ICRA'04. 2004 IEEE International Conference on* (Vol. 2, pp. 1059-1064). IEEE.

Li, G., Papannagari, R., E Defrate, L., Doo Yoo, J., Eun Park, S., & J Gill, T. (2006). Comparison of the ACL and ACL graft forces before and after ACL reconstruction an in-vitro robotic investigation. *Acta orthopaedica*, *77*(2), 267-274.

Ahmed, A. M., Burke, D. L., Duncan, N. A., & Chan, K. H. (1992). Ligament tension pattern in the flexed knee in combined passive anterior translation and axial rotation. *Journal of Orthopaedic Research*, *10*(6), 854-867.

Li, G., Most, E., Sultan, P. G., Schule, S., Zayontz, S., Park, S. E., & Rubash, H. E. (2004). Knee kinematics with a high-flexion posterior stabilized total knee prosthesis: an in vitro robotic experimental investigation. *The Journal of Bone & Joint Surgery*, *86*(8), 1721-1729.

Fleming, B. C., Renstrom, P. A., Beynnon, B. D., Engstrom, B., Peura, G. D., Badger, G. J., & Johnson, R. J. (2001). The effect of weightbearing and external loading on anterior cruciate ligament strain. *Journal of biomechanics*, *34*(2), 163-170.

Kanamori, A., Woo, S. L., Ma, C. B., Zeminski, J., Rudy, T. W., Li, G., & Livesay, G. A. (2001). The forces in the anterior cruciate ligament and knee kinematics during a simulated pivot shift test: a human cadaveric study using robotic technology. *Arthroscopy: The Journal of Arthroscopic & Related Surgery*, *16*(6), 633-639.

Cappozzo A: Gait analysis methodology. Hum Movement Sci 3:27-50, 1984

Kadaba, M. P., Ramakrishnan, H. K., & Wootten, M. E. (1990). Measurement of lower extremity kinematics during level walking. *Journal of Orthopaedic Research*, *8*(3), 383-392.

Chuckpaiwong, B., Charles, H. C., Kraus, V. B., Guilak, F., & Nunley, J. A. (2010). Age ‐associated increases in the size of the infrapatellar fat pad in knee osteoarthritis as measured by 3T MRI. *Journal of Orthopaedic Research*, *28*(9), 1149-1154.

Sanford, B. A., Williams, J. L., Zucker-Levin, A. R., & Mihalko, W. M. (2013). Tibiofemoral Joint Forces during the Stance Phase of Gait after ACL Reconstruction. *Open Journal of Biophysics*, *2013*.

Besier, T. F., Lloyd, D. G., & Ackland, T. R. (2003). Muscle activation strategies at the knee during running and cutting maneuvers. *Medicine and science in sports and exercise*, *35*(1), 119127.

McDowell MA, Fryar CD, Ogden CL, et al: Anthropometric reference data for children and adults:United States, 2003-2006. National Health Statistics Reports. Hyattsville, MD, National Center for Health Statistics, 2008

Winter, D. A., & Scott, S. H. (1991). Technique for interpretation of electromyography for concentric and eccentric contractions in gait. *Journal of Electromyography and Kinesiology*, *1*(4), 263-269.

Abreu, M. R., Chung, C. B., Trudell, D., and Resnick, D. (2008). Hoffa's fat pad injuries and their relationship with anterior cruciate ligament tears: New observations based on MR imaging in patients and MR imaging and anatomic correlation in cadavers. *Skeletal Radiology, 37*(4), pp. 301-306.

Culvenor, A. G., Cook, J. L,, Warden, S. J., and Crossley, K. M. (2011). Infrapatellar fat pad size, but not patellar alignment, is associated with patellar tendinopathy. *Scand J Med Sci Sports, 21*, pp. 405-411.

Butler, D. L., Sheh, M. Y., Stouffer, D. C., Samaranayake, V. A., & Levy, M. S. (1990). Surface strain variation in human patellar tendon and knee cruciate ligaments. *Journal of biomechanical engineering*, *112*(1), 38-45.

Song, Y., Debski, R. E., Musahl, V., Thomas, M., & Woo, S. L. Y. (2004). A three-dimensional finite element model of the human anterior cruciate ligament: a computational analysis with experimental validation. *Journal of biomechanics*, *37*(3), 383-390.

Kiapour, A. M., Kiapour, A., Demetropoulos, C. K., & Goel, V. K. (2013, June). A Novel Framework to Assess ACL Injury Risk Based on Validated Personalized Finite Element Models.
In *ASME 2013 Summer Bioengineering Conference* (pp. V01BT23A010-V01BT23A010). American Society of Mechanical Engineers.

Anderson, F. C., & Pandy, M. G. (2003). Individual muscle contributions to support in normal walking. *Gait & posture*, *17*(2), 159-169.

McKean, K. A., Landry, S. C., Hubley-Kozey, C. L., Dunbar, M. J., Stanish, W. D., & Deluzio, K. J. (2007). Gender differences exist in osteoarthritic gait. *Clinical Biomechanics*, *22*(4), 400409.

Cho, S. H., Park, J. M., & Kwon, O. Y. (2004). Gender differences in three dimensional gait analysis data from 98 healthy Korean adults. *Clinical biomechanics*, *19*(2), 145-152.

Kerrigan, D. C., Della Croce, U., Marciello, M., & Riley, P. O. (2000). A refined view of the determinants of gait: significance of heel rise. *Archives of physical medicine and rehabilitation*, *81*(8), 1077-1080.

Collins, J.J., 1995. The redundant nature of locomotor optimization laws. Journal of Biomechanics 28, 251–267.

Shelburne, K. B., Pandy, M. G., Anderson, F. C., & Torry, M. R. (2004). Pattern of anterior cruciate ligament force in normal walking. *Journal of biomechanics*, *37*(6), 797-805.

Smallman, T. V., Race, A., and Ekroth, S. (2012). The mechanical link between the Infrapatellar plica and the fat pad role in the etiology of anterior knee pain. *Journal of Bone & Joint Surgery, British Volume*, *94*(SUPP XXXVIII), p. 100.

Dragoo, J. L., Johnson, C., and McConnell, J. (2012). Evaluation and treatment of disorders of the infrapatellar fat pad. *Sports Medicine*, *42*(1), pp. 51-67.

Skiadas, V., Perdikakis, E., Plotas, A., and Lahanis, S. (2013). MR imaging of anterior knee pain: a pictorial essay. *Knee Surgery, Sports Traumatology, Arthroscopy*, *21*(2), pp. 294-304.

Han, W., Cai, S., Liu, Z., Jin, X., Wang, X., Antony, B., and Ding, C. (2014). Infrapatellar fat pad in the knee: is local fat good or bad for knee osteoarthritis? *Arthritis Research and Therapy*, *16*(4), R145.

Ballegaard, C., Riis, R. G., Bliddal, H., Christensen, R., Henriksen, M., Bartels, E. M., and Boesen, M. (2014). Knee pain and inflammation in the infrapatellar fat pad estimated by conventional and dynamic-contrast-enhanced magnetic resonance imaging in obese patients with osteoarthritis: A cross-sectional study. *Osteoarthritis and Cartilage*, *22*(7), pp. 933-940.

Collins, N. J., Bisset, L. M., Crossley, K. M., and Vicenzino, B. (2012). Efficacy of nonsurgical interventions for anterior knee pain. *Sports Medicine*, *42*(1), pp. 31-49.

Alentorn-Geli, E., Myer, G. D., Silvers, H. J., Samitier, G., Romero, D., Lázaro-Haro, C., and Cugat, R. (2009). Prevention of non-contact anterior cruciate ligament injuries in soccer players. Part 1: Mechanisms of injury and underlying risk factors. *Knee Surgery, Sports Traumatology, Arthroscopy*, *17*(7), pp.705-729.